INTERACTIONS BETWEEN SILICA-FILLED EPOXIDIZED NATURAL RUBBER AND FUMARIC ACID

ROHANI BT ABU BAKAR @ NASIR

FACULTY OF SCIENCE
UNIVERSITY OF MALAYA
KUALA LUMPUR

2016

INTERACTIONS BETWEEN SILICA-FILLED EPOXIDIZED NATURAL RUBBER AND FUMARIC ACID

ROHANI BT ABU BAKAR @ NASIR

DISSERTATION SUBMITTED IN FULFILMENT OF THE REQUIREMENTS FOR THE DEGREE OF MASTER OF SCIENCE

DEPARTMENT OF CHEMISTRY
FACULTY OF SCIENCE
UNIVERSITY OF MALAYA
KUALA LUMPUR

2016

UNIVERSITY OF MALAYA

ORIGINAL LITERARY WORK DECLARATION

Name of Candidate: ROHANI BT ABU BAKAR @ NASIR

Matric No: SGR[redacted]

Name of Degree: MASTER OF SCIENCE

Title of Project Paper/Research Report/Dissertation/Thesis ("this Work"):

INTERACTIONS BETWEEN SILICA-FILLED EPOXIDIZED NATURAL RUBBER AND FUMARIC ACID

Field of Study: POLYMER CHEMISTRY

I do solemnly and sincerely declare that:

(1) I am the sole author/writer of this Work;
(2) This Work is original;
(3) Any use of any work in which copyright exists was done by way of fair dealing and for permitted purposes and any excerpt or extract from, or reference to or reproduction of any copyright work has been disclosed expressly and sufficiently and the title of the Work and its authorship have been acknowledged in this Work;
(4) I do not have any actual knowledge nor do I ought reasonably to know that the making of this work constitutes an infringement of any copyright work;
(5) I hereby assign all and every rights in the copyright to this Work to the University of Malaya ("UM"), who henceforth shall be owner of the copyright in this Work and that any reproduction or use in any form or by any means whatsoever is prohibited without the written consent of UM having been first had and obtained;
(6) I am fully aware that if in the course of making this Work I have infringed any copyright whether intentionally or otherwise, I may be subject to legal action or any other action as may be determined by UM.

Candidate's Signature Date:

Subscribed and solemnly declared before,

Witness's Signature Date:

Name: Dr. Gan Seng Neon

Designation: Professor, Department of Chemistry, Faculty of Science

ABSTRACT

Vulcanization is a chemical process that forms crosslinks between the rubber and increases the elasticity and tensile strength of the rubber. The physical properties of the rubber vulcanizates could be further improved through the incorporation of filler, which at the same time reduce the cost of rubber products. Crosslinking of rubber using non-toxic fumaric acid and silica filler could offer a wide range of potential applications. In this work, interactions between silica-filled epoxidized natural rubber (ENR) and fumaric acid were investigated. The silica was isolated from rice husk. Amorphous silica could be produced by combustion of the rice husk and the results from X-Ray Diffraction (XRD) and X-Ray Fluorescence (XRF) analyses have shown a purity of ~95 %. Purer amorphous silica could be achieved by first leaching the rice husk with dilute acid before combustion. Thus amorphous silica with purity above 99 % was produced after leaching of the rice husk with dilute sulfuric acid prior to combustion at 600 °C for 2 h. ENR with 50 mol % epoxidation (ENR50) containing various loadings of silica was cured with low levels of fumaric acid at 160 °C. Crosslinking reactions of ENR50 with fumaric acid were first studied by Monsanto rheometer, attenuated total reflectance-Fourier transform infrared spectroscopy (ATR-FTIR), differential scanning calorimetry (DSC) and solvent swelling in toluene. The reactions led to the formation of ester linkages and the disappearance of epoxide peak as revealed by FTIR. Incorporation of silica at various loadings in the compound increased the rheometer torque due to the stiffening effect of filler, but there was no observable change in the glass transition temperature (T_g). For physical properties, the tensile strength of the samples slightly increased in spite of the decrease in elongation at break with increasing silica loading. As expected, the modulus at 100 % strain and hardness increased with addition of more filler due to the reduction in relative amount of rubber, resulting in more rigid samples. Upon ageing at 100 °C for 7 days, the tensile strength and elongation at break remained unchanged, but the modulus at 100 % strain slightly increased. On the other hand, sulfur-cured ENR50 containing 30 phr silica exhibited higher tensile strength and elongation at break and further addition of silica weakened these properties. After ageing, the tensile strength reduced by 5 to 7 MPa, whilst elongation at break and modulus at 100 % strain drastically decreased. This study has revealed that fumaric acid could effectively cure ENR to attain comparable physical properties of sulfur-cured ENR.

ABSTRAK

Pemvulkanan adalah proses kimia yang membentuk rangkai-silang di antara getah dan meningkatkan kekenyalan dan kekuatan regangan getah. Sifat fizikal getah vulkanizat dapat dipertingkatkan melalui penambahan pengisi, di mana pada masa yang sama mengurangkan kos produk getah. Rangkai-silang getah menggunakan asid fumarik yang tidak toksik dan pengisi silika dapat menyumbang kepada potensi kepelbagaian aplikasi. Dalam kajian ini, interaksi di antara isian silika-getah asli terepoksida dan asid fumarik disiasat. Silika tersebut telah diasingkan daripada sekam padi. Silika amorfus dihasilkan daripada pembakaran sekam padi dan keputusan daripada analisa *X-Ray Diffraction (XRD)* dan *X-Ray Fluorescence (XRF)* menunjukkan ~95 % ketulenan. Silika amorfus yang lebih tulen dapat dicapai dengan melarut resap sekam padi terlebih dahulu menggunakan asid mineral cair sebelum dibakar. Oleh itu silika amorfus dengan ketulenan melebihi 99 % dihasilkan selepas sekam padi dilarut resap menggunakan asid sulfurik cair sebelum dibakar pada suhu 600 °C selama 2 jam. Getah asli terepoksida dengan 50 mol % epoksida (ENR50) yang mengandungi pelbagai paras silika divulkan dengan paras asid fumarik yang rendah pada 160 °C. Tindakbalas rangkai-silang ENR50 dengan asid fumarik dikaji menggunakan *Monsanto rheometer*, *attenuated total reflectance-Fourier transform infrared spectroscopy (ATR-FTIR), differential scanning calorimetry (DSC)* dan pengembangan pelarut dalam toluena. Tindakbalas tersebut telah membawa kepada pembentukan ikatan ester dan kehilangan puncak epoksida seperti yang didedahkan oleh FTIR. Penambahan silika di pelbagai paras dalam sebatian telah meningkatkan kilas rheometer kerana kesan kekakuan pengisi, tetapi tiada perubahan pada suhu peralihan kaca (T_g). Untuk sifat fizikal, kekuatan regangan sampel meningkat sedikit manakala pemanjangan tahat putus menurun dengan penambahan paras silika. Seperti yang dijangka, modulus pada 100 % terikan dan kekerasan meningkat dengan penambahan lebih pengisi disebabkan oleh pengurangan jumlah relatif getah, meghasilkan sampel yang lebih kaku. Selepas penuaan pada 100 ^{o}C selama 7 hari, kekuatan regangan dan pemanjangan tahat putus tidak berubah, tetapi modulus pada 100 % terikan meningkat sedikit. Selain itu, sulfur-tervulkan ENR50 mengandungi 30 phr silika mempamerkan kekuatan regangan dan pemanjangan tahat putus paling tinggi dan penambahan silika seterusnya melemahkan sifat-sifat ini. Selepas penuaan, kekuatan regangan menurun sebanyak 5 hingga 7 MPa, manakala pemanjangan tahat putus dan modulus pada 100 % terikan menurun dengan drastik. Kajian ini telah menunjukkan bahawa asid fumarik dengan efektif boleh

mengikat-silang ENR untuk mendapatkan ciri fizikal yang setanding dengan sulfur-tervulkan ENR50.

ACKNOWLEDGEMENTS

First and foremost, I am deeply indebted to my main supervisor, Professor Dr Gan Seng Neon for his consistent guidance, support, encouragement and useful criticism throughout the research period and valuable suggestions in writing of journal papers and this dissertation. Next, I would like to express my sincere gratitude to my co-supervisor, Professor Dr Rosiyah Yahya, who has been very supportive throughout the period and she has been very persistence in proof-reading this dissertation.

Many thanks are due to all my friends and the staff of Chemistry Department, Faculty of Science especially Ms Nurshafiza Shahabudin, Mr Pejvak Rooshenass, Ms Ho Wei Ling and Mr Zulkifli Abu Hassan, for their cooperation and help.

A special thanks to my husband, Dr Jasril Hakeem Jaafar, and my children, Isyraf Izz Umar and Ili Nur Hannah for their love, patience and understanding shown to me throughout completing this study.

Last but not least, I would like to gratefully acknowledge the financial assistance of the Malaysian Rubber Board (MRB) and opportunity given to me to pursue this MSc study. Sincere thanks also to the MRB staff especially Dr Mazlina Mustafa Kamal and Mr Mohd Akram Zaki Abdullah for their support and advice. Also, research grant PG053-2014A from University of Malaya has made this project successful.

TABLE OF CONTENTS

LIST OF FIGURES

LIST OF TABLES

LIST OF SYMBOLS AND ABBREVIATIONS

Δ torque	:	Maximum torque (M_H) – minimum torque (M_L)
APTS	:	3-aminopropyl triethoxysilane
BET	:	Brunauer-Emmett-Teller
dN m	:	decinewton meter
DSC	:	Differential Scanning Calorimetry
ENR50	:	Epoxidized natural rubber with 50 % mol epoxidation
FTIR	:	Fourier Transform Infrared
IRHD	:	International Rubber Hardness Degrees
ISO	:	International Organization for Standardization
M_L	:	Minimum torque
M_H	:	Maximum torque
NR	:	Natural rubber
phr	:	parts per hundred of rubber
SBR	:	Styrene butadiene rubber
SEM	:	Scanning Electron Microscopy
t_{90}	:	Minutes to 90 % of maximum torque or optimum cure time
T_g	:	Glass transition temperature
TGA	:	Thermogravimetric Analysis
XNBR	:	Carboxylated nitrile rubber
XRD	:	X-ray diffractometer
XRF	:	X-ray fluorescence

LIST OF APPENDICES

CHAPTER 1: INTRODUCTION

1.1 Background

Natural rubber (NR) is obtained from *Hevea brasiliensis* tree and is one of the important commodities in Malaysia. It is used extensively in many rubber products such as gloves, rubber handgrips, kitchen utensils, toys, mats and rubber shoes. These products development require vulcanization process which is usually carried out by heating the mixture of rubber and various additives under pressure, to create durable and elastic material. Vulcanization process that includes vulcanizing agents such as sulfur, accelerators, antioxidants and other additives could release fumes during the manufacturing of rubber products. These hazardous by-products could cause adverse health effects to the workers. In addition, residual chemicals may also be leached from rubber products over time and subsequently induce skin dermatitis reactions. Thus it is important to seek chemicals that are non-toxic and environmental friendly to serve as alternatives to conventional additives in rubber vulcanization albeit careful attentions to safety practices have been implemented.

Vulcanizing or crosslinking agent in tandem with rubber additive such as filler is commonly used in rubber products development. In recent years silica has become an alternative filler to carbon black in rubber compounds. Although synthetic precipitated silica has been widely utilized in tire applications, shoe soles, hoses, rollers and conveyor belts, another source of silica is obtainable from agricultural waste material such as rice husk. With the growing concerns over environmental pollution, moving towards the use of sustainable material has captured the interests of many researchers to seek commercial use of rice husk. Many studies have demonstrated that combustion of rice husk generates rice husk ash, which consists of high silica content (> 80 % SiO_2).

In general, this dissertation investigated the potential use of fumaric acid in the absence of additives for curing of rubber, particularly ENR50. Secondly, the feasibility of silica used as filler in the ENR50 and fumaric acid compound were studied and further compared with sulfur vulcanization of silica-filled ENR50. The silica used throughout this work was produced from rice husk, wherein the production and properties of silica were described.

1.2 Problem statements

Vulcanization is a common crosslinking process in rubber, which involves utilization of sulfur or sulfur donors together with accelerators and activators. The presence of organic sulfur donor and accelerators such as thiuram, benzothiazoles and dithiocarbamates can cause bladder, lung and stomach cancers and respiratory diseases such as asthma, chronic lung changes and bronchitis (Sullivan et al., 2001), as well as allergic contact dermatitis (Jacob & Tace, 2006) to rubber product workers and users. For example, allergies to rubber chemicals from gloves are very common among healthcare workers and represent up to 30 % of total population, with 80 % caused by chemical accelerators (Ansell, 2010). Thus it is important to find an alternative towards a non-toxic crosslinking agent such as fumaric acid in rubber compound for product development.

Besides crosslinking agent, precipitated amorphous silica is one of the commercially available filler usually employed in rubber compounds to enhance physical properties of the rubber vulcanizates. A cheaper source of silica could be produced from rice husk. Large quantities of rice husk are usually burnt in rice mills and about 20 % of rice husk ash is generated. Upon complete combustion of the rice husk, grey to white ash is produced, whereas blackish ash is obtained after partial combustion. The white rice husk ash may consist of >90 % silica and small amount of metallic impurities,

depending on the combustion temperature. In addition to the process to extract silica from rice husk is simple, the advantages are not only to get valuable material from rice husk biomass, but also minimize environmental pollution and disposal problems.

1.3 Scope of study

Overall, the current work consists of three objectives. The main objective was to investigate the reactions between ENR50 and fumaric acid as a crosslinking agent. 100 parts of ENR50 was reacted with 1.5 – 19.5 phr of fumaric acid. This amounts to 0.66 mol of epoxide units reacting with 0.01 – 0.17 mol of fumaric acid. One molecule of fumaric acid can only react with two epoxide groups; thus, this low level of fumaric acid was used to avoid a high level of crosslinking so that the sample could remain as an elastomer. The second objective was to study the interactions of fumaric acid with ENR50 filled with silica, while the third objective was to produce high purity amorphous silica from rice husk for incorporating at loading range from 10 to 50 phr into ENR50 and mixed with fumaric acid. This work employed standard technique of rubber mixing using two-roll mill and compression molding. The objectives of this study were:

a) to prepare high purity amorphous silica from rice husk
b) to characterize silica properties using TGA, SEM, ATR-FTIR, XRD, particle size analyzer, XRF and BET method to be used as filler in rubber compound
c) to establish the reactions between ENR50 and fumaric acid
d) to find evidence on the interactions of silica-filled ENR50 with fumaric acid using Monsanto rheometer, ATR-FTIR spectroscopy, percentage of solvent swelling, DSC, and physical properties determination such as tensile strength, elongation at break, modulus at 100 % strain and hardness

e) to compare the interactions between fumaric acid-cured ENR50 filled with silica and sulfur vulcanization of silica-filled ENR50

1.4 Significance of study

The vulcanization process by heating natural rubber with sulfur was discovered by Charles Goodyear in 1841 (Coran, 2005). Since then, there has been continued progress towards the improvement of the process as well as in the usage of rubber chemicals. Substitution of less toxic materials in the vulcanization process presents a continuous challenge to the rubber industry. Despite precaution during raw material handling and storage, and use of proper ventilation in the processing and product manufacturing area, it is necessary to search a green material for crosslinking or in curing process of rubber. ENR is a semi-synthetic rubber, which provides dual functionality of unsaturated sites and epoxide groups. Besides the sulfur vulcanization *via* double bonds, alternative crosslinking reactions could take place *via* ring opening of epoxide groups by dicarboxylic acid such as fumaric acid. Since both the crosslink structures are distinctly different from each other, it is crucial to establish the predominant reactions between the epoxide groups of ENR and fumaric acid.

Fumaric acid has been widely used as acidulant in food industry. Currently, the production of fumaric acid includes the use of petrochemical feedstock, but it also can be produced through fermentation of *Rhizopus oryzae* fungus. Other than its non-toxic nature, it can be produced from renewable resources, and the two carboxylic acid groups in fumaric acid structure could give chain modification *via* ester formation during crosslinking of ENR.

Apart from crosslinking which increases elasticity and strength of rubber, most of the rubber industry use filler to obtain desired processing characteristics, ultimate properties

and simultaneously lower the cost of rubber products. Precipitated amorphous silica is among the most widely used filler for rubber reinforcement. Most of the processes to produce precipitated silica start with sodium silicate solution, with subsequent acid/base aqueous precipitation processes. Precipitated amorphous silica in commercial production is synthesized from pure quartz sand and sodium carbonate at 1100 – 1200 ^{o}C (Bhattacharya & Ali, 2015) to produce sodium silicate. On the other hand, it has been well known and investigated that rice husk produces rice husk ash upon burning. In Malaysia, combustion of rice husk as fuel in rice mill to produce hot air for drying rice has resulted in the production of ash as a by-product. On top of the emission of CO_2, SO_x and NO_x during combustion of rice husk, the rice husk ash has been disposed-off to landfills (Theeba et al., 2012), thereby leading to air and land pollutions. The rice husk ash has been reported to consist of high silica content (James & Rao, 1986) and thus the abundance of rice husk ash could be the promising option of silica source. This would also provide a new income source to the rice processors and at the same time greatly reduce space for agricultural wastes.

Nowadays, increased awareness of safety and health has created a trend towards the use of green and environmental friendly materials. This dissertation presents a study on the potential use of fumaric acid, which is a non-toxic compound, in crosslinking of ENR. Also, silica isolated from rice husk could be a value-added material to function as filler in the ENR50 compound and concurrently could overcome environmental problems.

1.5 Summary

This chapter discusses the issues pertaining to current vulcanization process and precipitated amorphous silica filler used in the rubber industry. The crosslinking in ENR by fumaric acid could introduce some new properties in comparison with sulfur

vulcanization, and subsequently recommends new applications. Utilization of silica obtained from rice husk could also give new application for a waste material. The following chapter will address relevant literature relating to the subjects that have been discussed here.

CHAPTER 2: LITERATURE REVIEW

2.1 Introduction

Chapter 2 gives a detailed review on the general information about ENR, followed by vulcanization or crosslinking process that can take place in ENR. The origin and advantages of fumaric acid as crosslinking agent is also addressed. Next, the common types of filler used in rubber and its properties are discussed. A more detailed preparations and properties of pure silica filler isolated from rice husk are given in the following section.

2.2 Epoxidized natural rubber (ENR)

NR exhibits outstanding properties such as high tensile strength, high resilience, outstanding fatigue and cut growth resistance, low heat build-up, and good low temperature resistance. As a result of non-polar nature, NR has certain disadvantages and these include poor wet grip properties, low heat, oxygen and ozone resistances, and swell in oil, grease, fuel and hydrocarbon solvent. The non-polar property and unsaturation of NR have restricted its usefulness in certain applications. Therefore, many efforts have been made to modify the NR by chemical or physical means to impart special properties.

Chemical modification of NR by epoxidation reaction has produced ENR, where a portion of the carbon-carbon double bonds of the NR is chemically converted into the polar epoxide groups. Currently, ENR is marketed as Ekoprena® by Malaysian Rubber Board and produced by Felda Rubber Industries Sdn. Bhd. Two grades of Ekoprena® are available, namely Ekoprena25® and Ekoprena50® which contain 25 mol % and 50 mol % epoxide group, respectively.

2.2.1 Preparation of ENR

Epoxidation of NR was discovered as early as in 1922, whereby NR was treated with peroxycarboxylic acids (Gelling & Porter, 1988). Ever since, various methods of preparation and reaction conditions in the synthesis of ENR were reported, including with preformed peroxyacetic acid (peracetic acid) or 'in-situ' peroxyformic acid (performic acid) (Burfield et al., 1984; Gelling, 1985). The most preferred route has been found by using performic acid, generated by reversible reaction between hydrogen peroxide and formic acid as shown in Figure 2.1. The performic acid transfers an oxygen atom to the double bond of polyisoprene in a cyclic, single-step mechanism. The result is the syn addition of the oxygen to the double bond, with formation of an epoxide and a formic acid (Solomons & Fryhle, 2000). Thus only hydrogen peroxide is consumed, whilst formic acid acts as catalysts in epoxidation reaction (Figure 2.2).

Figure 2.1: Reversible reaction between hydrogen peroxide and formic acid

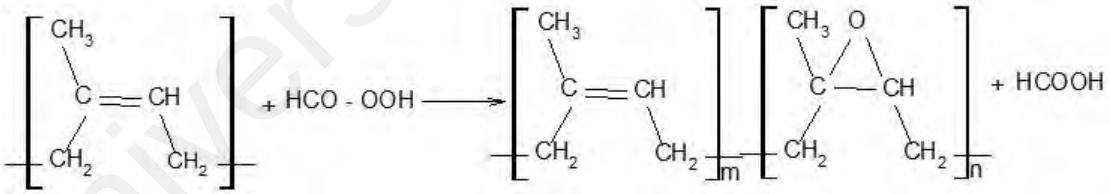

where, m = number of polyisoprene repeating unit
n = number of epoxide repeating unit

Figure 2.2: Epoxidation reaction of NR

Owing to high acid concentration and elevated temperature, the epoxidation of NR favors the formation of secondary products resulted from the ring opening reaction of the epoxide groups. The types of secondary ring-opened products vary depending on the level of epoxidation. At low level of modification, the majority of epoxide groups are

isolated in the rubber chains, thus the *trans* diol is normally the ring-opened products. On the other hand, at high level of modification, the number of adjacent epoxide groups increases, intra-molecular attack of hydroxyl group on neighbouring epoxide groups will result in the formation of five-membered cyclic ether as a major product (Gelling, 1985). Under carefully controlled conditions such as temperature and total acid concentration of the epoxidation reaction, NR latex can be epoxidized up to 75 mol % without formation of secondary ring-opened products.

2.2.2 Properties of ENR

Epoxidation reactions of NR have changed the physical and chemical properties of NR and these properties are observed to change systematically with the level of epoxidation. The introduction of random epoxide groups along a stereo-regular *cis*- 1,4-polyisoprene backbone (Davey & Loadman, 1984) increases the rubber polarity and thus enhances its resistance towards oils and hydrocarbon solvents as well as reduction in gas permeability. Glass transition temperature (T_g) also increases linearly with increasing epoxidation level because of restriction in chain mobility.

Typically, chemical modification of NR disrupts the stereo-regularity of NR backbone and thus inhibits strain crystallization, with a subsequent reduction in strength properties. However, since epoxidation reaction of NR is known to be stereo-specific (Witnauer & Swern, 1950), ENR is also able to undergo strain crystallization similar to NR for up to 50 mol % epoxidation (Davies et al., 1983). This is revealed by significantly higher tensile strength of unfilled ENR compared to nitrile butadiene rubber (NBR) with much improved fatigue performance. Furthermore, the increase in T_g of carbon black-filled ENR has resulted in improved damping capability, decreased resilience, reduced gas permeability and better wet traction (Baker et al., 1985).

2.2.3 Applications of ENR

As a result of the increase in T_g and polarity on epoxidation reaction, in combination with the ability of ENR to undergo strain crystallization, a wide range of potential applications for ENR has been suggested. In applications dependent on properties related to T_g, which results in an increase in damping properties, decrease gas permeability and low resilience, ENR can be used in tire inner liner and inner tubes. Since tire is the largest market for rubber, thus it also provides the largest potential market for ENR. The increase in ambient temperature hysteresis, also results in an increase in wet grip which is an important property for tire tread compounds. Typically improvement in wet grip is followed by the increase in rolling resistance. Compared to common tread rubbers, silica-filled ENR25 tread compounds exhibit both low rolling resistance and high wet grip properties (Baker et al., 1985).

The combinations of properties exhibited by ENR suggest applications in a wide range of general rubber goods. The high strength and oil resistance properties of ENR are being utilized for an application in oil resistant tubular conveyors, milking inflations and oil resistant cut tread. Also the high fatigue lives and damping properties of ENR compounds have been applied in vibration isolation mounts (Gelling, 1987). The high wet grip properties of ENR have also being applied to produce non-slip flooring materials and shoe soling compounds. Patents have been filed on the ENR based adhesives compositions which could be developed for the bonding of vulcanized rubbers of differing polarity and rubber compounds to steel (Loo, 1989), for use in the area of epoxy resin technology and to develop glazing sealing systems.

2.2.4 Vulcanization and crosslinking of ENR

In development of rubber products and applications, vulcanization is a crucial process, which involves insertion of crosslinks between polymer chains through the

action of heat and pressure. The crosslink may be a group of sulfur atoms in a short chain, a carbon to carbon bond, a polyvalent organic radical, an ionic cluster or a polyvalent metal ion (Coran, 2005). Vulcanization converts rubber from a linear polymer to a three-dimensional network structure by crosslinking the polymer chains through the use of vulcanizing or crosslinking agents. Vulcanizing agents containing elemental sulfur is the most important chemicals and widely used in rubber industry because it is easily available, abundant and very cheap. The most basic requirement for sulfur vulcanization is the availability of –C=C– groups on the rubber chains. Thus similar to NR, ENR can be vulcanized by sulfur in the presence of accelerators. In addition, ENR can also be cured through the crosslinking of the epoxide groups with various chemicals and polymers.

2.2.4.1 Sulfur vulcanization

In almost every industrial practice sulfur vulcanization is conducted in the presence of other ingredients such as accelerators, activators, retarders and pre-vulcanization inhibitors. Typical ingredients for sulfur vulcanization include sulfur and/or a sulfur donor, accelerators, zinc oxide as activator and stearic acid as co-activator. Generally, in sulfur vulcanization system, the sulfur-sulfur bonds in the elemental S_8 sulfur rings start to break at the temperature in the range of 120 – 160 ^{o}C. The primary sites of attack are hydrogen on the α-carbon on the double bond. The structure is shown in Figure 2.3.

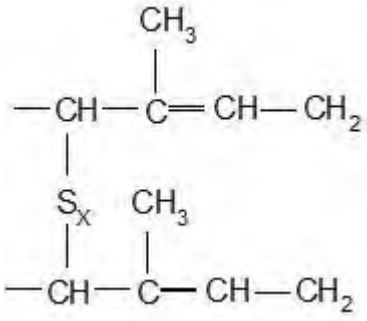

where, x = 2,4,6,8

Figure 2.3: Crosslinking of NR *via* sulfur vulcanization

Sulfur vulcanization systems can be categorized as conventional (CV), semi-efficient (semi-EV) and efficient (EV) systems, depending on the amount of sulfur and the ratio of accelerator to sulfur, as illustrated in Table 2.1. A CV system contains high amounts of sulfur and low amounts of accelerator. The vulcanizates contain 95 % poly- and disulfidic crosslinks and 5 % monosulfidic crosslinks. Although these network structures exhibit good fatigue, tensile and tear properties, and excellent resistance to low-temperature crystallization, the structures are poor in reversion resistance (resistance to non-oxidative thermal ageing or overcure), high compression set and stress relaxation at elevated temperature, due to polysulfidic crosslinks that are able to rearrange under stress.

Table 2.1: Classification of sulfur vulcanization system

Type	Sulfur (S, phr)	Accelerator (A, phr)	A/S ratio
CV	2.0 – 3.5	1.2 – 0.4	0.1 – 0.6
Semi-EV	1.0 – 1.7	2.5 – 1.2	0.7 – 2.5
EV	0.4 – 0.8	5.0 – 2.0	2.5 – 12

Source: Akiba and Hashim (1997).

Vulcanization of NR using high amounts of accelerator and low amounts of sulfur efficiently utilizes sulfur to form crosslinks and known as efficient vulcanization (EV) system. The crosslinks are mainly monosulfidic (80 %) with low level of main chain

modifications. EV systems give vulcanizates that are excellent reversion resistance and good resistance to oxidative ageing, due to the higher thermal stability of monosulfidic crosslinks. Monosulfidic crosslinks are not able to exchange, rearrange or break to relieve stress without the breakage of main chains. However, EV vulcanizates exhibit lower properties in tensile strength, resilience, fatigue and abrasion resistances, thus EV systems are used for the vulcanization of thick articles and those used at elevated temperatures.

Semi-EV is defined as an intermediate vulcanization system between CV and EV systems, with 50 % poly- and disulfidic crosslinks, and 50 % monosulfidic crosslinks. The use of semi-EV systems exhibit physical properties intermediate between those of CV and EV vulcanizates. Compared with CV vulcanizates, semi-EV gives some improvements in ageing and reversion resistance, but resistance to low-temperature crystallization and fatigue is impaired. Figure 2.4 shows general structures in sulfur-vulcanized NR.

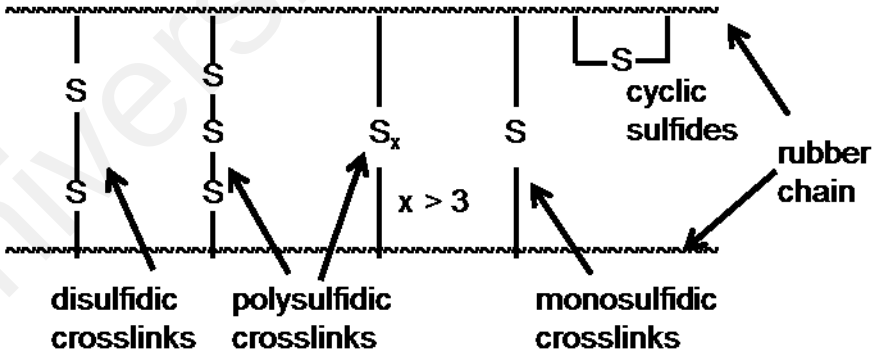

Figure 2.4: Structure in sulfur vulcanization systems

ENR can be vulcanized using standard sulfur formulation normally employed for NR. Gelling and Morrison (1985) reported that ENR vulcanized by sulfur alone is faster and more efficient compared to NR. However, a CV system which contains high

amounts of sulfur was not recommended for ENR due to poor ageing characteristics. The sulfur-containing acids produced from thermal decomposition of oxidized sulphides induced the ring opening of the epoxide groups, with a subsequent increase in T_g, crosslink density and formation of ether crosslinks. These result in significant increase in modulus and consequently decrease in tensile strength and elongation at break. Therefore semi-EV and EV systems are recommended for ENR. Although the semi-EV provides better fatigue and inferior ageing properties compared to EV systems, generally, the properties of semi-EV and EV vulcanizates of ENR was comparable to NR (Baker et al., 1985). To optimize the ageing resistance of ENR, it is important to maintain the vulcanizates at basic conditions and this can be achieved by adding small amount of base such as calcium stearate in the compound (Gelling, 1991).

2.2.4.2 Crosslinking involving epoxide groups of ENR

While sulfur-cured ENR utilizes the residual of –C=C– groups, the epoxide groups in ENR can also be used as crosslinking sites. ENR cured by amine compounds *via* ring opening of the epoxide groups has been investigated by Hashim and Kohjiya (1994). Curing of ENR with *p*-phenylenediamine catalyzed by bisphenol A was carried out at 180 ^{o}C, and it was found to have an activation energy of 67.5 kJ/mol, much higher than in a typical sulfur-cured ENR (36 – 52 kJ/mol). Further reinforcement with carbon black filler in ENR cured by amine has resulted in significantly higher tensile strength and modulus at 100 % strain compared to sulfur-cured ENRs. The relatively high T_g of the carbon black-filled vulcanizates could be attributed to the bulkiness of the amine crosslinks and hydrogen bonding effect of bisphenol A.

Other crosslinking reactions involving the epoxide group in ENR and reactive functional groups in two or more polymers has led to the development of self-crosslinkable blends. Alex et al. (1989) developed self-crosslinkable rubber blends

based on ENR and carboxylated nitrile rubber (XNBR). ENR and XNBR were first masticated separately on the two-roll mill for 6 min. Then masticated rubbers were blended on the mill for 10 min, followed by curing at 140 ^{o}C for 45 min in the absence of crosslinking agent and additives. It was found that the proportions of carboxyl group in XNBR and epoxide group in ENR contribute significantly to the increase in crosslinking between the rubber blends, resulting in the formation of ester together with ether crosslinks. In addition to the higher maximum torque (M_H) that indicates the extent of crosslinking in XNBR/ENR blends, the higher tensile strength, tear resistance, resilience and hardness, and lower value of compression set were achieved with higher composition of XNBR. Figure 2.5 (a) shows probable mechanism of crosslinking between ENR/XNBR.

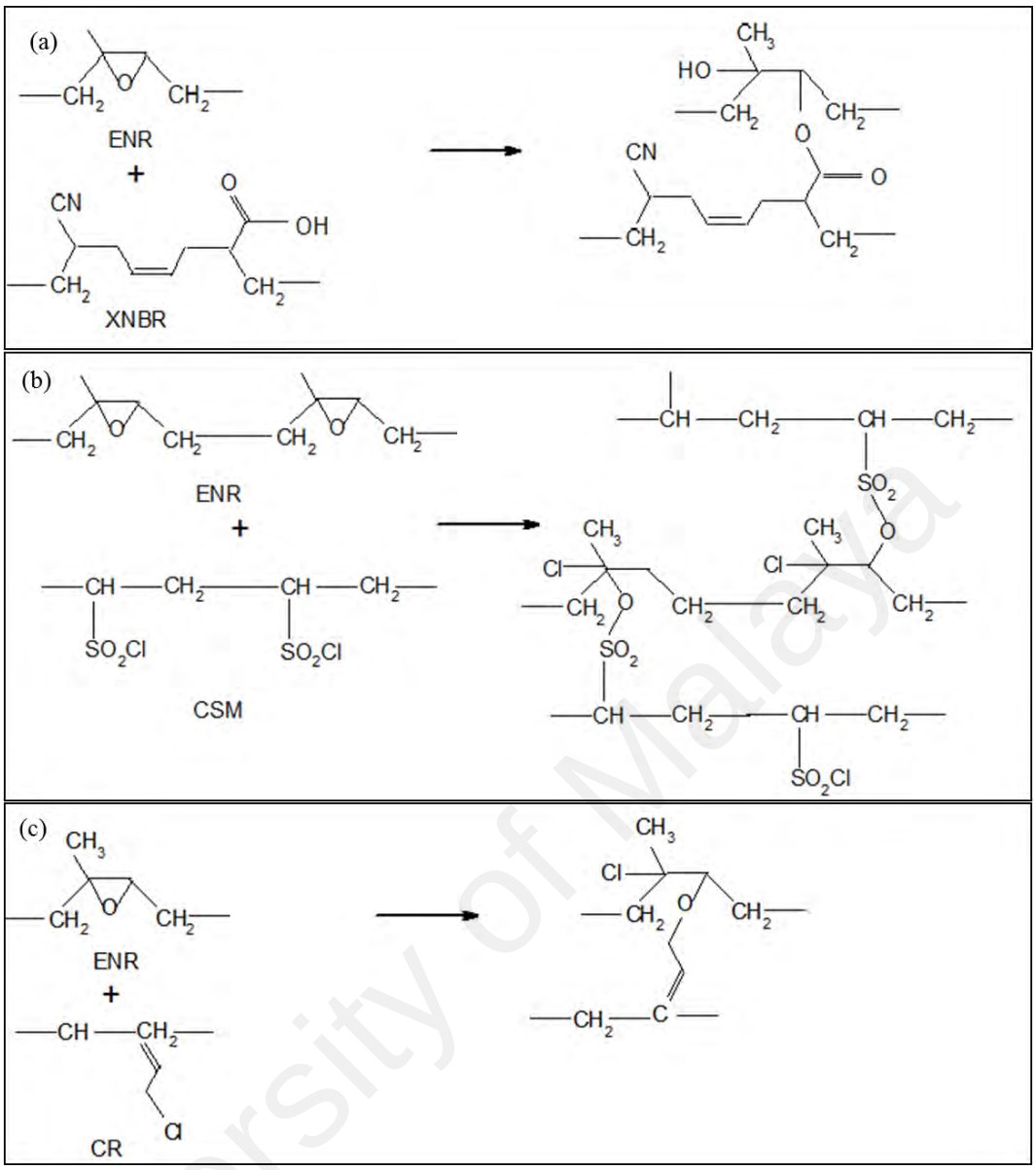

Figure 2.5: Probable mechanism of crosslinking in (a) ENR/XNBR blends, (b) ENR/CSM blends and (c) ENR/CR blends

Other self-crosslinkable rubber blends which include ENR/chlorosulphonated polyethylene (CSM) (Mukhopadhyay & De, 1991) and ENR/polychloroprene (CR) (Alex & De, 1991) have also been investigated. In ENR/CSM blends, sulfonate type of linkage was formed between the epoxide group of ENR and the $-SO_2Cl$ group of CSM, whereas in ENR/CR blends, ether crosslinks were formed by the reaction of the epoxide group of ENR and the allylic chlorine of CR. The probable mechanisms of crosslinking

in ENR/CSM and ENR/CR blends are shown in Figure 2.5 (b) and Figure 2.5 (c), respectively.

Besides self-crosslinking of binary rubber blends discussed above, ternary blends such as CR/XNBR/ENR (Alex et al., 1991) and CSM/XNBR/ENR (Roychoudhury et al., 1992) blends have also been reported to be self-crosslinkable. ENR and alkyd could also form a self-crosslinkable blend in toluene solution at ambient temperature (Khong & Gan, 2013). The crosslinking reactions between the epoxide groups of ENR and –COOH groups of alkyd have formed ester linkages, with a subsequent increase in T_g and gel content of the blend.

Curing of ENR with a series of saturated dicarboxylic acids *via* ring opening of the epoxide groups at 170 ^oC has been reported by Loo (1985). ENR50 mixed with dicarboxylic acids having smaller pK_a^1 value such as oxalic (pK_a^1 ~1.27) and malonic (pK_a^1 ~2.85) acids formed hard crumbs during and after mixing process, presumably due to complete furanization in ENR50 during mixing as there was no observable of T_g. In contrast, ENR50 mixed with dicarboxylic acids having pK_a^1 value in the range of 4.21 to 4.55 produced smooth samples. The reactions exhibited a marching increase in rheometer torque with time. The shorter chain of dicarboxylic acids [$HOOC(CH_2)_{2-3}COOH$] revealed a faster cure rate and higher extent of cure. However, the rate and extent of cure become less significant with increasing in the pK_a value and chain length [$HOOC(CH_2)_{4-8}COOH$] of dicarboxylic acids. The extent of reaction is highly dependent on the concentration of carboxylic acid, the temperature, and the reaction time. Changes in physical properties such as T_g, hardness, modulus, and resilience are associated with the crosslinking reaction between ENR and dicarboxylic acid. Furthermore, the vulcanizates have been found to give higher air permeability and lower oil swell when compared to the semi-EV sulfur-cured ENR vulcanizates. But, the

crosslinking reaction may not be the only cause for the increase in T_g as a similar increase has been observed in the reaction of ENR with monofunctional benzoic acid that could not incur crosslinking (Gan & Burfield, 1989). The T_g of the sample increases proportionally with the benzoic acid loading when heated at elevated temperature (125 – 160 ^oC). Benzoic acid has ring-opened the epoxide ring and generate polar –OH groups in the ring-opened structure, which might be involved in the inter-molecular and intra-molecular hydrogen bonding. The reaction was found to be first order with activation energy of 70 kJ/mol.

Studies on the crosslinking reactions between ENR and dodecanedioic acid (DA) at 180 ^oC was carried out by Pire et al. (2010). T_g of the samples increased non-linearly with the high amount of DA. Further investigation based on the reaction of ENR and lauric acid showed the T_g of the grafted elastomer remained unchanged at ~42.5 ^oC similar to that of raw ENR25 for all proportions of acid. It has been suggested that the formation of hydroxyl and ester, as a result of ring opening of epoxide groups by lauric acid, does not induce any increase in T_g. Thus main chain modifications could not explain the deviation from linearity in T_g of ENR cured by DA for high proportions of acid. This was disputed by the results of Gan and Burfield (1989) that suggested it could be due to the linear lauric acid used, which is less bulky than benzoic acid and does not interfere in the main chain mobility. The deviation in T_g of the sample at high amounts of DA is hypothesized to be due to the polar interactions between the pendant chains in DA with other carboxylic groups (from pendant chains) and epoxide sites. The physical properties of the vulcanizates were as good as sulfur-cured ENR when curing at similar conditions (180^oC, 3 h), but the curing time led to the degradation of the properties of sulfur-cured ENR. Accelerating the reaction using 1,2-dimethylimidazole (DMI) has reduced the detrimental effect of heat treatment, with a subsequent improvement in the

physical properties of vulcanizates (Pire et al., 2011). DMI acts as an accelerator *via* the formation of an imidazolium dicarboxylate that enables the solubilization and the activation of the crosslinking agent in ENR (Pire et al., 2012).

2.2.5 Summary

From the interesting findings reported by the researchers as discussed in section 2.2.4.2, it reveals that curing or crosslinking of ENR at elevated temperatures with compounds containing amine, chlorine and carboxyl groups were viable through ring-opening of the epoxide groups. Thus, the ideas of investigating the reaction of ENR with unsaturated dicarboxylic acid of fumaric acid were proposed.

2.3 Fumaric acid

Fumaric acid or *trans*-butenedioic acid is a white crystalline powder of organic acid. Currently, fumaric acid is manufactured from petroleum based derivatives maleic anhydride, which is produced from butane *via* fluid-bed or fix-bed processes (Sim, 2005, May 18). The increasing prices of petroleum has led to the development of fermentation process to produce fumaric acid from *Rhizopus* species (Sood et al., 2014). This microorganism has been found to produce the highest yield and productivity of fumaric acid, *via* a combination of the citrate cycle and reductive pyruvate carboxylation.

Fumaric acid has many potential industrial applications. It has been used in foods and beverages as acidulant since 1946 to provide persistent, long lasting sourness and flavor stability. Other uses of fumaric acid can be found in paper resins, alkyd resins, plasticizers, inks, personal care additives, lacquers, lubricating oil, carboxylating agent for styrene-butadiene rubber, and in the production of unsaturated polyester resins (Du et al., 2015). Apart from two carboxylic acid groups and carbon-carbon double bond of

fumaric acid as shown in Figure 2.6, that is important in polymerization and esterification reactions, the non-toxic nature of fumaric acid provides better option than the other carboxylic acids in polymer industry (Roa Engel et al., 2008). Table 2.2 shows properties of fumaric acid.

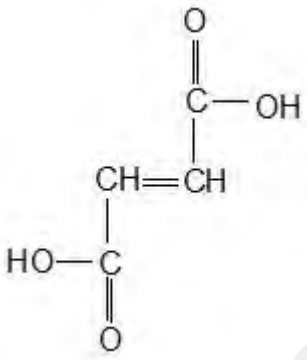

Figure 2.6: Chemical structure of fumaric acid

Table 2.2: Properties of fumaric acid

Properties	
Molar mass	116 g/mol
Density	1.64 g/cm^3
Melting point	287 ^{o}C
Solubility in water	7 g/L at 25 ^{o}C
Acidity (pK_a)	pK_{a1} 3.03, pK_{a2} 4.44

Source: National Center for Biotechnology Information (NCBI) (2016).

2.4 Fillers in rubber

Fillers are particulate solids, essentially rigid and non-deformable. Incorporation of filler could lead to an increase in tensile strength, modulus, hardness, abrasion resistance and tear resistance (Edwards, 1990). The most commonly used reinforcing fillers known are carbon black and silica. Non-reinforcing fillers can be used as diluents to reduce compound cost and to improve processing. Examples of non-reinforcing fillers are clay, mica, talc and ground calcium carbonate.

2.4.1 Carbon black

Carbon black is made up of mostly carbon atoms in a graphite-like structure, and also covered with various functional groups on the surface such as phenol, carboxyl, lactone, ketone, quinone and pyrone in very small quantities (Wolff, 1996) as shown in Figure 2.7.

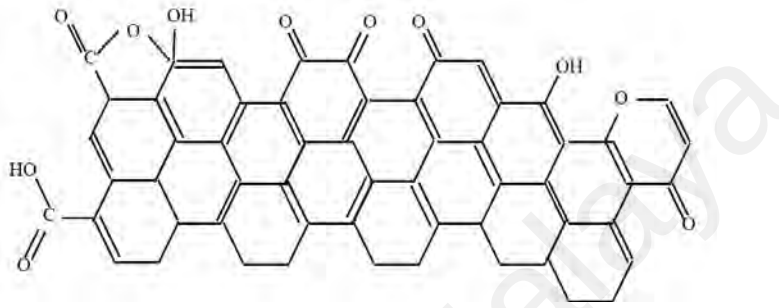

Figure 2.7: Surface chemistry of carbon black

Carbon blacks are produced by thermal cracking or incomplete combustion of hydrocarbon and widely used in tires. Other than tires, it has also been used in rubber products such as conveyor belts, weatherstrip, dock fenders, windshield wipers and hoses (Norman, 1990). Carbon black is graded with a letter and three digit numbers as described in ASTM D1765. The letter is either 'N' for normal or 'S' for slow curing material. The first of the three digits indicate the average particle sizes. The last two digits describe the structure of the aggregate. For example N340 and N327 have essentially the same average particle sizes, and N340 is more reinforcing than N327 (Byers, 1987).

2.4.2 Non-black fillers

The non-black fillers which include calcium carbonate, clay, silica and silicate are incorporated in many rubber compounds to modify processing and performance of rubber products (Wagner, 1987). Two types of calcium carbonates are available, natural and precipitated calcium carbonates. Natural calcium carbonate can be derived from

marble or high dolomitic limestone. The limestone is classified either wet-ground (grades 1 – 4) or dry-ground (grades 5 – 8). Grade 5 (dry ground) is mainly used in rubber industry for general purposes, whereas Grade 2 (wet ground) for maximum brightness. Precipitated calcium carbonate is produced by direct carbonation of hydrated lime, known as the milk of lime process.

Kaolin is one of the examples of clay widely used in rubber because it is cheap, serves moderate reinforcement and processing benefits. After the high purity deposits (>90 % kaolin) is mined, the ore is dried, pulverized and refined by either air-separation or water-separation processes. A relatively coarse particle sizes (soft clays) and fine particle sizes (hard clays) are produced through a combination of mineral-source and particle-size classification. The particle sizes of hard and soft clays influence the changes in tensile strength and tear properties.

Silica can exist in amorphous and crystalline forms. While there are three major forms of crystalline silica, which are quartz, cristobalite and tridynamite, synthetic amorphous silica are available in two forms, which are precipitated silica and fumed silica. Amorphous silica is categorized based on the preparation method. Fumed silica is prepared from flame pyrolysis of silicon tetrachloride or from quartz sand vaporized in a 3000 ^{o}C electric arc, with properties of high purity (99 % silica), extremely fine particle size (7 – 15 nm) and low adsorbed water (<1 %). Precipitated silica is synthesized by reacting alkaline silicate solution with a sulfuric acid, followed by filtration, washing and drying of the resulting white precipitate. Figure 2.8 shows chemical reactions for manufacturing of precipitated silica. Additionally, silica is polar and hydrophilic reinforcing filler due to the presence of three types of silanol groups and siloxane bridge on the silica surface. Figure 2.9 shows siloxane bridge and types of silanol groups, which are geminal, vicinal and isolated silanol groups on silica surface.

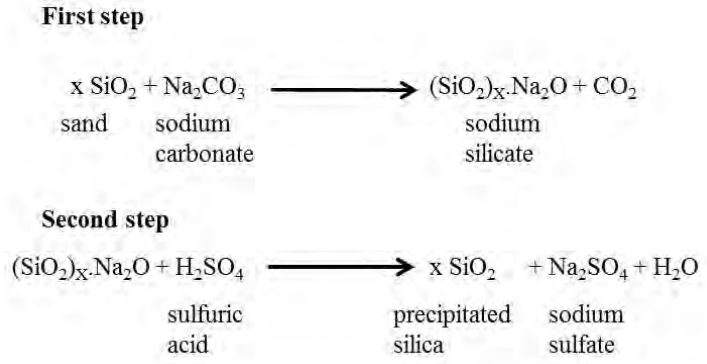

Figure 2.8: Chemical reactions for manufacturing of precipitated silica

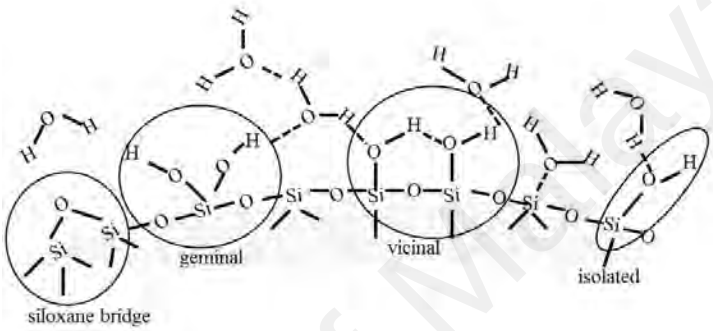

Figure 2.9: Silanol groups and siloxane bridge on a silica surface

2.4.3 Properties of rubber filler

Reinforcement of rubber by filler is associated with a strong interaction between the filler surface and rubber. Although mechanism of the reinforcement between rubber and filler is still lacking, it appears that the interaction is due to both physical and chemical depending on physico-chemical property of the filler surface and chemical nature of the rubber (Dannenberg, 1986). The reinforcing capability of a filler is governed by its particle size or specific surface area, structure and surface activity (Leblanc, 2002).

2.4.3.1 Particle size

Generally, the larger the particle sizes of filler, the poorer the reinforcement capability and the lower the cost of the material. Particle size larger than 1000 nm does not have reinforcing capabilities. The smaller the particle size of filler, the greater the total amount of surface area of filler in contact with the elastomer (Leblanc, 2002).

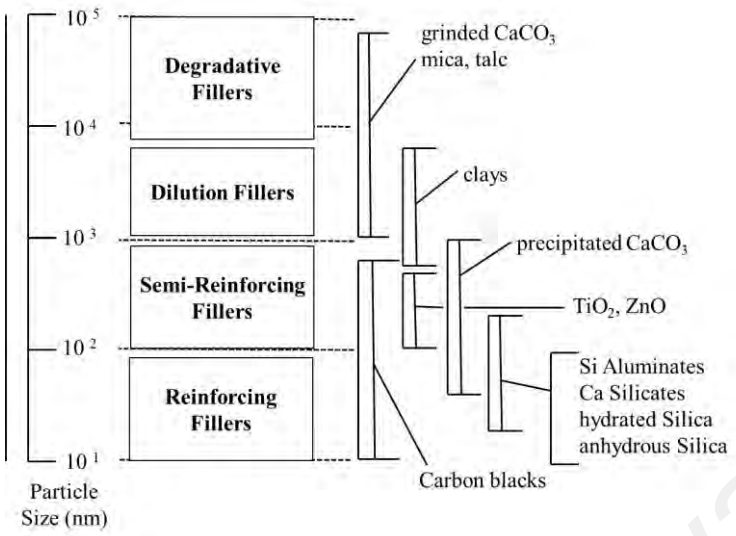

Figure 2.10: Category of fillers according to average particle size. Adapted from Leblanc J.L. © 2002 Elsevier Science Ltd.

Figure 2.10 shows category of fillers according to average particle size. Particle sizes of carbon black and silica are considerably smaller and hence offer significant reinforcing capabilities than the clay. There is a wide range of carbon black with surface areas ranging from 6 m^2/g to 250 m^2/g. The surface areas of the precipitated silica are in the range of 125 – 200 m^2/g and typical hard clays ranges from 20 m^2/g to 25 m^2/g.

2.4.3.2 Particle structure

'Structure' is used to describe the degree of aggregation of the particles. High structure blacks may have a high number of primary particles per aggregate, for example up to 200 particles per aggregate is called a strong aggregation. A low structure blacks exhibit a weak aggregation that may have an average of 30 particles per aggregate (Frohlich et al., 2005). These aggregates (primary structure) may form agglomerates (secondary structure) linked by van der Waals interactions which are easily broken during mixing and dispersion of carbon black into rubber compound. Thus the well dispersed of the smallest form of aggregates in an elastomer increases the reinforcing capabilities. In contrast, silica aggregates cannot be broken during mixing, but tends to form agglomerates through hydrogen bonding due to the surface chemistry

of silica. Silica specific areas are larger than carbon black at similar reinforcing capabilities.

2.4.3.3 Surface activity

The surface activity of filler is a major factor pertaining to filler-filler and filler-rubber interaction. Many authors have demonstrated that the chemical crosslinks existing between the functional groups on the filler surface and the reactive rubbers induce reinforcement (Rajeev & De, 2002).

(a) ***Carbon black***

Bandyopadhyay et al. (1996b) reported interactions of 75 parts of carbon black per hundred parts of XNBR, without crosslinking agent, has increased the Δ torque and the effect was more prominent with the oxidized carbon black as compared to the non-oxidized carbon black. This is attributed to the reaction between –COOH groups of XNBR interacting chemically with the reactive groups of the carbon black. The same group (Bandyopadhyay et al., 1996a) has reported that the tensile strength, modulus at 100 % and 300 % elongations and tear resistance further increased with addition of 3-aminopropyl triethoxysilane (APTS). It was postulated that $–NH_2$ groups of the silane interact with –COOH groups of the XNBR, whereas $–OC_2H_5$ groups of the silane interact with –OH groups on the carbon black. Besides assisting in the crosslinking of the rubber by filler, APTS reduced the filler-filler interaction with improved dispersion of the carbon black in rubber.

Reinforcement of ENR by oxidized carbon black in the absence of crosslinking agents has been discussed by Roychoudhury and De (1993), in which the extent of crosslinking reaction depends on the epoxy content of ENR and concentration of surface oxygen functional groups of the carbon black. Despite higher surface oxidation of

carbon black, following investigation by Manna et al. (1997) have also shown the extent of crosslinking reaction between ENR and oxidized carbon black increased with increasing filler content from 40 to 100 phr and higher molding temperatures ranging from 170 to 190 ^{o}C. Supporting evidence of the reactions was provided by the increase in bound rubber value, higher Δ torque, and decrease in percentage of solvent swelling, with a subsequent increase in the tensile strength and modulus properties. FTIR studies have revealed that the interaction between ENR and oxidized carbon black formed ester and phenolic ether linkages. In addition, incorporating N-(4-vinylbenzyl)-N'-[3-(trimethoxysilyl)propyl]ethane-1,2-diamine mono hydrogen chloride salt coupling agent into the compound has resulted in the formation of silyl ether, silyl ester and amide linkages (Manna et al., 1999).

(b) ***Silica***

The reinforcement of rubber by silica is different from carbon black. The silica surface composed of siloxane and silanol groups can be characterized by the surface energy. The surface free energy of filler, γ_s can be represented as in Figure 2.11, where γ_s^d is the dispersive component, whereas γ_s^{sp} is the specific component of the surface free energy.

$$\gamma_s = \gamma_s^d + \gamma_s^{sp}$$

Figure 2.11: Surface energy of filler

Specific interaction measure the filler-filler interactions (hydrogen bonding, polar and acid-base interactions), whilst non-specific such as van der Waals interactions are dispersive interactions between rubber and filler. A lower γ_s^d and a higher γ_s^{sp} of the surface energies of silica would result in low filler-rubber interaction and strong agglomeration of silica in the rubber (filler-filler interaction), respectively. These

resulted in higher viscosity of silica-filled rubber compounds, higher hardness and higher low strain-moduli of the vulcanizates. In contrast, the higher γ_s^d of carbon black gives strong filler-rubber interaction (Wolff & Wang, 1992).

Crosslinking reaction between XNBR and precipitated silica at 50 phr as studied by Bandyopadhyay et al. (1996c), resulted in an increase in Δ torque which was attributed to the reaction between the –COOH groups of the XNBR and the silanol groups of silica. Other evidence showed that by heating the silica at 800 ^oC for 4 h, in order to condense the silanol groups to form siloxane linkages, has not formed any appreciable amount of bound rubber and there was no significant increase in Δ torque. Thus decrease in silanol groups has reduced the extent of the rubber-silica interaction. Incorporation of silane coupling agent, APTS, has further increased Δ torque and bound rubber value of XNBR-silane-silica compound, as a result of silica reacting with the silane, and subsequently reacting with the –COOH groups of the XNBR. Furthermore, the tensile strength, modulus and tear strength were higher compared to those without coupling agent.

The active epoxy group of ENR has attracted Varughese and Tripathy (1992) to study the interaction mechanism between ENR50 and silica without conventional crosslinking agents. Cure characteristics of ENR50 mixed with 50 phr silica was studied on the Monsanto rheometer at 180 ^oC for 1 h, resulting in a slight increase in torque (~10 dN m), but heating the silica before mixing decreased the torque by 3 units, indicating crosslinking was formed through silanol groups. These findings have then captured the interest of Manna et al. (1999) to study the bonding between precipitated silica and ENR50 in the presence of N-3(N-vinyl benzyl amino) ethyl-γ-amino propyl trimethoxy silane mono hydrogen chloride and then compared with sulfur vulcanization system. When ENR was mixed with 60 phr silica, similar M_H value (10.8 dN m) was

reported. FTIR studies showed that chemical crosslinks was formed between silanol groups of silica and ENR through formation of Si–O–C linkages. The proposed reaction mechanism is shown in Figure 2.12. Incorporating silane coupling agent (5 phr) in silica-filled ENR50 has significantly increased the M_H to 20.8 dN m. Addition of silane coupling agent formed C–N bond between epoxy group of ENR and amine groups of the silane, whereas trimethoxy silane reacted with silanol groups on the silica, leading to silyl ether linkages. However, sulfur-cured ENR50 filled with the same amount of silica exhibited greater extent of crosslinking as revealed from the higher M_H (27.1 dN m), and addition of silane at 5 phr had little effect on the value (29.0 dN m), indicating coupling agent did not participate in sulfur vulcanization of silica-filled ENR50 at 150 ^oC.

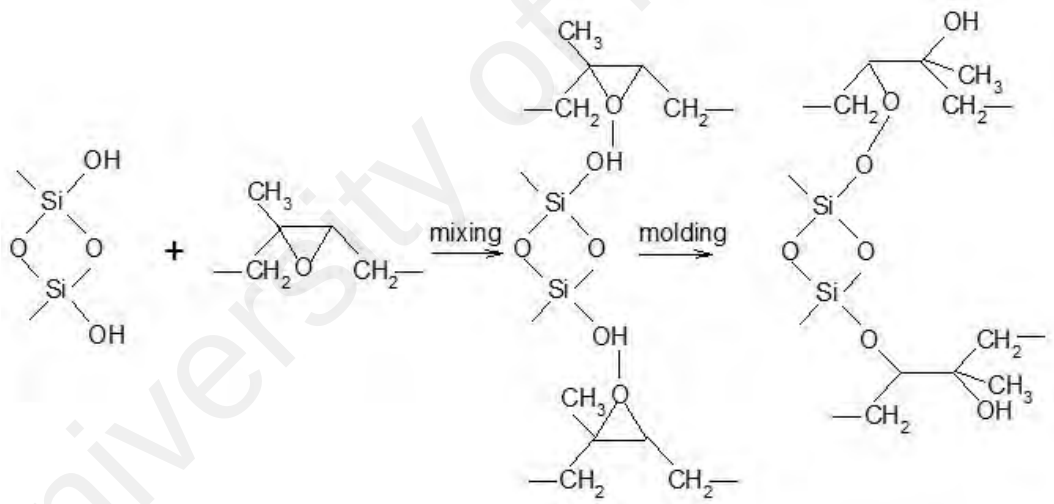

Figure 2.12: Proposed reaction mechanism between ENR and silica. Reproduced from Manna et al. © 1999 John Wiley & Sons, Inc.

Another findings by the same groups (Manna et al., 2002) revealed that increasing molding time from 2 min to 60 min at 180 ^oC, led to the increase in T_g from -3.1 to -1.2 ^oC, showing chemical crosslinks was formed between ENR chains and silica surface. Incorporation of silane coupling agent has shifted the T_g to higher temperature, but

adding silane up to 10 phr decreased the T_g, attributed to the plasticizing effect of the unreacted coupling agent.

2.4.4 Summary

From the work listed above, it is apparent that the presence of surface silanol groups of precipitated silica contributes to the crosslinking in ENR. Despite the fact that precipitated amorphous silica has been known for a long time and typically used in rubber compound, this study focuses on the high purity amorphous silica produced from rice husk.

2.5 Rice husk

Rice is one of the major food crops in many regions of the world. Global paddy production was approximately 744 million tons in 2014 (FAO, 2014) with Malaysia contributing about 2.6 million tons (FAO, 2015). Rice husk, the outer covering of the rice grain is removed from paddy during the milling process. It is one of the by-products of rice that represents 20 % of the total production of rice. Although rice husk is generated in all rice producing countries, the composition of rice husk differs from region to region. This is reported to be due to the crop year, paddy types, geographic location, soil chemistry, and fertilizer used (Chandrasekhar et al., 2003). Generally, rice husk consists of 75 – 90 % organic materials such as celluloses and lignin. The average compositions of rice husk are given in Table 2.3.

Table 2.3: Composition of rice husk

Compositions	Weight %
Cellulose	35
Hemicellulose	25
Lignin	20
Ash	17
Crude Protein	3

Source: Ugheoke and Mamat (2012).

Rice husk is an abundantly available agricultural waste material, thus it creates disposal problems and environmental pollution. Furthermore, rice husk is tough, high abrasive character, low nutritional value, low bulk density (~100 kg/m^3) and resistant to degradation due to its high lignin and silica content which subsequently limits the direct use of rice husk.

2.5.1 Uses of rice husk

Direct use of rice husk has been seen in admixture of poultry feed (Aggarwal, 2003, March 12) and widely used as a fuel in rice parboiling boilers to generate steams (Ahiduzzaman, 2007; Sadrul Islam & Ahiduzzaman, 2013). It is also an alternative fuel for household energy replacing wood fuel (Assureira, 2002, June 11). Kumar et al. (2012) has reviewed various applications of rice husk. The organic materials of rice husk could be used to produce xylose ($C_5H_{10}O_5$), furfural ($C_5H_4O_2$), xylitol, ethanol, acetic acid and lignosulphonic acid, with a subsequent use as cleaning agent in metal and machine industries.

Rice husk has also been used as filler in plastics such as polypropylene (Sun & Gong, 2001) and polystyrene (Rozman et al., 2000). Rice husk can act as a fibre to reinforce the plastics. However, chemical modification of the rice husk is necessary to

impart the mechanical properties of the composites, due to the polar character of rice husk which provides incompatibility with most polymer matrices.

2.5.2 Silica in rice husk ash

Combustion of rice husk produces 17 – 20 % of rice husk ash which contains >90 % silica and small amount of metallic impurities. Depending on the combustion temperature, silica (SiO_2) in rice husk ash could be in the form of both amorphous and crystalline. Numerous studies (Chakraverty et al., 1988; Hamad & Khattab, 1981) have reported that amorphous silica was generated at temperatures above 500 ^{o}C and it depends on the combustion time. Increasing combustion temperatures beyond 700 ^{o}C could lead to crystallization of amorphous silica to cristobalite and tridymite forms. However, the crystalline silica forms such as cristobalite and quartz have been pointed to pose carcinogenic risks to humans (Borm et al., 2011).

2.5.3 Pre-treatment effects on silica production

High purity silica with white color could be produced by controlling the combustion conditions (temperature and time) and treatments of rice husk with various chemicals. Utilization of rice husk ash as a source of high purity silica is based on the removal of metallic impurities such as sodium (Na), potassium (K), magnesium (Mg), calcium (Ca), manganese (Mn), and iron (Fe), as well as black particles of unburned carbon. Several attempts are made either by pre-treatments of rice husk or post-treatments of rice husk ash with various chemicals to remove or reduce these metallic impurities. It was claimed that pre-treatments of rice husk before combustion is more advantageous (Yalcin & Sevinc, 2001).

Pre-treatment of rice husk by leaching with dilute mineral acids such as nitric, hydrochloric and sulfuric acids of varying concentrations have been employed

(Chakraverty et al., 1985; Rahman et al., 1997). Investigation by Krishnarao et al. (2001) revealed potassium has caused black particles in the silica. The presence of potassium has accelerated carbon fixation in the rice husk ash due to surface melting of silica. It was further reported by the same researchers that pre-treatment of the rice husk with hydrochloric acid before combustion could produce white silica, attributed to the removal of metallic impurities including potassium during acid leaching. However, dilute mineral acids have caused significant hazards to the environment and human life and also has increased the processing cost. Thus organic acid treatments such as oxalic, citric and malic acids have been suggested (Chandrasekhar et al., 2005; Olawale et al., 2012; Umeda et al., 2007) . Pre-treatment of the rice husk with alkalis such as sodium hydroxide (NaOH) and ammonium hydroxide (NH_4OH) solutions have also been researched (Conradt et al., 1992; Patel et al., 1987). Comparisons between alkali solutions, organic and mineral acids used in the pre-treatment of the rice husk revealed that hydrochloric acid was the most effective in removing metallic impurities with the production of white color silica (Chakraverty et al., 1988). Although leaching of the rice husk influence its chemical composition, it does not transform amorphous silica into crystalline form.

2.5.4 Properties of amorphous silica

Properties of silica are largely dependent on the pre-treatment of the rice husk and combustion conditions. The properties such as structure, reactivity, whiteness, surface area and porosity render it suitable for applications.

2.5.4.1 Structure

The structure of silica is often investigated using X-ray diffractometer. A broad, diffused peaks of X-ray diffraction (XRD), with maximum intensity at about $2\theta = 21.8^{o}$ revealed a single phase amorphous silica. The amorphous nature of silica could be

obtainable from the combustion of rice husk at temperature below 700 ^{o}C (Hamdan et al., 1997). Other researchers (Chandrasekhar et al., 2006; Kapur, 1985) reported that combustion of rice husk above 900 ^{o}C resulted in crystallization of amorphous silica to cristobalite and tridymite.

2.5.4.2 Chemical reactivity and whiteness

Reacting the silica with saturated slaked lime, $Ca(OH)_2$ solution could determine the chemical reactivity of silica. The work of Rao et al. (1989) found that the maximum reactivity of silica was achieved at combustion temperature between 400 and 600 ^{o}C and combustion time from 6 to 12 h. Further increase in combustion temperature and time led to the formation of cristobalite and consequently reduced the silica reactivity. Extensive studies carried out by Chandrasekhar et al. (2006) revealed that the chemical reactivity and whiteness of silica could be enhanced with pre-treatment of rice husk. The lime reactivity increased from 34 mg CaO/g to 120 mg CaO/g after leaching the rice husk with dilute hydrochloric acid, followed by combustion at 600 ^{o}C for 2 h.

2.5.4.3 Surface area and porosity

In the work of Real et al. (1996), pre-treatment of rice husk with hydrochloric acid before combustion at 600 ^{o}C produced pure silica (~99.5 %) with approximately 260 m^2/g specific surface area. Following post-treatment of the pure silica with hydrochloric acid decreased the surface area to 1 m^2/g with similar purity. Combustion of hydrochloric acid-leached rice husk at 800 ^{o}C has maintained the surface area of silica. Another work by Kapur (1985) described that the surface area of silica has increased from 60 m^2/g to 80 m^2/g with increasing combustion temperature of un-leached rice husk from 350 ^{o}C to 600 ^{o}C, respectively. Nevertheless, the silica surface area was reduced from 40 m^2/g to 1 m^2/g upon combustion of the rice husk between 700 to 900 ^{o}C due to the presence of alkali metals.

Liou (2004b) studied the combustion of hydrochloric acid-leached rice husk at heating rates, ranging from 5 to 20 K/min. The amounts of metallic impurities were found lower with the highest purity silica obtained at 5 K/min compared to other heating rates, resulting in highly porous silica and larger BET surface area. On the other hand, the silica surface area was significantly smaller without leaching the rice husk, attributed to the metallic impurities that promote the structural changes of the silica during combustion (Conradt et al., 1992).

2.5.5 Applications of silica from rice husk ash

Rice husk ash with high silica content (> 85 % SiO_2) has wide variety of uses and many more potential applications. Rice husk ash has been utilized as a source of amorphous silica which some of the uses are discussed below.

2.5.5.1 In the production of silicon-based materials

Rice husk ash has been used in the production of silicon-based materials including silica, silicon tetrachloride ($SiCl_4$), silicon carbide (SiC), silicon nitride (Si_3N_4) and zeolite. The specific properties of silica will determine each application. Amorphous silica with large surface area, high porosity and high purity combined with precursor gel at constrained composition (SiO_2/Al_2O_3 molar ratio), improves the dissolution of silicate and aluminate species. Consequently, the nucleation and crystallization rate, and stability of ZSM-5 zeolite has thermodynamically sped up (Panpa & Jinawath, 2009).

The high purity mixture of carbon and silica (C/SiO_2) powder could be produced after acid leaching of the rice husk, followed by high temperature combustion in a non-oxidizing atmosphere. The C/SiO_2 has been utilized as a starting material in the production of silicon tetrachloride ($SiCl_4$) (Chen & Chang, 1991), silicon nitride (Si_3N_4) and silicon carbide (SiC) (Liou, 2004a; Liou et al., 1997). These high quality ceramic

powders of Si_3N_4 and SiC find application in turbine engines, whereas $SiCl_4$ in the production of silicon esters, silicone polymers, organosilicon halides, organosilicates and solar-grade Si.

2.5.5.2 As an adsorbent and catalyst support

Recently, rice husk ash has been successfully used as adsorbents in water and wastewater treatment (Ahmaruzzaman & Gupta, 2011). Although treatment processes that include chemical precipitation, reverse osmosis, ion exchange, ozonation, solvents extraction, oxidation/reduction, coagulation, irradiation, photochemical, electrochemical, membrane filtration and adsorption are existing technologies for the removal of pesticides, dyes, heavy metals and other organic pollutants from wastewaters, these processes have few drawbacks. Amongst the technologies, adsorption process has attracted many researchers due to its easy operation and handling, sludge free operation and regeneration capacity. Thus various agricultural wastes including rice husk ash has been researched as adsorbents for removal of various contaminants. Besides being utilized as an absorbent, rice husk ash is used as a catalyst support in fine chemical synthesis because of its high purity, small particle size and large surface area of the amorphous silica (Adam et al., 2006; Chang et al., 2006; Tsay & Chang, 2000).

2.5.5.3 As a filler

Silica in rice husk ash has potential application as filler in cement, plastic and rubber. It has been classified as 'highly active pozzolans' due to its similar properties to those of condensed silica fumed and thus suitable for use as filler in Portland cement, mortar and concrete. Incorporation of rice husk ash in both the mortar and concrete has increased the compressive strength (Kilinçkale, 1997; Zhang & Malhotra, 1996), but it has no significant effect on the compressive strength of the cement (Ajiwe et al., 2000;

Zhang et al., 1996). Work by Chandrasekhar et al. (2002) revealed that microsilica from rice husk ash has potential in substituting condensed silica fumed for high performance concrete. The lime reactivity of rice husk ash pertaining to silica content, large surface area with ultrafine particle size and amorphous structure was found superior compared to the commercially available microsilicas.

Incorporation of rice husk ash filler in plastic such as polypropylene has been extensively studied by Fuad et al. (1993). Increasing filler content has decreased the impact strength, tensile strength and elongation at break, whereas the density and flexural modulus increased. The poor interfacial adhesion between filler and polypropylene could be the caused in the reduction of strengths (Fuad et al., 1995) Thus the effect of surface modifiers including titanate, zirconate and silane coupling agents has been attempted by the same researchers to enhance the silica-filled polypropylene properties. Amongst these coupling agents, silane showed better effect in improving mechanical properties of silica-filled polypropylene (Fuad et al., 1995).

In addition, rice husk ash could also be incorporated in rubber. Haxo and Mehta (1975) revealed that rice husk ash could be used as reinforcing filler in ethylene-propylene-diene rubber (EPDM), styrene-butadiene rubber (SBR), nitrile butadiene rubber (NBR), neoprene, butyl rubber and NR. Studies has also indicated a potential use of rice husk ash as filler in ENR cured by semi-EV sulfur formulation (Ishak & Bakar, 1995; Ismail et al., 1997) with white rice husk ash (>95 % SiO_2) showing better properties compared to black rice husk ash (~54 % SiO_2). In comparison with commercial fillers at similar loading of 20 phr, the physical properties including tensile strength, modulus at 100 % and 300 % strain, and hardness of the ENR50 filled with precipitated silica and carbon black were better than those of rice husk ash-filled ENR vulcanizates. Supporting evidence from SEM studies disclosed that larger particle sizes

hence smaller surface area and filler agglomeration in the vulcanizate have contributed to the reduction in properties due to poor filler-rubber interactions. However, the properties of rice husk ash-filled ENR was further improved by the addition of silane coupling agent (Ismail et al., 1997; Nasir et al., 1989); this is attributed to the chemical bonding between the silane coupling agent and both the rice husk ash and the ENR.

2.5.6 Summary

From the work discussed above, it shows that amorphous silica could be produced after combustion of rice husk at temperature above 500 ^{o}C, whereas high purity silica could be obtained after pre-treatment of the rice husk with mineral acid, prior to the combustion. The pure form of silica gives better properties in rubber vulcanizates compared to that of impure silica. Thus the current work involves production of high purity amorphous silica from rice husk that has been leached with dilute hydrochloric and sulfuric acids. In the next chapter, the experimental work carried out in this study is given in details.

CHAPTER 3: MATERIALS AND METHODS

3.1 Introduction

This chapter focuses on the experimental work for preparation of high purity amorphous silica from rice husk and samples of ENR50 mixed with fumaric acid and silica. Samples of ENR50 mixed with silica and semi-EV sulfur formulation were also prepared. Further, these samples were analyzed and characterized before and after curing at elevated temperature.

3.2 Characterizations of silica

Experimental study was conducted by leaching the rice husk with mineral acids, followed by combustion of rice husk at various temperatures to determine the conditions to produce pure form of silica. The properties of silica were then characterized.

3.2.1 Materials

Rice husk was obtained from BERNAS rice mill (Selangor, Malaysia). Hydrochloric acid (HCl), sodium dodecyl sulfate and potassium bromide (KBr) powder were purchased from Merck (Germany) and sulfuric acid (H_2SO_4), from R&M Chemicals (Malaysia).

3.2.2 Methods

Two mineral acids, namely hydrochloric acid and sulfuric acid were diluted accordingly and used in the pre-treatment of rice husk. Subsequently, combustion of un-leached rice husk and acid-leached rice husk were performed in a muffle furnace.

3.2.2.1 Preparation of chemical reagents

(a) ***Preparation of 1.0 M hydrochloric acid solution***

1.0 M of hydrochloric solution (37 % HCl, ρ 1.19 g/ml, M_w 36.46 g/mol) was prepared by slowly adding 82.12 mL of 37 % HCl into 250 mL of distilled water in 1.0

L volumetric flask. The final volume of solution was adjusted to 1000 mL with distilled water.

(b) ***Preparation of 0.5 M sulfuric acid solution***

0.5 M of sulfuric solution (30 % H_2SO_4, ρ 1.84 g/ml, M_w 98.08 g/mol) was prepared by slowly adding 88.84 mL of 30 % H_2SO_4 into 250 mL of distilled water in 1.0 L volumetric flask. The final volume of solution was adjusted to 1000 mL with distilled water.

(c) ***Preparation of 1 wt % sodium dodecyl sulfate solution***

A solution of 1 wt % sodium dodecyl sulfate was prepared by dissolving 10 g of sodium dodecyl sulfate in 1000 mL distilled water.

3.2.2.2 Production of silica from rice husk

The rice husk (~500 g) was washed with 1 wt % sodium dodecyl sulfate aqueous solution for 10 min to remove dirt and water soluble impurities, followed by rinsing with distilled water to remove the surfactant. The washed rice husk was left to air dry at ambient temperature for 3 h and later dried in an air-oven at 110 ^oC for 24 h. The washed rice husk obtained was designated as un-leached rice husk. Another sample of the washed rice husk were separately treated with 1.0 M dilute hydrochloric acid or 0.5 M dilute sulfuric acid at 60 ^oC for 30 min with constant stirring. After the acidic solution was drained off, the rice husk was rinsed with distilled water until free from acid, filtered and dried in an air-oven at 110 ^oC for 24 h. The un-leached rice husk and acid-leached rice husk were placed in a muffle furnace and heated at 600, 700, 800 and 900 ^oC for 2 h to produce the samples (each ~25 g) of silica.

3.2.3 Analyses of rice husk

The samples of un-leached and acid-leached rice husks were analyzed using thermogravimetric (TGA) analyzer and scanning electron microscope (SEM).

3.2.3.1 Thermogravimetric Analysis (TGA)

TGA was used to study the thermal decomposition of organic components in rice husk. The thermogram from TGA is usually plotted in weight percentage against temperature.

TGA measurement was performed on a TGA6 analyzer (Perkin Elmer). A sample of 5 – 7 mg was loaded in the ceramic pan and heated at a heating rate of 20 ^{o}C/min from 50 to 850 ^{o}C under nitrogen atmosphere with a flow rate of 20 mL/min.

3.2.3.2 Scanning Electron Microscope (SEM)

The sample was examined using SEM to study the surface morphology of the rice husk. SEM was conducted on a FESEM JSM 6701F (JOEL). The sample was placed onto the specimen stub and coated with platinum evaporative coating under high vacuum. It was operated at 15 kV with 15 mm working distance.

3.2.4 Analytical techniques for characterizing silica properties

After combustion of un-leached and acid-leached rice husks in a muffle furnace at respective temperatures, silica samples were produced. The properties of silica were determined using Fourier Transform Infrared Spectrometer, X-Ray Diffractometer, Zeta Potential and Particle Size Analyzer, X-Ray Fluorescence Spectrometer and surface area and porosity analyzer.

3.2.4.1 Fourier transform infrared (FTIR) spectroscopy

Infrared spectroscopy is a valuable method in structural identification of materials. FTIR is a modern infrared spectrometer, with greater speed and sensitivity compared to dispersive infrared spectrometer (Ferry & Becker, 2004).

The functional groups in silica were examined using KBr pellet method. KBr powder was first dried in an oven at 110 ^{o}C overnight. Silica/KBr powder (1:6) was finely ground and pressed into pellet. Then, Nicolet 6700 FTIR spectrometer (Thermo Scientific) was used to record the infrared spectra with 32 scans at a resolution of 4 cm^{-1} in the range of 4000 – 600 cm^{-1}. A pure KBr pellet was scanned as the background.

3.2.4.2 X-ray diffraction (XRD)

XRD method is a powerful tool used to investigate orderly arrangements of atoms or molecules through the interaction of electromagnetic radiation (Billmeyer, 1984).

The X-ray pattern of silica was obtained using a D8 Discovery X-ray Diffractometer (Bruker) with CuKα operated at 40 kV and 40 mA, and 2Theta between 5^{o} to 50^{o}. EVA™ software was used to record and analyze the structural pattern of the silica.

3.2.4.3 Particle size analysis

Particle sizes of silica were measured using ZetaPlus Zeta Potential Analyzer (Brookhaven Instruments Corporation). Approximately 0.05 g of the silica was dispersed in 10 g distilled water, and then the solution was vigorously mixed and sonicated for 30 min to minimize any particle agglomerates that may have been present in the suspension.

3.2.4.4 X-ray fluorescence (XRF)

XRF is a simple and most economic analytical method used to determine the chemical composition of many types of materials including silica.

The silica content (SiO_2) and metallic impurities were estimated using an Axios^{mAX} Wavelength Dispersive X-Ray Fluorescence Spectrometer (PANalytical).

3.2.4.5 Brunauer-Emmett-Teller (BET) surface area and porosity analysis

BET method was developed in 1938 (Brunauer et al., 1938). The method is based on physical adsorption of a gas on the surface of the solid in which the amount of gas adsorbed at a given pressure allows the surface area to be determined. Barrett-Joyner-Halenda (BJH) method is used to determine pore volume and average pore diameter using adsorption and desorption technique.

The surface area and pore volume of silica were measured by the BET and BJH methods, respectively, according to ASTM D3663-03 by using TriStar II surface area and porosity analyzer (Micromeritics).

3.3 Investigation of the interactions of silica-filled ENR50 with fumaric acid and sulfur vulcanization of silica-filled ENR50

ENR50 was mixed with fumaric acid at ambient temperature, followed by curing at elevated temperature. The reactions between ENR50 and fumaric acid before and after curing were studied. Then, silica was added into ENR50 and fumaric acid compound, where the samples before and after curing were also characterized. Finally, for comparison, sulfur vulcanization of silica-filled ENR50 was prepared and characterized.

3.3.1 Materials

ENR50 containing 50 mol % epoxide group was obtained from Malaysian Rubber Board (Sg Buloh, Malaysia). Fumaric acid and toluene were purchased from Sigma-Aldrich (Switzerland) and Merck (Germany), respectively. The washed rice husk was leached with dilute sulfuric acid (0.5 M) using similar procedure as detailed in Section 3.2.2.2. The sulfuric acid-leached rice husk was placed in a muffle furnace and heated at 600 ^{o}C for 2 h and the silica sample produced was used throughout this work.

Other ingredients were used as received. Sulfur and stearic acid were purchased from Centre West Industrial Supplies Sdn. Bhd. (Malaysia). N-oxydiethylenebenzothiazole-2-sulfenamide (Santocure® MBS) and tetramethylthiuram monosulfide (Perkacit® TMTM) were supplied by Flexsys Co., Ltd. (Belgium). Zinc oxide (ZnO) was obtained by Metacorp Industries Sdn Bhd. (Malaysia).

3.3.2 Methods

Generally, the term 'mixing' in rubber is used for blending or compounding one or more elastomers with additives. Rubber mixing can be done on the two-roll mill, internal mixer or continuous mixer. In this study, ENR50 was mixed with fumaric acid and silica using two-roll mill. Following the mixing process, rubber compound was submitted to molding process.

3.3.2.1 Mixing of ENR50 with fumaric acid

ENR50 (100 g) was masticated on the two roll mill with a nip setting of 0.5 mm for ~30 s before addition of the specified amount of fumaric acid. The ENR50 and fumaric acid were mixed for 5 min. Finally, the compound was passed through the gap of 1.5 mm to produce a sheet.

3.3.2.2 Mixing of ENR50 with fumaric acid and silica

ENR50 (100 g) was masticated on the two roll mill with a nip setting of 0.5 mm for ~30 s before addition of the specified amount of fumaric acid. The ENR50 and fumaric acid were mixed for 2 min, followed by the addition of the specified amount of silica and further mixed for another 3 min. Finally, the compound was passed through the gap of 1.5 mm to produce a sheet.

3.3.2.3 Mixing of ENR50 with silica and semi-EV sulfur formulation

ENR50 (100 g) was masticated for ~30 s, then silica was added and mixed for 1 min on the two roll mill, followed by addition of the specified amount of zinc oxide, stearic acid, sulfur, Santocure® MBS and Perkacit® TMTM and further mixed for another 4 min. Finally, the compound was passed through the gap of 1.5 mm to produce a sheet.

3.3.2.4 Compression molding

Molding process is described as vulcanization or curing of compound and may be done by compression, injection or transfer moldings, depending on the shape, size and overall structure of the desired product (Melotto, 1990).

In this study, the sample for characterizations and physical properties determinations was prepared in dimension of 120 mm x 150 mm x 2 mm by compression molding at 160 ^{o}C to the respective optimum cure time (t_{90}) or otherwise stated in the text, in an electrically heated hydraulic press under a pressure of 10 MPa.

3.3.3 Characterizations of sample

After mixing, the cure characteristic of compound was measured by Monsanto rheometer. Further, the sample was characterized before and after molding using FTIR spectrometer, solvent swelling test and differential scanning calorimeter (DSC). The

physical properties of the sample including tensile strength, modulus, elongation at break and hardness were determined according to ISO standard test method.

3.3.3.1 Cure characteristic using Monsanto rheometer

Cure meter is utilized to measure the vulcanization or cure characteristic of rubber compound. It has been extensively used to control the uniformity and quality of rubber compound in the factory. Vulcanization is measured by increase in the torque required to maintain given amplitude of oscillation at a given temperature. The torque is automatically plotted against time, in which the increase in torque is proportional to the number of crosslinks formed per unit volume of rubber (Coran, 2005).

Cure characteristic of the compound was measured by MDR2000 Monsanto moving die rheometer (Alpha Technologies) (1.66 Hz frequency, ±0.5 ^{o} oscillation amplitude) at the specified temperature and time prior to compression molding. 5 g of the compound was used for each measurement. The optimum cure time (t_{90}), maximum torque (M_H) and minimum torque (M_L) were determined from the cure curve as shown in Figure 3.1.

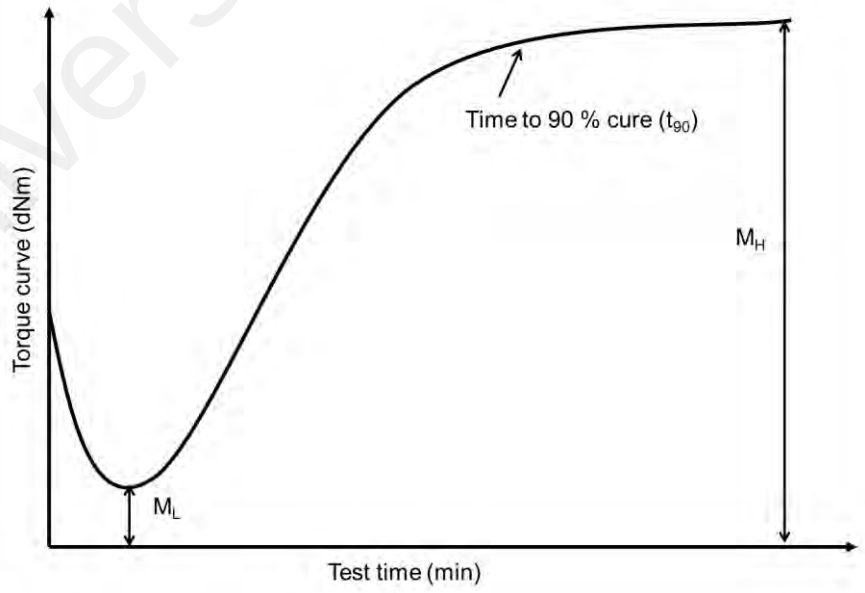

Figure 3.1: Cure meter curve

3.3.3.2 FTIR spectroscopy

The functional groups in the sample were examined by FTIR using the attenuated total reflectance (ATR) accessory. Nicolet 6700 FTIR spectrometer (Thermo Scientific) was used to record the infrared spectra with 32 scans at a resolution of 4 cm^{-1} in the range of 4000 – 600 cm^{-1}.

3.3.3.3 Solvent swelling test

0.4 g of the sample was immersed in 20 mL toluene for 48 h at ambient temperature in a closed glass bottle. The swollen sample was picked by forceps, and excess toluene on the surface of sample was removed by gently wiping with filter paper. The sample was then transferred into a pre-weighed glass bottle (W_a). The weights of swollen sample and glass bottle were recorded as W_1. The sample was dried in vacuum oven at 60 °C overnight and the dried weight was recorded as W_2. The equilibrium swelling percentage of the sample was calculated using (Eqn 3.1), where $W_2 - W_a$ was slightly smaller than the initial sample weight (<10 %), presumably due to a small amount of low molecular weight fraction of the sample being dissolved into toluene during the immersion of the sample in toluene for 48 h.

$$\text{Swelling (\%)} = \frac{W_1 - W_2}{W_2 - W_a} \, x \, 100$$

(Eqn 3.1)

3.3.3.4 Crosslink density *via* Flory-Rehner equation

The equilibrium degree of swelling for a swollen rubber network is related to the physical effective crosslink density, η_{phys} and thus, Flory-Rehner equation (Flory & Rehner, 1943) was employed to determine the crosslink density of the sample, as shown in (Eqn 3.2):

$$-\ln(1 - V_r) - V_r - \chi V_r^2 = 2\rho V_o \eta_{phys} V_r^{1/3}$$

(Eqn 3.2)

where, V_r is the volume fraction of rubber in swollen gel, V_o is the molar volume of solvent (106.11 mL/mol), χ is the rubber-solvent interaction parameter (0.42) and ρ is the density of rubber. Density of rubber, ρ was determined in accordance to ISO 2781. The test piece of rubber sample was weighed in air and then in water using a balance accurate to 1 mg. ρ is given as follows:

$$\rho = \frac{\text{weight of sample in air (g)}}{\text{weight of sample in air (g)} - \text{weight of sample in water (g)}}$$

(Eqn 3.3)

V_r and ρ were measured experimentally and tabulated in Appendix F. Details of the calculations have been described elsewhere (Lee, 2009).

3.3.3.5 Differential scanning calorimetry (DSC)

DSC measurement was performed on a DSC 822e (Mettler Toledo) instrument that was first calibrated with indium. Approximately 5 – 8 mg of sample was weighed and encapsulated in an aluminium pan. A similar empty pan was used as the reference. T_g was measured over a temperature range of -60 to 100 ^oC at scanning rate of 10 ^oC/min. The sample was scanned twice, and the midpoint temperature of the second transition was taken as the T_g of the sample.

3.3.3.6 Physical properties determination

Tensile tests are commonly practised in laboratory to measure general quality of material and to predict product performance. In this study, tensile properties and hardness of samples were determined in accordance with ISO procedures.

(a) ***Tensile stress-strain properties***

Stress is the force applied to the test piece per unit area of the original cross-section of the test length. Strain is the elongation expressed as a percentage of the original test length. ISO37 outlines method for determining properties including tensile strength, elongation at break and modulus (stress at specified strain).

(i) Tensile strength

Tensile strength is defined as the maximum tensile stress reached in stretching the test piece to breaking point. It was calculated as follow:

$$\text{Tensile strength (MPa)} = \frac{\text{force at break}}{\text{initial cross-sectional area}}\ x\ 100$$

(Eqn 3.4)

(ii) Modulus (stress at specified strain) – The tensile stress in the test length subjected to a given strain, for example modulus at 100 % strain.

(iii) Elongation at break – The percentage tensile strain in the test length at breaking point.

Five dumb-bell test pieces were prepared using the type 2 die as described in Table 3.1 and shown in Figure 3.2. The tensile properties before and after heat aging were measured using an AG-XPlus universal testing machine (Shimadzu), at a crosshead

speed of 500 mm/min with a 1 kN load cell. The average of five measurements was reported.

For heat aging studies, test pieces were placed in an oven and aged at 100 ^{o}C for 7 days. Retention in properties was calculated using (Eqn 3.5):

$$\text{Retention (\%)} = \frac{\text{value after aging}}{\text{value before aging}}\ x\ 100 \qquad \textbf{(Eqn 3.5)}$$

Table 3.1: Dimension of dumb-bell test piece

Dimension		Type 2
A	Overall length (minimum) (mm)	75
B	Width of ends (mm)	12.5±1
C	Length of narrow portion (mm)	25±1
D	Width of narrow portion (mm)	4±0.1
E	Transition radius outside (mm)	8±0.5
F	Transition radius inside (mm)	12.5±1

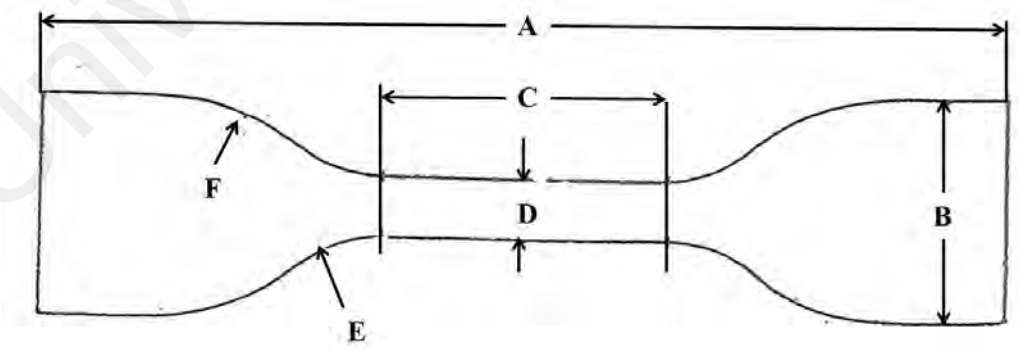

Figure 3.2: Typical dimension of dumb-bell test piece

(b) ***Hardness***

Hardness is a measure of elastic modulus of a rubber by determining its resistance to indentation and is expressed in international rubber hardness degrees (IRHD). ISO48 (Rubber, vulcanized or thermoplastic – Determination of hardness (hardness between 10 IRHD and 100 IRHD) describes the testing procedure. The hardness of test specimen of 8 mm in thickness was measured at five different positions on the sample using Digitest (Bareiss) and average of the value was reported.

Findings from the characterizations and physical properties determinations of the samples will be explicitly discussed in Chapter 4.

CHAPTER 4: RESULTS AND DISCUSSION

4.1 Introduction

In Chapter 4, through analysis of silica properties, the conditions to produce pure form of amorphous silica from rice husk, to be used as filler in rubber compound were established. Before adding silica, reactions between ENR50 and fumaric acid, as crosslinking agent were first investigated. Afterwards, the interactions of silica-filled ENR50 with fumaric acid were studied and further compared with sulfur vulcanization of silica-filled ENR50.

4.2 Properties of silica

Rice husk before and after leaching with 1 M hydrochloric acid and 0.5 M sulfuric acid solutions were conducted for thermal analysis and surface morphology examination, using TGA and SEM, respectively, prior to the combustion. Subsequently, properties of silica samples produced after the combustion were determined.

4.2.1 Analyses of rice husk

Rice husk comprises of organic and inorganic components. As a result of acid leaching, the changes in composition were studied by thermal analysis, whereas the changes in morphology were observed by SEM.

4.2.1.1 Thermal analysis

Rice husk was characterized with TGA in order to quantify its organic and inorganic components. Figure 4.1 shows TGA thermogram of un-leached, hydrochloric acid-leached and sulfuric acid-leached rice husks, which exhibit three stages of weight loss and the results are summarized in Table 4.1. The initial weight loss occurs within the range of 50 – 150 ^{o}C, with a weight loss of 1 – 2 % corresponds to the loss of water and

other volatile substances. The second stage reveals a rapid decomposition starting from 200 to 400 ^{o}C, with a weight loss of 52 – 58 %. This, as reported by Shafizadeh (1968), corresponds to the thermal decomposition of hemicellulose and cellulose, a major organic components in the rice husk. Several researchers (Antal, 1983; Shafizadeh & DeGroot, 1976) revealed hemicellulose decomposes mainly at 150 – 350 ^{o}C, the least stable component of the rice husk and cellulose decompose between 275 – 350 ^{o}C. Table 4.1 shows sulfuric-acid leached rice husk revealed remarkably large mass loss compared to those un-leached and hydrochloric acid-leached rice husks. The combustion of sulfuric acid-leached rice husk was accelerated more rapidly due to the increase of organic components exposed areas.

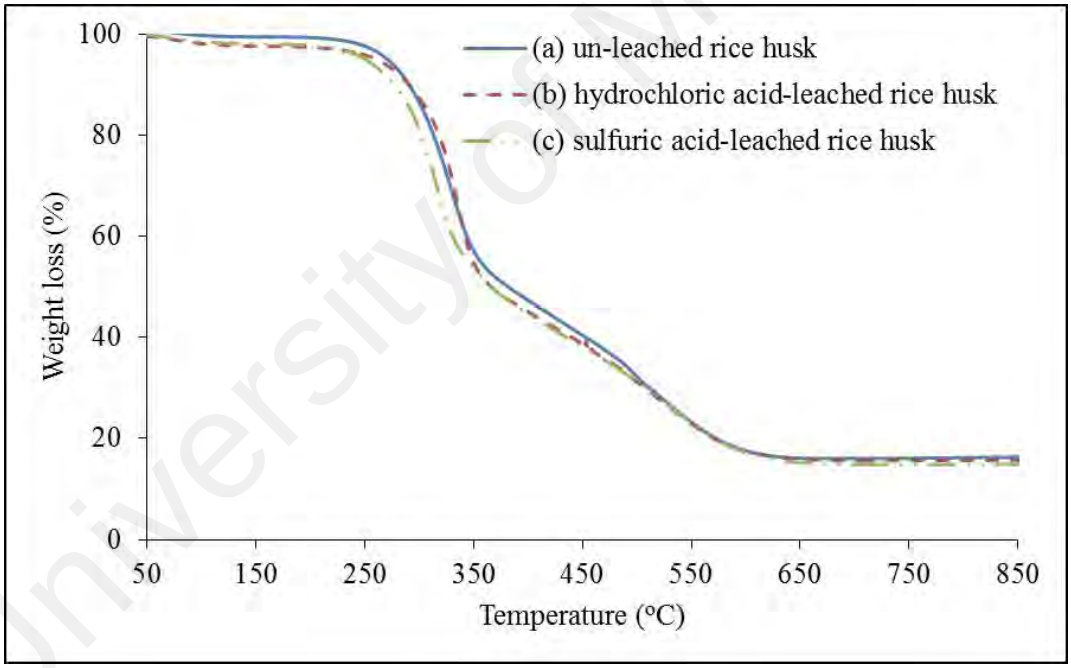

Figure 4.1: TGA curves of (a) un-leached, (b) hydrochloric acid-leached and (c) sulfuric acid-leached rice husks

The third stage of decomposition begins from 400 to 680 ^{o}C and it is characterized by the decomposition of lignin with a weight loss 26 – 31 %, a thermally more stable aromatic polymer. The residual of ash is mainly the non-combustible silica (~16 %,

>600 ^{o}C). TGA results show that the organic and inorganic components are in the range of typical rice husk composition.

Table 4.1: Weight loss (%) of un-leached and acid-leached rice husks

Sample	Weight Loss (%)			Residual weight (%)
	Stage 1	Stage 2	Stage 3	
Un-leached rice husk	1.1	52.3	31.1	16.0
Hydrochloric acid-leached rice husk	1.8	52.4	29.1	15.8
Sulfuric acid-leached rice husk	1.6	57.6	25.5	15.0

4.2.1.2 Surface morphology

Figure 4.2 shows morphology of outer surfaces of un-leached and acid-leached rice husks. The outer surface of rice husk was uneven and highly roughened. After acid leaching, a significant change in rice husk morphology can be seen. The surfaces, particularly the dome-shaped protrusions of un-leached rice husk show greater degree of roughness than those that have been leached with dilute acids, presumably due to the hydrolysis of some organic components by the acids.

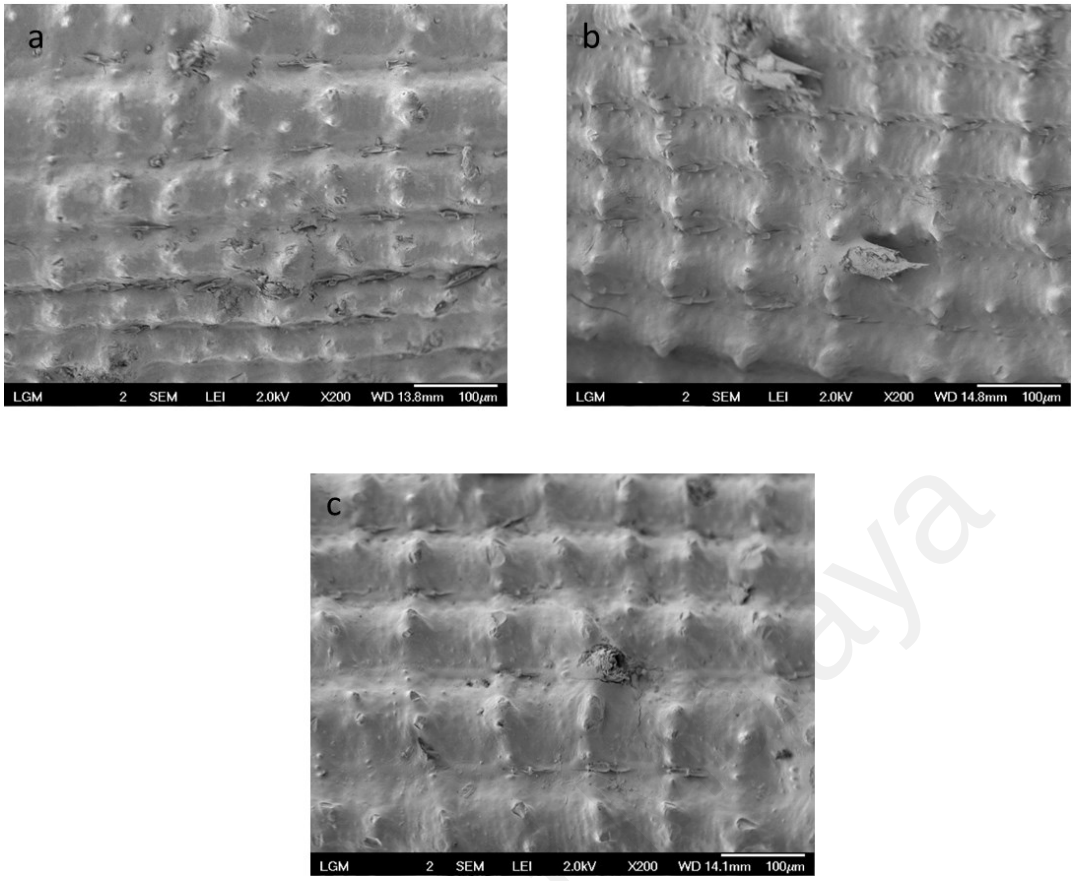

Figure 4.2: Morphology of (a) un-leached, (b) hydrochloric acid-leached and (c) sulfuric acid-leached rice husks

4.2.2 Characterizations of silica

After combustion the un-leached and acid-leached rice husks at 600, 700, 800 and 900 ^{o}C for 2 h, the silica samples were produced and characterized using FTIR spectroscopy, XRD, particle size, XRF and BET surface area analyses.

4.2.2.1 FTIR spectroscopy

FTIR spectra of silica produced from un-leached and acid-leached rice husks after combustion at 600 ^{o}C are shown in Figure 4.3. The spectra of silica at other combustion temperatures of 700, 800 and 900 ^{o}C are shown in Appendix A.1, A.2 and A.3, respectively. As expected, the spectra appear identical, with the notable absorbance peaks at 1094 and 804 cm^{-1} corresponding to O-Si-O asymmetric and symmetric stretching, respectively. The broad absorbance peak at 3200 – 3600 cm^{-1} corresponds to

the surface hydroxyl groups of the silica and the chemically adsorbed water, whereas the peak at 1640 cm^{-1} is attributed to the bending vibration of water molecules.

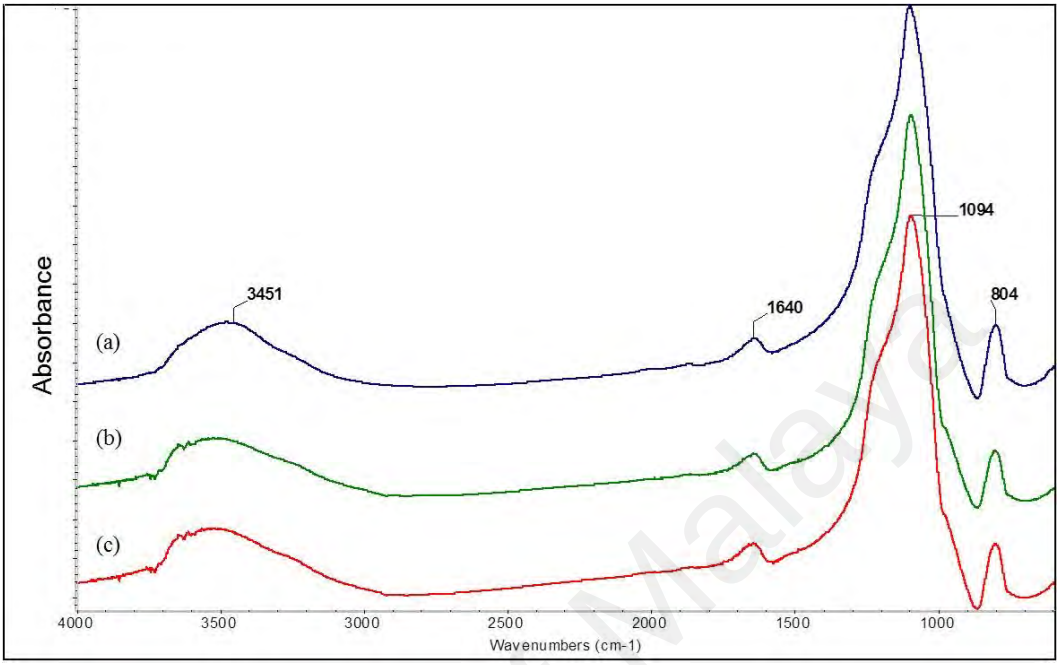

Figure 4.3: FTIR spectra of silica produced from (a) un-leached, (b) hydrochloric acid-leached and (c) sulfuric acid-leached rice husks at 600 ^{o}C for 2 h

4.2.2.2 XRD analysis

XRD patterns of silica produced from un-leached, hydrochloric acid-leached and sulfuric acid-leached rice husks at various combustion temperatures are similar to each other, as shown in Figure 4.4 (A), (B) and (C). The broad diffused peaks with maximum intensity at $2\theta = 22^{o}$ and the absence of sharp peaks in the patterns, confirm the amorphous nature of the silica. However, the sharpness of this peak increases with combustion temperatures for silica produced from un-leached rice husk (Figure 4.4 A), indicating the crystallization transformation of silica starts to occur at 900 ^{o}C. On the other hand, silica produced from acid-leached rice husks show completely amorphous structures upon combustion below 900 ^{o}C, due to the removal of alkali metals during acid-leaching, which hinders eutectic reaction with silica (Venezia et al., 2001).

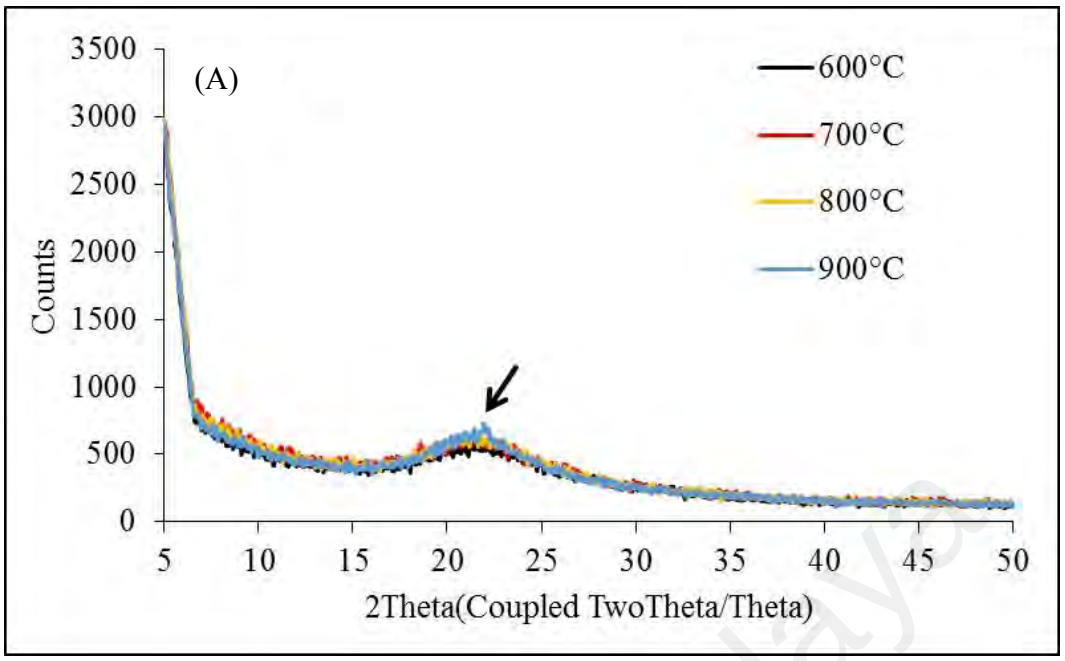

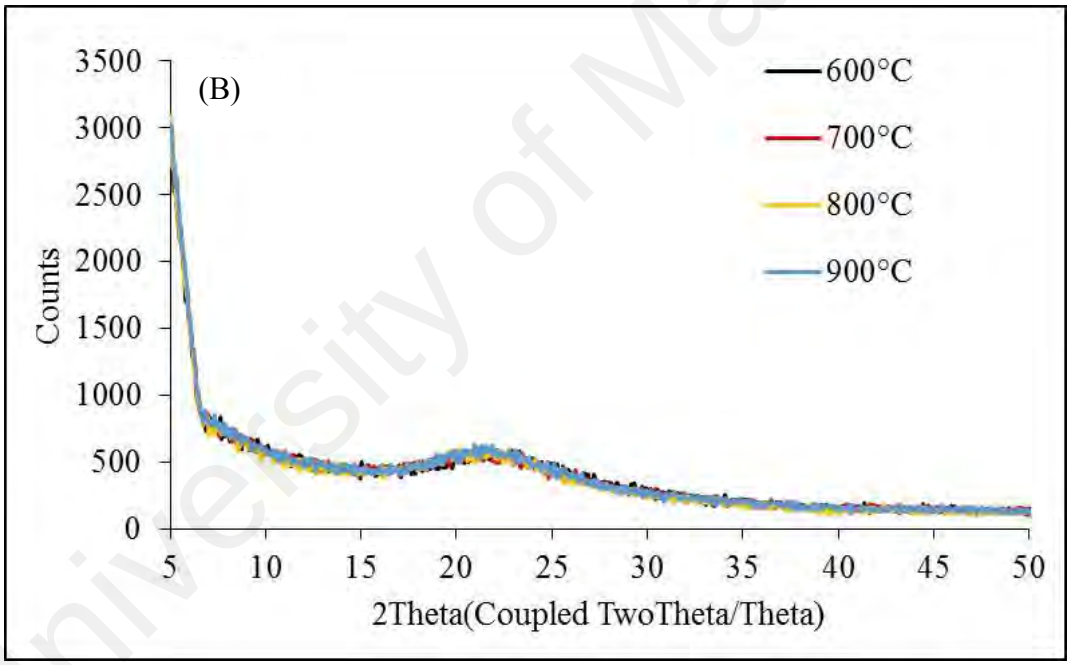

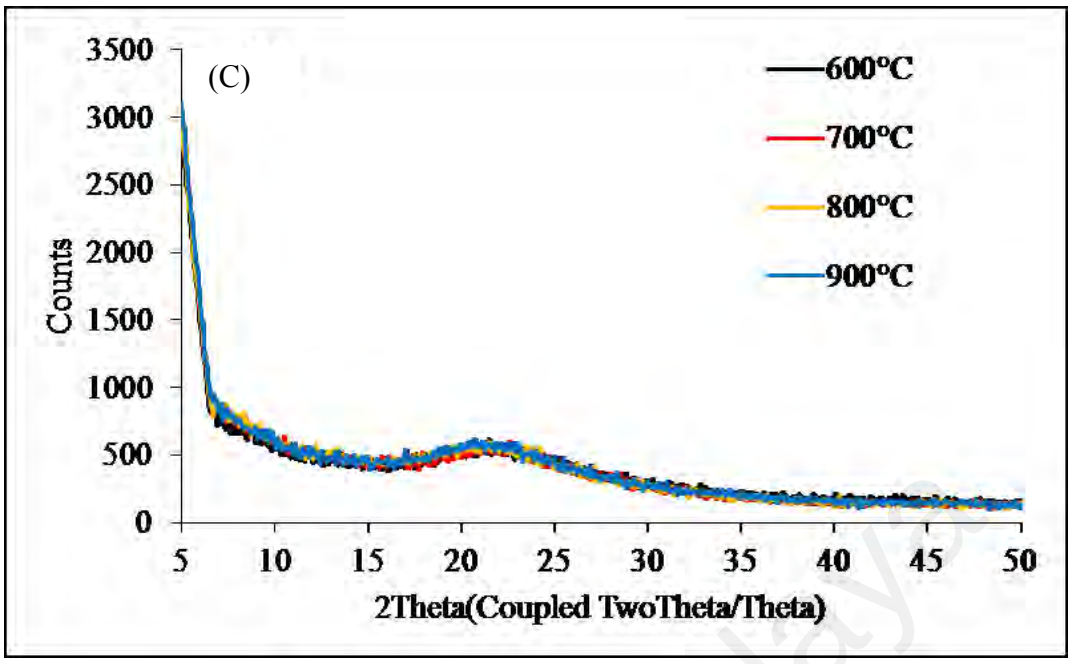

Figure 4.4: XRD patterns of silica produced from (A) un-leached, (B) hydrochloric acid-leached and (C) sulfuric acid-leached rice husks

4.2.2.3 Particle size analysis

The average particle size of silica at various combustion temperatures are given in Table 4.2. It varied from 0.50 to 0.70 µm and had no significant change between combustion temperatures investigated.

Table 4.2: Average particle size of silica produced from un-leached, hydrochloric acid-leached and sulfuric acid-leached rice husks

Sample / ^{o}C	600	700	800	900
Silica from un-leached rice husk	0.53	0.64	0.59	0.60
Silica from hydrochloric acid-leached rice husk	0.52	0.43	0.57	0.72
Silica from sulfuric acid-leached rice husk	0.49	0.52	0.69	0.74

Since the properties of silica revealed by FTIR spectroscopy, XRD and particle size analysis after combustion at 600, 700, 800 and 900 ^{o}C were comparable, thus only the

properties of silica after combustion at 600 ^{o}C were further characterized by XRF and BET surface area and porosity analysis.

4.2.2.4 XRF analysis

XRF analysis was employed to identify the chemical compositions as well as level of purity of silica produced from rice husk. Table 4.3 reveals the high purity of silica, with >95 % SiO_2 being produced from the rice husk after combustion. Leaching of the rice husk with dilute hydrochloric acid and dilute sulfuric acid significantly reduced the amount of metallic impurities in rice husk, and consequently >99 % SiO_2 was produced.

Table 4.3: Composition of silica produced from un-leached and acid-leached rice husks at 600 ^{o}C for 2 h

Elements as oxide, %	Silica from un-leached rice husk	Silica from hydrochloric acid - leached rice husk	Silica from sulfuric acid-leached rice husk
SiO_2	95.77	99.58	99.08
MgO	0.40	0.02	0.04
Al_2O_3	0.05	0.17	0.61
P_2O_5	0.46	0.11	0.13
SO_3	0.65	0.02	0.05
K_2O	0.62	0.02	0.02
CaO	0.67	0.04	0.05
MnO	0.05	0	0.01
Fe_2O_3	0.05	0.03	0.02
ZnO	0.02	0	0
Cl	0.01	0	0
Na_2O	1.26	0	0
TiO_2	0	0	0
SrO	0	0	0
ZrO_2	0	0	0

4.2.2.5 Surface area and porosity

The surface area, pore volume and pore diameter of silica are shown in Table 4.4. The BET surface area was higher for the silica produced after leaching the rice husk with dilute acids compared with silica produced from un-leached rice husk. Acid leaching had a significant effect on the surface area of the silica. Presumably, acid leaching serves to hydrolyze the hemicellulose and cellulose into smaller compounds that could decompose more readily during the combustion, thereby leading to a more porous structure, as confirmed by the increase in pore volume. The average pore diameters for silica produced from rice husk were in the range of 5 to 7 nm, indicating that the silica produced was mainly mesoporous.

Table 4.4: BET surface area of silica produced from un-leached and acid-leached rice husks at 600 ^{o}C for 2 h

Sample	BET surface area, m^2/g	Total pore volume, cm^3/g	Average pore diameter (4V/A by BET), nm
Silica from un-leached rice husk	116	0.23	7.84
Silica from hydrochloric acid-leached rice husk	218	0.32	5.56
Silica from sulfuric acid-leached rice husk	208	0.31	5.68

4.2.3 Summary

One of the objectives of this study was to prepare high purity amorphous silica from rice husk to be utilized as filler in rubber compound. Amorphous silica of high purity (> 99 %) was produced from the combustion at 600 ^{o}C of rice husk that was leached with dilute sulfuric acid. Subsequently, it was incorporated as filler into ENR50 mixed with fumaric acid.

4.3 Reactions between ENR50 and fumaric acid

Before adding silica as filler in the rubber compounds, the reactions between ENR50 and fumaric acid at various amounts, before and after curing at elevated temperatures were studied through cure characteristic, FTIR spectroscopy, percentage of solvent swelling and T_g measurement. Formulations of the sample are given in Table 4.5.

Table 4.5: Formulation of ENR50 and fumaric acid compound

Sample / Ingredients	ENR50 / parts	Fumaric acid / phr	Ratio $\frac{\text{epoxide}}{\text{-COOH}}$
ENR50	100	-	-
E-FA2	100	2	38.7
E-FA11.5	100	11.5	6.7
E-FA19.5	100	19.5	3.9

4.3.1 Effect of cure temperature

Characterization of the vulcanization process using cure meter such as moving die rheometer is a regular practice in the rubber industry. In this study, cure characteristic related to the curing process of the ENR50 and fumaric acid compound was studied on the Monsanto rheometer at 130, 140, 150, 160, 170 and 180 ^{o}C for 1 h.

4.3.1.1 Cure characteristic by Monsanto rheometer

Figure 4.5 (A), (B) and (C) show cure curves of the samples E-FA2, E-FA11.5 and E-FA19.5 at various cure temperatures, respectively. E-FA2 sample showed a marching increase in torque with increasing cure temperature. Samples of E-FA11.5 and E-FA19.5 showed similar trend, suggesting progressive crosslinking occurred between ENR50 and fumaric acid, but the increase in torque for E-FA2 was much slower than the other two samples. When increasing cure temperatures to 170 ^{o}C and 180 ^{o}C, the

cure curves of E-FA11.5 and E-FA19.5 samples showed a fast initial increase in torque during the first 10 min and followed by a slowing down to a plateau at 20 min. Higher temperature and greater amount of fumaric acid led to a faster curing reaction that reached a plateau curves.

Thus in the following work, cure temperature of 160 ^{o}C was selected with prolonged curing time (3 h) at the rheometer and the effect of amounts of fumaric acid were further investigated.

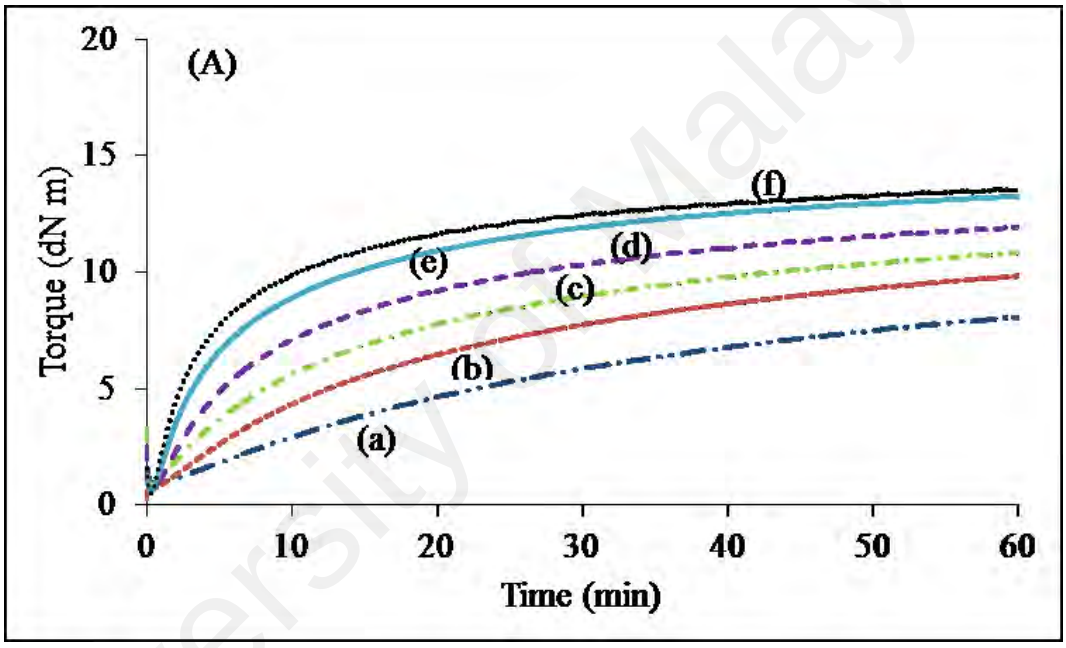

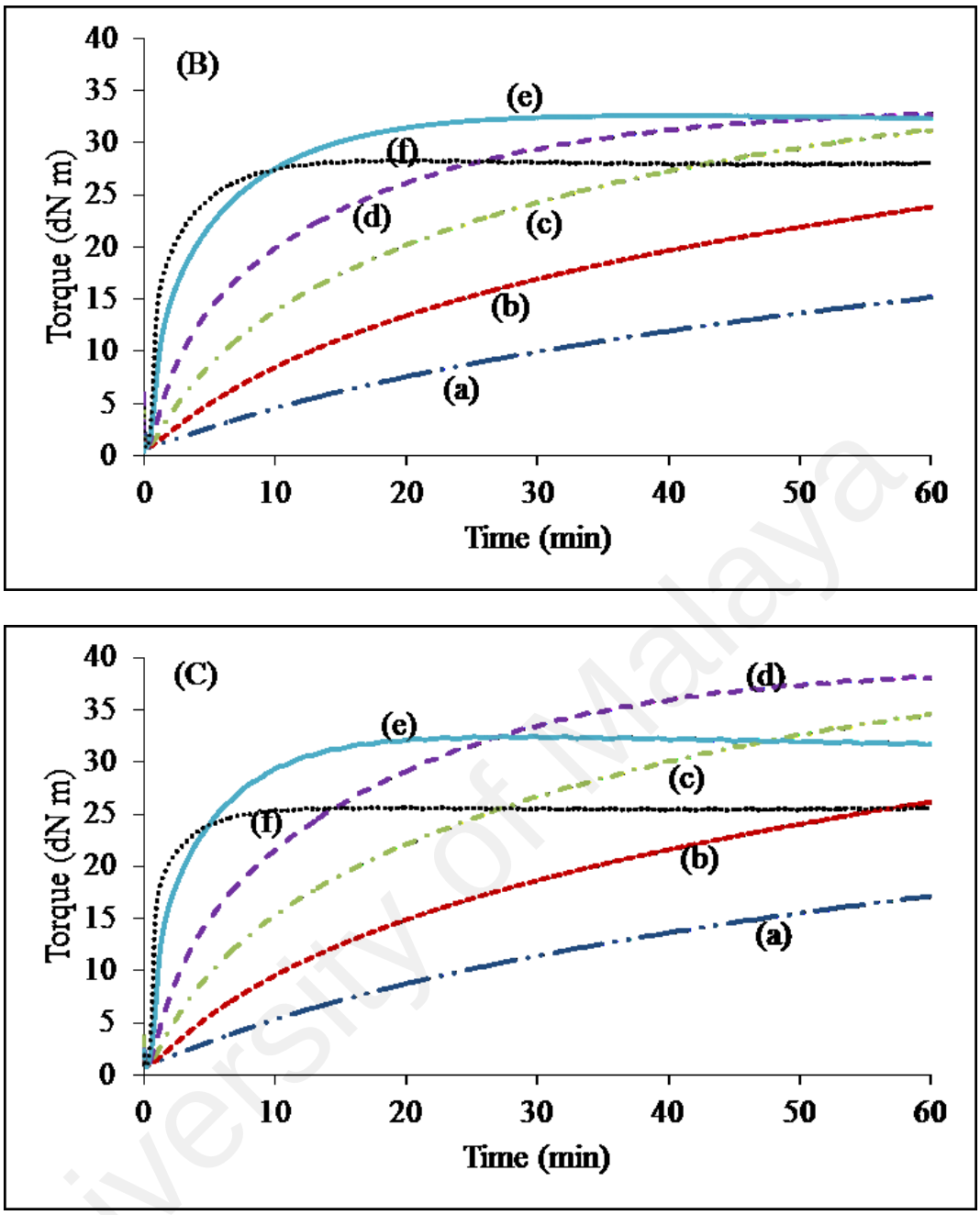

Figure 4.5: Cure curves of (A) E-FA2, (B) E-FA11.5 and (C) E-FA19.5 at (a) 130, (b) 140, (c) 150, (d) 160, (e) 170 and (f) 180 ^{o}C

4.3.2 Effect of amount of fumaric acid

In addition to the cure characteristic, the samples were characterized before and after curing at 160 ^{o}C for 1 h.

4.3.2.1 Cure characteristic by Monsanto rheometer

The cure characteristic of ENR50 mixed with fumaric acid was assessed on the rheometer at 160 ^{o}C, and the results are summarized in Figure 4.6 and Table 4.6. The first curve (curve a) shows no change in torque when ENR50 alone was measured in the rheometer. Addition of 2 phr of fumaric acid (curve b) showed a gradual increase in torque for the first 30 min. As the level of fumaric acid was increased to 11.5 phr (curve c) and 19.5 phr (curve d), there was a faster initial increase in torque during the first 30 min and followed by a slowing down to a plateau at 50 min, reflecting the much faster crosslinking reactions that occurred between ENR50 and fumaric acid. The extent of crosslinking increased with increasing amount of fumaric acid (curves (b-d)).

Furthermore, the maximum torque (M_H) and minimum torque (M_L) increased, whereas optimum cure time (t_{90}) decreased with increasing amount of fumaric acid as shown in Table 4.6. A shorter t_{90} was achieved with greater amount of fumaric acid, thereby leading to a faster cure time.

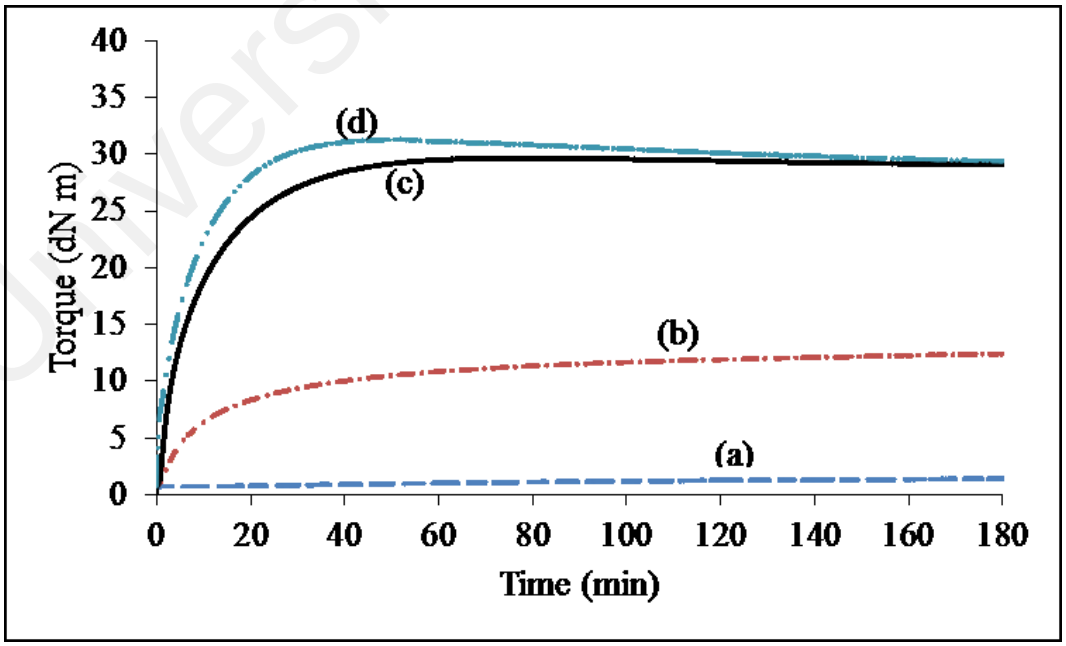

Figure 4.6: Cure curves of (a) ENR50, (b) E-FA2, (c) E-FA11.5 and (d) E-FA19.5 at 160 ^{o}C

Table 4.6: Cure characteristic of samples heated at 160 ^{o}C

Sample	M_H (dN m)	M_L (dN m)	t_{90} (min)
ENR50	1.42	0.72	-
E-FA2	12.02	0.61	75.59
E-FA11.5	28.15	0.74	31.81
E-FA19.5	36.00	0.82	28.79

4.3.2.2 Characterization by FTIR spectroscopy

FTIR spectra of ENR50, fumaric acid and ENR50 mixed with fumaric acid (E-FA2, E-FA11.5 and E-FA19.5 samples) at ambient temperature are shown in Figure 4.7. The spectra exhibit absorbance peaks at 2959, 2856, 1450, 1376, and 836 cm^{-1} that correspond to C-H asymmetrical stretching, C-H symmetrical stretching, C-H asymmetrical bending vibration, C-H symmetrical bending, and =CH wagging, respectively of the *cis*-1,4-polyisoprene in ENR50. The peaks at 878 cm^{-1} and 1251 cm^{-1} are attributed to the epoxide groups in ENR. The spectrum of fumaric acid (e) shows absorbance peak at 1668 cm^{-1} that corresponds to the –C=O groups in conjugation with the C=C bond (Yadav, 2005). The absorbance peaks of ENR50 mixed with fumaric acid (spectra (b - d)) at ambient temperature are similar to each other. But the peak at 1668 cm^{-1} is clearly seen with increasing amount of fumaric acid, suggesting that there no significant reaction has occurred at ambient temperature.

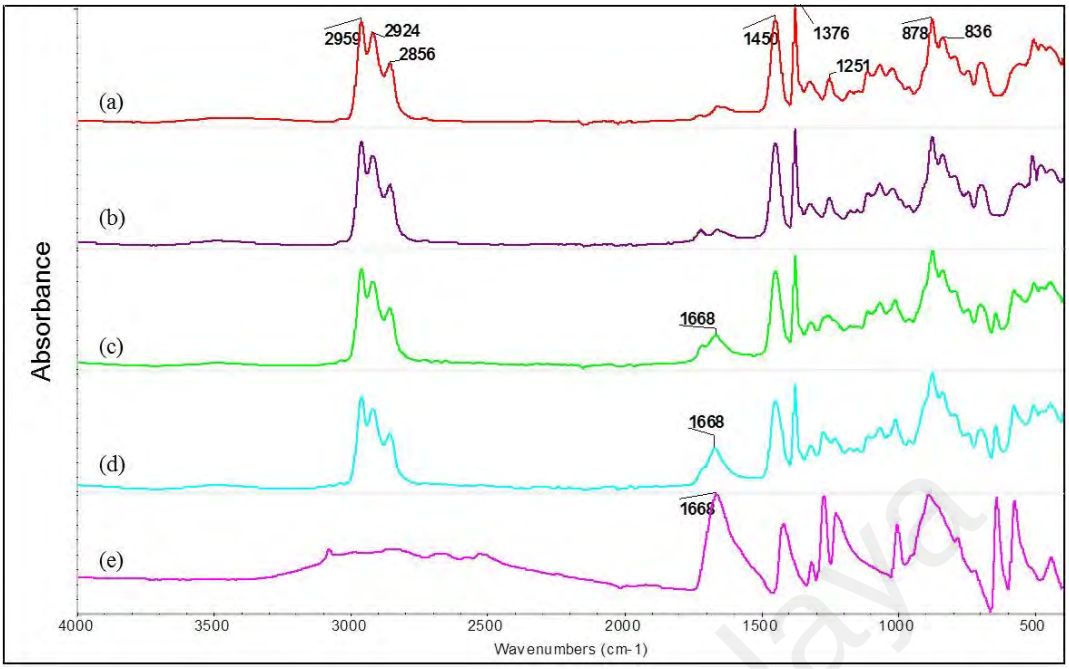

Figure 4.7: FTIR spectra of (a) ENR50, (b) E-FA2, (c) E-FA11.5, (d) E-FA19.5 and (e) fumaric acid, mixed at ambient temperature

FTIR spectra of E-FA2, E-FA11.5 and E-FA19.5 samples after curing or heating at 160 ^{o}C for 1 h are shown in Figure 4.8. The new peak at 3450 cm^{-1} corresponds to –OH stretching, and peaks at 1714 cm^{-1} (C=O stretching) and 1260 cm^{-1} (C–O stretching) corresponds to the ester groups. Other peaks at 1067 cm^{-1} and 1028 cm^{-1} are attributed to C–O stretching of 2^{o} alcohol groups. The –C=O peak of fumaric acid at 1668 cm^{-1} has shifted to 1714 cm^{-1}, suggesting that –COOH group of fumaric acid has converted to ester group *via* ring opening of the epoxide group of ENR50. In contrast, the absorbance peak of epoxide group at 875 cm^{-1} has diminished with increasing amount of fumaric acid, as more epoxide groups are consumed. A new absorbance peak at 897 cm^{-1} corresponds to CH_2 out of plane deformation of vinylidene groups >C=CH_2 (Roychoudhury & De, 1992). Calculations of the absorbance peaks ratio with reference to internal peak at 1450 cm^{-1} are listed in Table 4.7. The peak at 1450 cm^{-1} corresponding to C–H bending of the –CH_2 group is not involved in any reaction. The increase in the absorbance peak ratios of A_{1714}/A_{1450} and A_{3450}/A_{1450} with increasing amounts of fumaric acid suggest that the –COOR and –OH groups are formed during

reaction. Pire et al. (2012) reported the formation of β-hydroxyesters along the rubber chains when ENR was crosslinked with dodecanedioic acid. The plausible crosslinking reaction is shown in Figure 4.9.

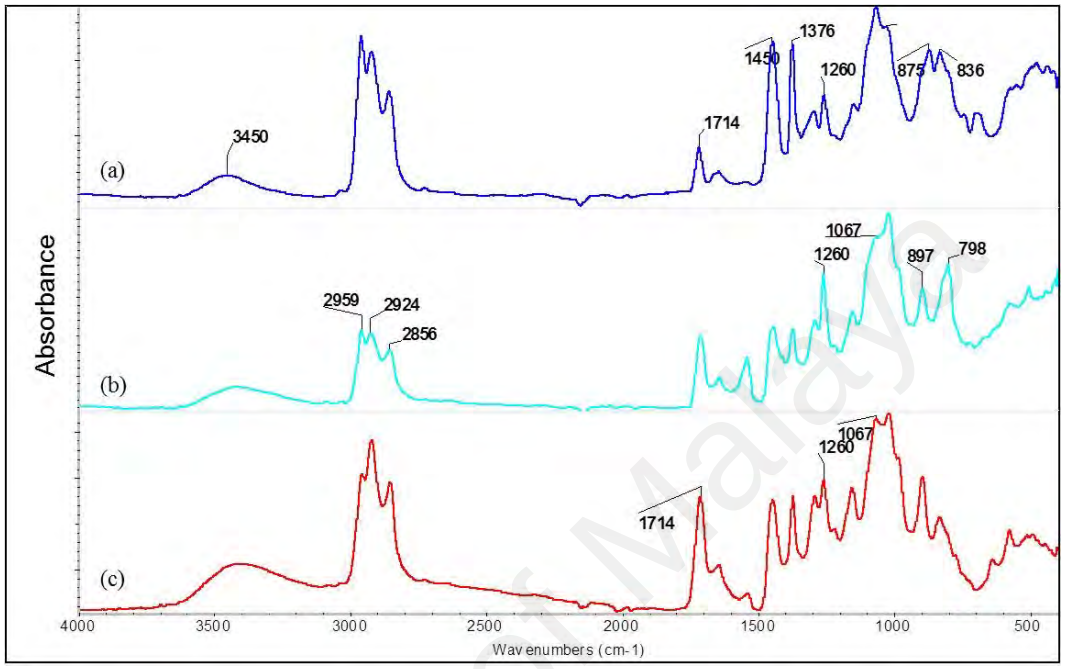

Figure 4.8: FTIR spectra of (a) E-FA2, (b) E-FA11.5 and (c) E-FA19.5 after reaction at 160 ^{o}C

Table 4.7: Absorbance ratio of samples after reaction at 160 ^{o}C

Sample	A_{1714}/A_{1450}	A_{3450}/A_{1450}
E-FA2	0.29	0.20
E-FA11.5	1.16	0.37
E-FA19.5	1.19	0.48

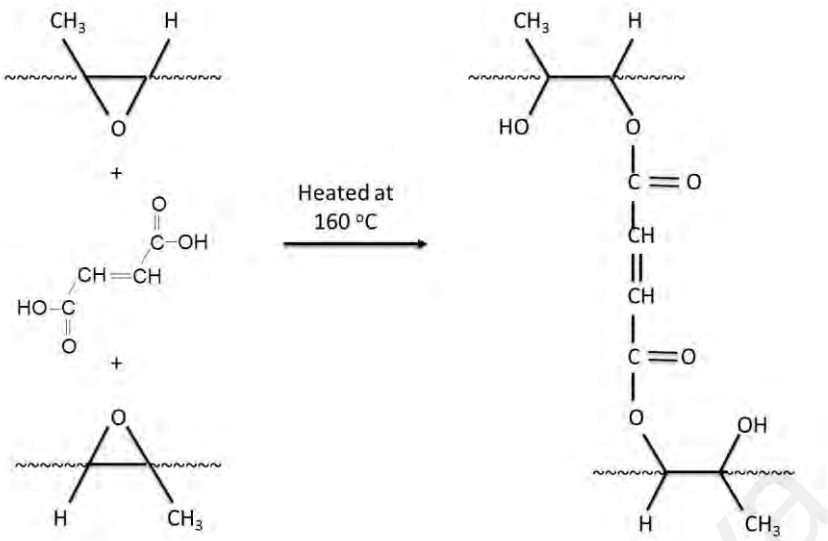

Figure 4.9: Plausible reaction between ENR50 and fumaric acid

4.3.2.3 Percentage of solvent swelling

Further evidence of crosslinking reactions in ENR50 at elevated temperature was provided by a reduction in percentage of solvent swelling after immersion in toluene for 48 h (Table 4.8). At ambient temperature, when there was no reaction between the ENR50 and fumaric acid, the percentages of solvent swelling of samples ENR50, E-FA2, E-FA11.5 and E-FA19.5 were shown to be of the similar order, ranging from 2900 to 3000 %. After heating the samples at 160 °C for 1 h, ENR50 still exhibited 2400 % solvent swelling, whereas those of E-FA2, E-FA11.5 and E-FA19.5 were reduced drastically to 264, 140 and 120 %, respectively, with higher reduction in percentage of swelling being observed for a higher amount of fumaric acid. The reduction in swelling in toluene is primarily due to the increase in the number of crosslinks. In addition, the formations of hydroxyl and ester groups increased the polarity of the sample, which could affect the interaction with the non-polar toluene. Consequently, percentage of swelling has deviated from linearity with the amount of fumaric acid.

Table 4.8: Percentage of solvent swelling of samples before and after reaction at 160 ^{o}C

Sample	% solvent swelling	
	Initial	After heating at 160 ^{o}C
ENR50	2850±90	2380±68
E-FA2	2970±99	264±3
E-FA11.5	2950±16	140±5
E-FA19.5	3050±32	120±6

4.3.2.4 Characterization by DSC

Results of DSC measurements of the samples are summarized in Table 4.9 and the DSC thermograms are shown in Appendix B.1 and B.2 for samples at ambient temperature and after heating at 160 ^{o}C, respectively. The T_g of the samples of ENR mixed with fumaric acid at ambient temperature were approximately -19 ^{o}C, similar to that of ENR50 since there was no reaction between ENR and fumaric acid. However, the T_g increased significantly after the reaction at 160 ^{o}C due to two factors: the increase in the number of crosslinks and the amount of polar groups. The presence of epoxide groups, -OH groups as a result of ring-opening reaction and –COOH groups from pendant chain could induce polar interactions with –COOH groups in fumaric acid and subsequently increased the T_g of the sample.

Table 4.9: T_g of samples before and after reaction at 160 ^oC

Sample	Glass transition temperature (T_g)	
	Initial	After heating at 160 ^oC
ENR50	-19.5	-21.0
E-FA2	-19.6	-6.1
E-FA11.5	-18.8	36.9
E-FA19.5	-18.7	40.7

4.3.3 Summary

Crosslinking reactions of ENR50 with fumaric acid could occur at elevated temperature. ENR was predominantly reacted with fumaric acid *via* ring opening of the epoxide groups of ENR during the reactions at 160 ^oC to form crosslinked structures.

As a result from the viability of ENR50 being crosslinked by fumaric acid, silica as filler was subsequently added into the compound and the interactions of the silica-filled ENR50 with fumaric acid were investigated.

4.4 Interactions of silica-filled ENR50 with fumaric acid

Silica produced from sulfuric acid-leached rice husk after combustion at 600 ^oC for 2 h was added at various loadings into ENR50 and fumaric acid compound. In this part of work, the amount of fumaric acid was kept constant at 4 phr. The samples were brittle for 11.5 phr and 19.5 phr fumaric acid. Thus, lower amount of fumaric acid was used to determine the physical properties of the samples. The interactions of the samples before and after curing/heating at 160 ^oC to the respective t_{90} were investigated. Formulations of the samples are given in Table 4.10.

Table 4.10: Formulation of ENR50 mixed with fumaric acid and silica

Ingredients	phr
ENR50	100
Fumaric acid	4
Silica	Varied at 0, 10, 20, 30, 40, 50

4.4.1 Monsanto rheometer

Cure characteristic of ENR50 mixed with silica at various loadings (10, 20, 30, 40, 50 phr) are shown in Figure 4.10. Besides the torque of ENR50 alone being negligible as reported in section 4.3.2.1, the torque of the ENR50 and silica compounds were also insignificant (<1 dN m) with increasing silica loading, indicating no interactions between ENR50 and silica, up to 50 phr.

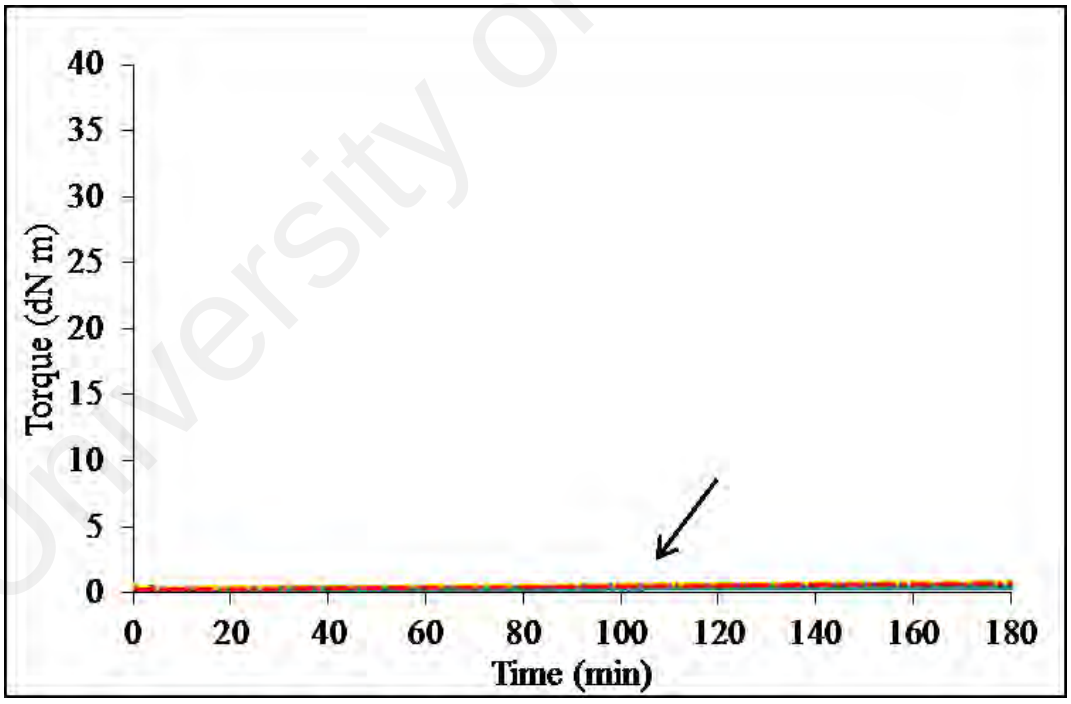

Figure 4.10: Cure curves of ENR50 mixed with silica at various loading at 160 ^{o}C

Figure 4.11 shows cure curves of ENR50 mixed with fumaric acid and silica at various loadings, and the cure characteristic are summarized in Table 4.11. Addition of 4 phr of fumaric acid (curve a) showed a fast initial increase in torque during the first 30

min and followed by a slowing down to a plateau at 80 min, suggesting crosslinks has formed between ENR50 and fumaric acid. Curves (b – f) show a similar trend as curve (a) because of the similar amount of fumaric acid in the samples; the higher final torque was due to the higher silica filler content. As illustrated in Table 4.11, incorporating silica at every 10 phr loading has increased the M_H by 7 to 8 units; due to the stiffening effect of the filler, but the t_{90} has slightly decreased with increasing silica loading. The M_L which indicates the viscosity of the samples prior to the onset of vulcanization has slightly increased with silica loading.

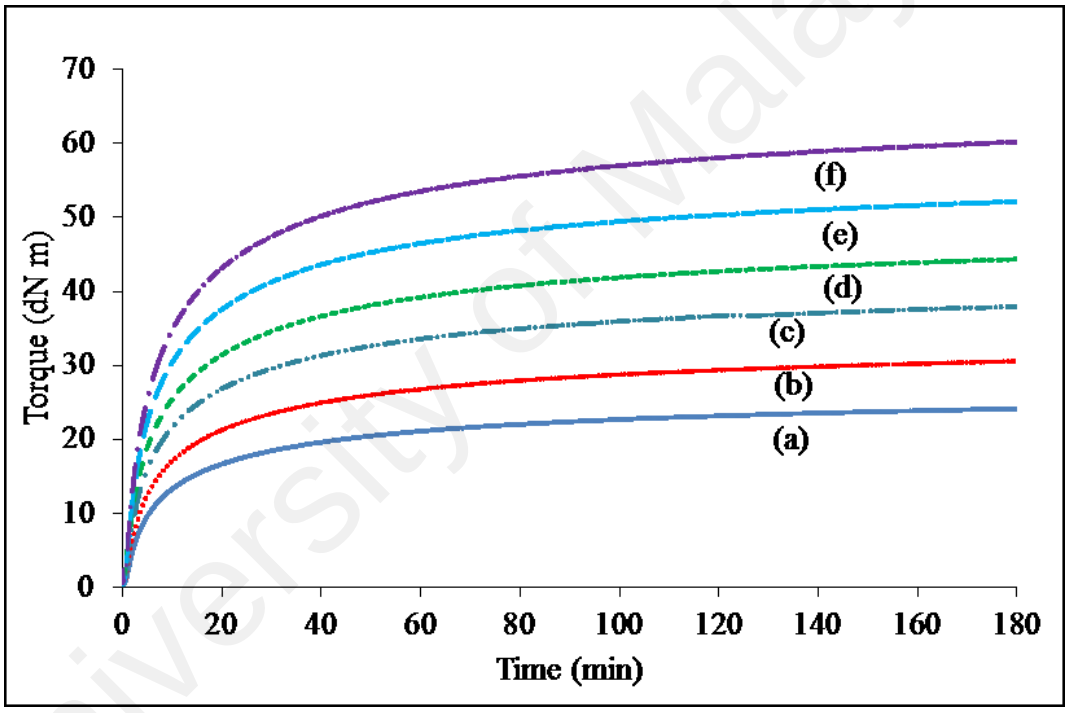

Figure 4.11: Cure curves of ENR50 mixed with 4 phr fumaric acid and silica loading at (a) 0, (b) 10, (c) 20, (d) 30, (e) 40 and (f) 50 phr at 160 ^{o}C

Table 4.11: Cure characteristic of silica-filled ENR50 mixed with fumaric acid

Silica loading (phr)	M_H (dN m)	M_L (dN m)	t_{90} (min)
0	24.13	0.49	72.94
10	30.59	0.46	72.29
20	37.99	0.53	68.30
30	44.38	1.26	69.53
40	52.20	0.58	64.90
50	60.25	0.78	66.08

4.4.2 FTIR spectroscopy

FTIR spectra of silica-filled ENR50 mixed with fumaric acid at ambient temperature are shown in Figure 4.12 (A). The spectra of the samples are similar to each other, which correspond to the *cis*-1-4-polyisoprene and epoxide groups of ENR as discussed in section 4.3.2.2, but the appearances of the peak at 1067 cm^{-1} due to –O-Si-O- stretching is more prominent with increasing silica loading. This suggests no significant reaction between silica and the compound of ENR50 and fumaric acid has occurred at ambient temperature.

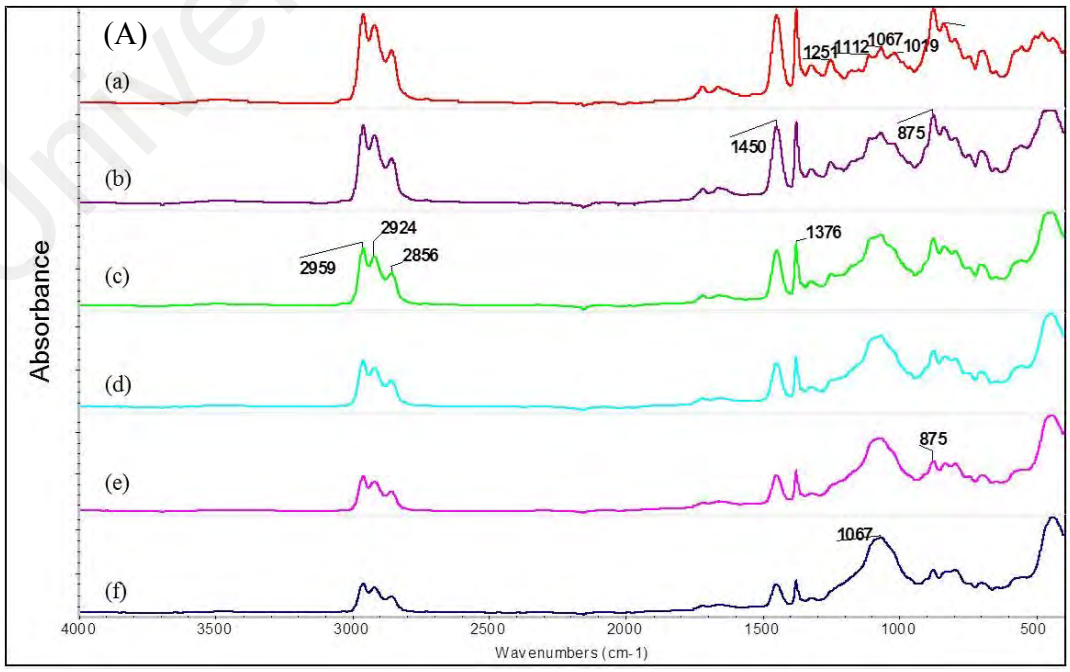

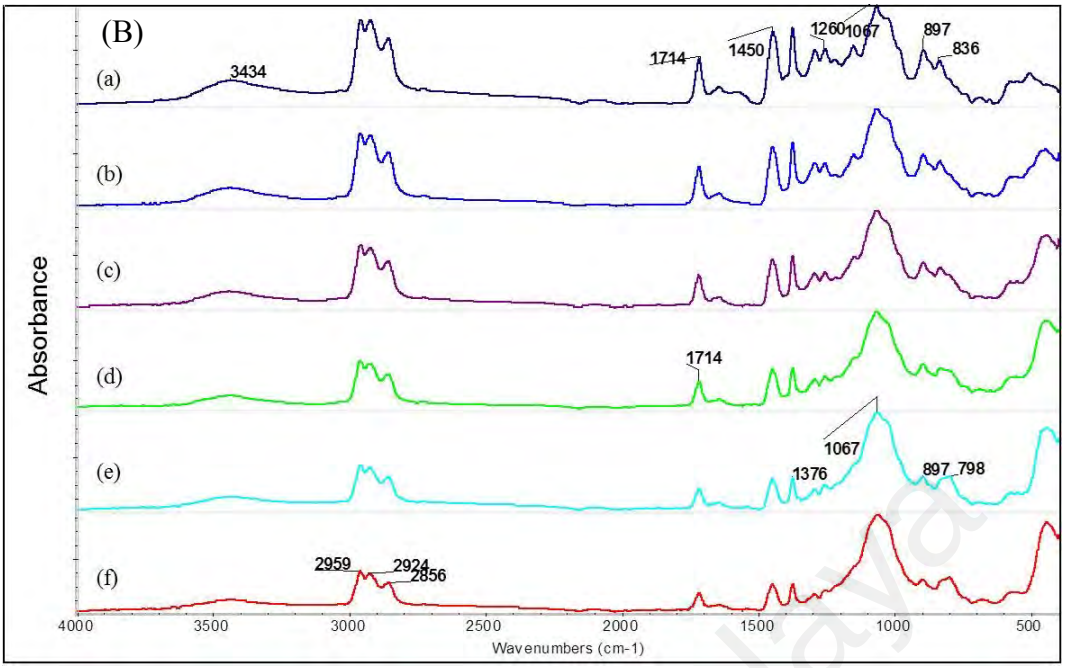

Figure 4.12: FTIR spectra of silica-filled ENR50 with 4 phr fumaric acid (A) mixed at ambient temperature and (B) after heating at 160 ^{o}C at silica loading of (a) 0, (b) 10, (c) 20, (d) 30, (e) 40 and (f) 50 phr

Figure 4.12 (B) shows spectra of silica-filled ENR50 with fumaric acid after heating at 160 ^{o}C. As expected, the reaction of ENR50 with 4 phr fumaric acid (spectrum a) has resulted in the diminishing of the peak at 875 cm^{-1} attributed to the epoxide group, whereas the new peak appeared at 897 cm^{-1} corresponds to CH_2 out of plane deformation of vinylidene groups >C=CH_2 (Roychoudhury & De, 1992). The peaks at 1714 cm^{-1} and 3434 cm^{-1} corresponds to –COOR and –OH groups were formed during reaction. Presumably, the absorbance peaks at 1067 cm^{-1} could be due to polar-polar interaction between –COOH group of fumaric acid and –OH group. The plausible interaction is shown in Figure 4.13.

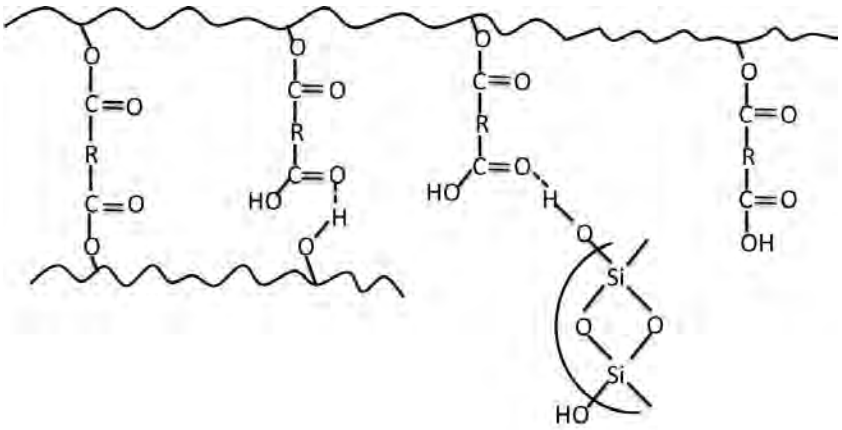

Figure 4.13: Plausible interaction between –OH of silica and –COOH of fumaric acid

4.4.3 Percentage of solvent swelling

Table 4.12 shows percentage of solvent swelling of silica-filled ENR50 with fumaric acid before and after heating at 160 ^{o}C. When ENR50 was mixed with fumaric acid and silica at ambient temperature, considerable reduction in solvent swelling from 436 to 288 %, with increasing silica loading was obtained, presumably due to the reduction of rubber content and some polar interaction between silica and ENR50 in the sample. After heating at 160 ^{o}C, crosslinking reactions between ENR50 and fumaric acid have led to 90 % reduction in solvent swelling. The percentage of swelling was reduced drastically by 67 to 75 % from the initial with silica loading. However, the percentage of swelling slightly decreased with increasing silica loading after heating.

Table 4.12: Percentage of swelling of samples before and after heating at 160 ^{o}C

Silica loading (phr)	% solvent swelling	
	Initial	After heating at 160 ^{o}C
0	1062±68	104±2
10	436±30	107±1
20	382±21	127±10
30	366±35	105±11
40	311±25	86±10
50	288±24	73±14

4.4.4 DSC analysis

The DSC thermograms of ENR50 mixed with fumaric acid and silica before and after heating at 160 ^{o}C are shown in Appendix C.1 and C.2, respectively, and the results are summarized in Table 4.13.

Table 4.13: T_g of samples before and after heating at 160 ^{o}C

Silica loading (phr)	Glass transition temperature (T_g)	
	Initial	After heating at 160 ^{o}C
0	-17.2	10.1
10	-16.3	10.2
20	-16.4	10.1
30	-16.0	11.9
40	-16.7	11.0
50	-15.7	10.5

In this part of work, T_g of the ENR50 mixed with fumaric acid, without silica filler has registered -17 ^{o}C. Incorporation of silica in the compound at ambient temperature showed no significant change in T_g. After heating at 160 ^{o}C, T_g of the samples

drastically increased by 27 ^{o}C, due to the reduction of chain mobility of rubber molecules, but there was no significant change in T_g with increasing silica loading.

4.4.5 Physical properties

The physical properties of silica-filled ENR50 cured with fumaric acid were measured in accordance with ISO standard test methods and the results are summarized in Appendix E.1. The tensile strength has slightly increased in spite of the decrease in elongation at break with increasing silica loading shown in Figure 4.14, presumably due to the structural changes of the rubber chain.

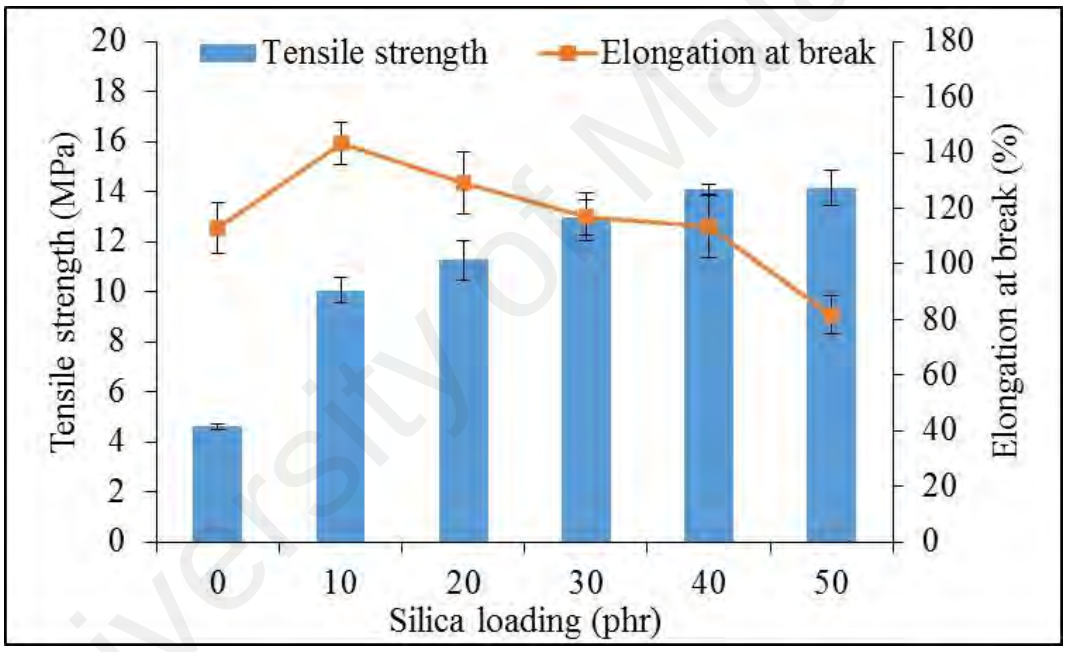

Figure 4.14: Tensile strength and elongation at break of silica-filled ENR50 cured with fumaric acid

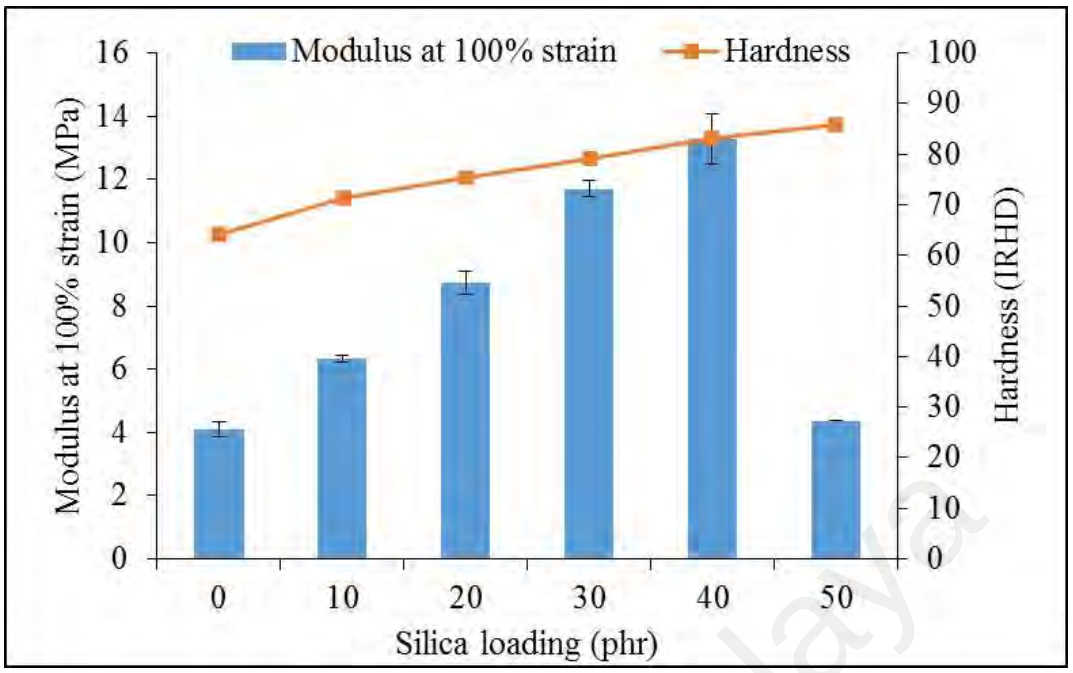

Figure 4.15: Modulus at 100 % strain and hardness of silica-filled ENR50 cured with fumaric acid

Figure 4.15 shows modulus at 100 % strain and hardness of silica-filled ENR50 cured with fumaric acid. The modulus at 100% strain and hardness increases with addition of more filler due to the reduction in relative amount of rubber, resulting in more rigid samples. The modulus at 100 % strain drastically decreased at 50 % silica loading, presumably due to the silica exceeding the optimum level as filler.

4.4.6 Summary

Findings from this work show that fumaric acid could be utilized as crosslinking agent in rubber and silica isolated from rice husk could be used as filler in the rubber compound. The properties from the silica-filled ENR50 cured with fumaric acid may suggest different types of applications to the existing sulfur vulcanization. Thus, in the next section, curing of silica-filled ENR50 with fumaric acid and sulfur vulcanization of silica-filled ENR50 were compared.

4.5 Curing of silica-filled ENR50 with fumaric acid *versus* sulfur vulcanization

ENR50 was mixed with fumaric acid and silica, where the amount of fumaric acid was similar to that of sulfur at 1.5 phr. The semi-EV sulfur formulation which consisted of accelerators, activator and co-activator was selected for ENR. The formulations are given in Table 4.14. Curing of silica filled-ENR50 with fumaric acid and sulfur vulcanization were carried out at 160 ^{o}C for the duration of the respective t_{90}. Both the fumaric acid-cured and sulfur-cured ENR50s filled with silica were characterized using FTIR spectroscopy, percentage of solvent swelling, DSC and physical properties determination.

Table 4.14: Formulations of the fumaric acid-cured and sulfur-cured ENR50s filled with silica

Ingredients (phr)/ Sample	Fumaric acid-cured ENR50	Sulfur-cured ENR50
ENR50	100	100
Fumaric acid	1.5	-
Zinc oxide	-	5
Stearic acid	-	2
Sulfur	-	1.5
MBS	-	1.5
TMTM	-	1.5
Silica	Varied at 0, 10, 20, 30, 40, 50 phr	

4.5.1 Cure characteristics

Figure 4.16 (A) and (B) show cure curves of silica-filled ENR50 mixed with fumaric acid and sulfur formulation at 160 ^{o}C, respectively, and the cure characteristics are summarized in Table 4.15.

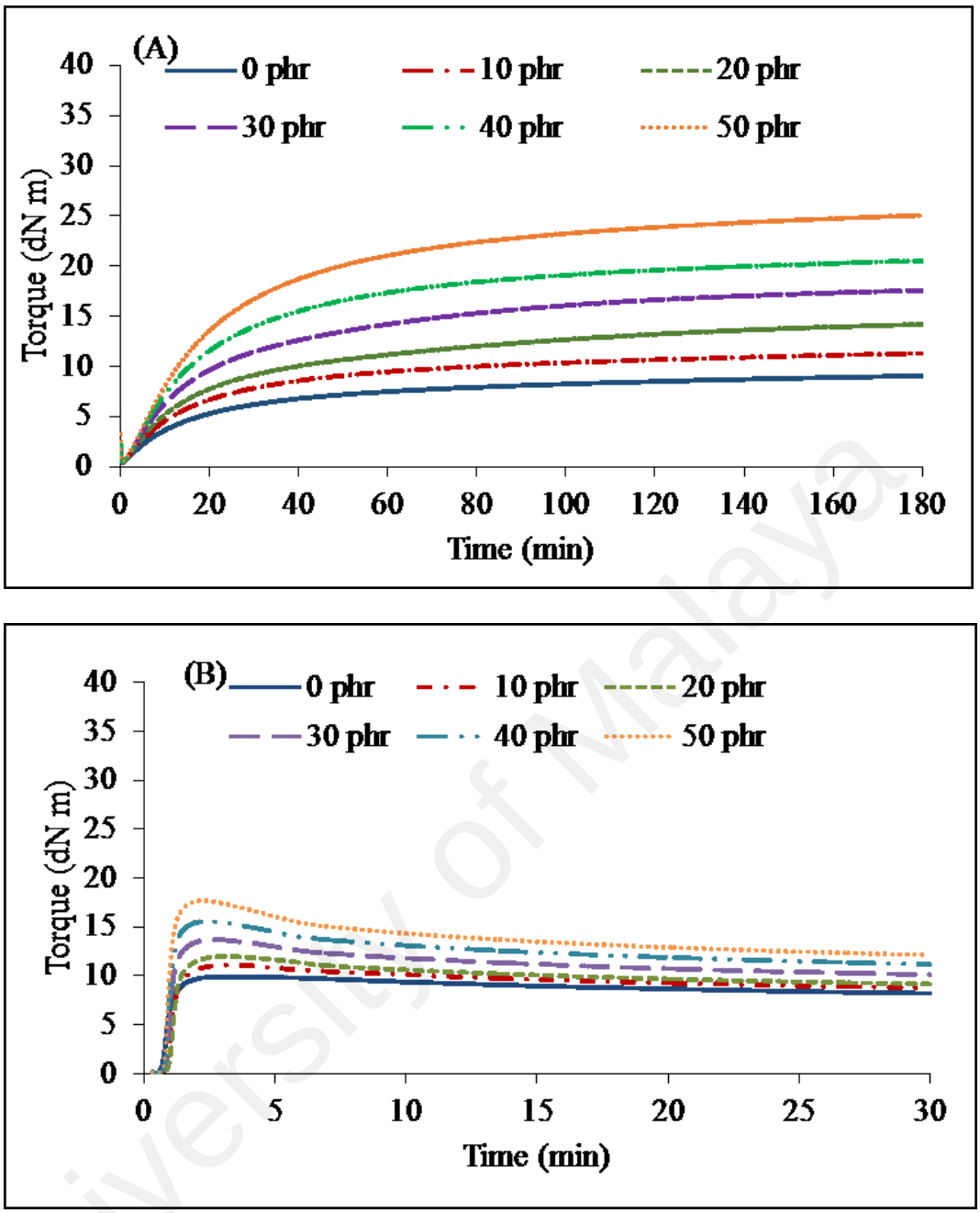

Figure 4.16: Cure curves of ENR50 mixed with (A) fumaric acid, (B) sulfur formulation, and silica at various loading at 160 ^{o}C

Curing of ENR50 with fumaric acid filled with silica shows a long marching increase in torque, presumably due to the continuing ring-opening of the epoxide groups. But ENR50 sulfur-curing has suffered from reversion as shown in Figure 4.16 (B), attributed to the decomposition of di- and polysulphidic crosslinks as studied by Poh et al. (1995). Both the samples show similar trend, wherein the torque gradually increased with increasing silica loading.

As shown in Table 4.15, ENR50 mixed with 1.5 phr fumaric acid, without silica filler, has increased the M_H to 9 dN m, indicating crosslinking reactions have occurred between ENR50 and fumaric acid. Incorporating silica at every 10 phr loading has increased the M_H by 3 to 4 units; suggesting stiffening effect of the filler. On the other hand, the M_H of ENR50 sulfur-curing has also shown similar increase of about 10 dN m, but the M_H has increased by 1 to 2 units only with increasing silica loading. The M_L has no significant effect with silica loading for both the samples. Noticeably, the t_{90} of ENR50-fumaric acid curing is slower and further decreased with increasing silica loading compared to those ENR50-sulfur curing. There was no significant effect on the t_{90} in the ENR50-sulfur curing and it has been concluded by Fetterman (1973) that other than type of elastomer and accelerator systems, cure retardation of rubber is directly proportional to the total surface area of silica and the functionality of sulfur is dependent on both the particle size and the total content of silica. In addition, as reported by Nasir et al. (1988), silica would react with zinc oxide which subsequently reduces the zinc reactivity, thus delays the sulfur reaction.

Table 4.15: Cure characteristics of silica-filled ENR50 compounds

Silica loading (phr)	Fumaric acid-cured ENR50			Sulfur-cured ENR50		
	M_H (dN m)	M_L (dN m)	t_{90} (min)	M_H (dN m)	M_L (dN m)	t_{90} (min)
0	9.07	0.50	97.8	9.92	0.14	1.4
10	11.31	0.49	90.5	11.12	0.12	1.6
20	14.21	0.44	104.9	12.01	0.11	1.6
30	17.59	0.40	93.4	13.72	0.12	1.4
40	20.54	0.44	82.5	15.59	0.14	1.3
50	25.07	0.50	84.3	17.71	0.13	1.3

4.5.2 FTIR analysis

FTIR spectrum of ENR50 (spectrum a), fumaric acid-cured ENR50 (spectra b – e) and sulfur-cured ENR50 (spectrum f) filled with silica are shown in Figure 4.17. The peaks between 2958 and 2859 cm^{-1} represent the methyl and methylene groups and peaks at 1250 and 875 cm^{-1} correspond to the epoxide groups of ENR. Spectra (a) and (b) are almost identical except the peak at 1718 cm^{-1}, which attributes to C=O from ester group and the broad peak in the region of 3300 - 3600 cm^{-1}, suggesting the presence of –OH groups, for (b). With increasing silica loading (spectra c – e), the peak at 1067 cm^{-1} could be due to the presence of –O–Si–O– stretching of silica. In contrast, sulfur-cured ENR50 filled with 50 phr silica (spectrum f), the peak at 875 cm^{-1} remained unchanged, whilst the peak at 835 cm^{-1} has diminished, indicating crosslinking reaction has taken place *via* double bonds. FTIR spectra of sulfur-cured ENR50 filled with silica at other loadings are shown in Appendix D.1.

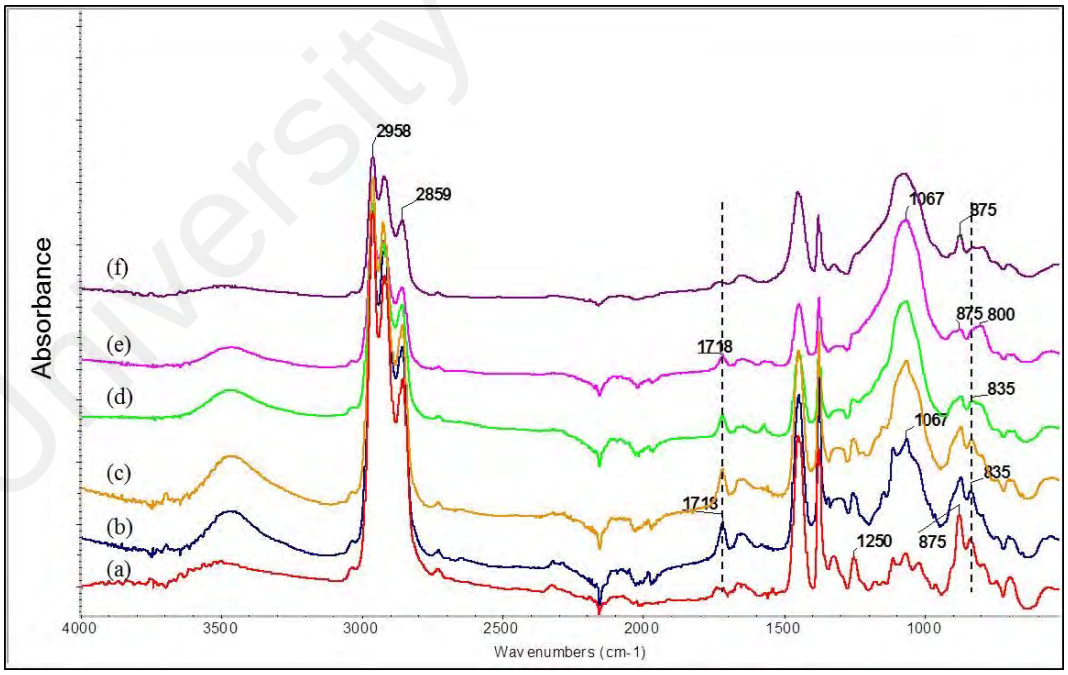

Figure 4.17: FTIR spectra of (a) ENR50 and ENR50 cured with 1.5 phr fumaric acid at silica loading of (b) 0 phr, (c) 10 phr, (d) 30 phr, (e) 50 phr and (f) sulfur-cured ENR50 filled with 50 phr silica

4.5.3 Percentage of solvent swelling and crosslink density

The percentage of solvent swelling and crosslink density of fumaric acid-cured and sulfur-cured ENR50s are given in Table 4.16. The percentage of swelling of both the samples gradually decreased with increasing silica loading, with greater reduction in the fumaric acid-cured ENR50. Besides the reduction of rubber content with increasing silica loading, further decrease in percentage of swelling could be due to the increase in the number of crosslinks which is in agreement with the increase in crosslink density of the samples. The crosslink density of fumaric acid-cured ENR50 is shown to be remarkably higher than sulfur-cured ENR50 at similar amount of crosslinking agent (1.5 phr), indicating fumaric acid has effectively cured the ENR without additives.

Table 4.16: Percentage of solvent swelling and crosslink density of fumaric acid-cured and sulfur-cured ENR50s filled with silica

Silica loading (phr)	Fumaric acid-cured ENR50		Sulfur-cured ENR50	
	% solvent swelling	Crosslink density (10^{-5} mol/cm^3)	% solvent swelling	Crosslink density (10^{-5} mol/cm^3)
0	212±3.0	11.6	274±6.0	6.7
10	189±4.4	12.6	239±3.0	7.6
20	152±2.0	16.3	206±2.4	8.7
30	135±0.7	18.0	191±2.9	9.4
40	127±1.2	18.8	176±2.9	10.0
50	113±0.8	21.4	152±1.7	12.0

4.5.4 DSC analysis

As expected, silica-filled ENR50 mixed with fumaric acid and sulfur formulation at ambient temperature has no significant effect on the T_g as shown by DSC thermograms in Appendix C.3 and C.4, respectively. The T_g was approximately -20 ^oC similar to the ENR50, indicating no significant interactions at ambient temperature. On the other

hand, crosslinking reactions at 160 ^{o}C between ENR50 and fumaric acid; and sulfur led to the increase in T_g from -20 ^{o}C to -13 ^{o}C and -15 ^{o}C, respectively, thus reduced the chain mobility between the rubber molecules. Fumaric acid-cured and sulfur-cured ENR50s filled with silica at various loading have revealed similar T_g to the initial (Table 4.17). Nevertheless, fumaric acid-cured ENR50 showed higher T_g compared with sulfur-cured ENR50 at any silica loading, due to the higher crosslink density, and presumably due to the existence of more polar groups in ENR50 cured with fumaric acid. DSC thermograms of fumaric acid-cured and sulfur-cured ENR50s filled with silica are shown in Appendix C.5 and C.6, respectively.

Table 4.17: T_g of fumaric acid-cured and sulfur-cured ENR50s filled with silica

Silica loading (phr)	Fumaric acid-cured ENR50	Sulfur-cured ENR50
0	-13.3	-15.0
10	-12.4	-15.4
20	-13.0	-15.8
30	-12.5	-15.9
40	-13.3	-16.9
50	-13.3	-16.6

4.5.5 Physical properties

Appendix E.2 and E.3 summarize tensile strength and elongation at break of fumaric acid-cured and sulfur-cured ENR50s filled with silica at various loading, respectively. The tensile strength of fumaric acid-cured ENR50 slightly increased but, elongation at break decreased with increasing silica loading as shown in Figure 4.18. As for sulfur-cured ENR50 filled with silica, the tensile strength and elongation at break increased up to 30 phr silica and further addition of silica weakened these properties. Similar observation was reported by Ishak and Bakar (1995) and it was deduced that adding

more filler after maximum point was reached, the silica particles were no longer adequately separated and wetted by the rubber phase. Thus, reduction in strength may be due to the poor dispersion of the filler particles in the rubber phase. However, this is not the case with the fumaric acid-cured ENR50 filled with silica. The differences in the trend between fumaric acid-cured and sulfur-cured ENR50s may presumably be attributed to the network structure of the samples.

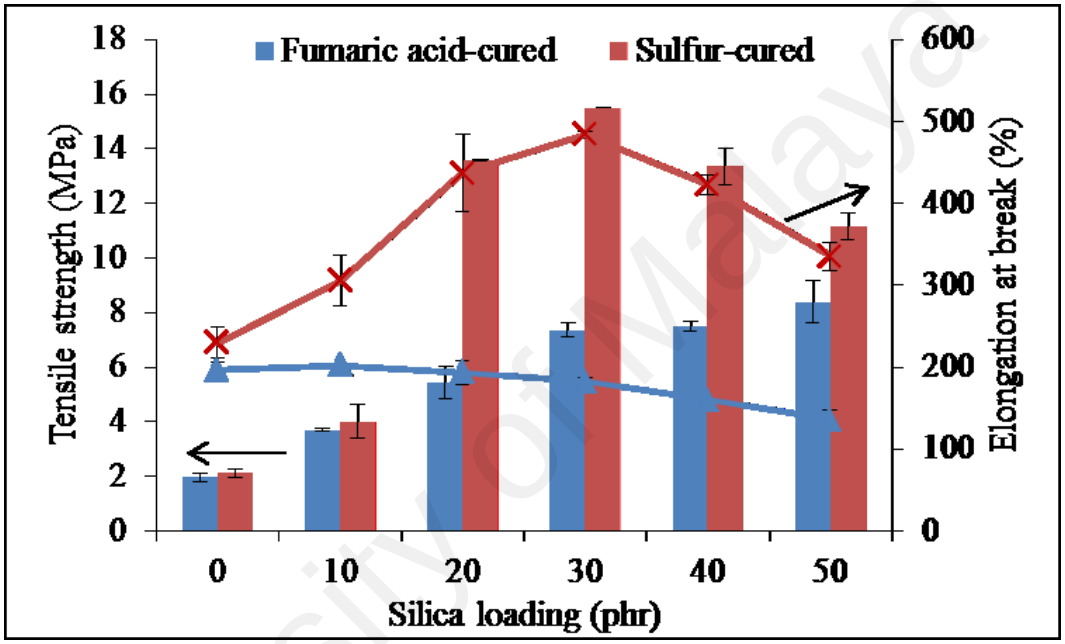

Figure 4.18: Tensile strength and elongation at break of fumaric acid-cured and sulfur-cured ENR50s filled with silica - Unaged

However, both samples exhibited similar trend with the modulus at 100% strain while hardness increased with increasing silica loading, with greater increment in fumaric-acid cured ENR50 as shown in Figure 4.19 and Appendix E.4.

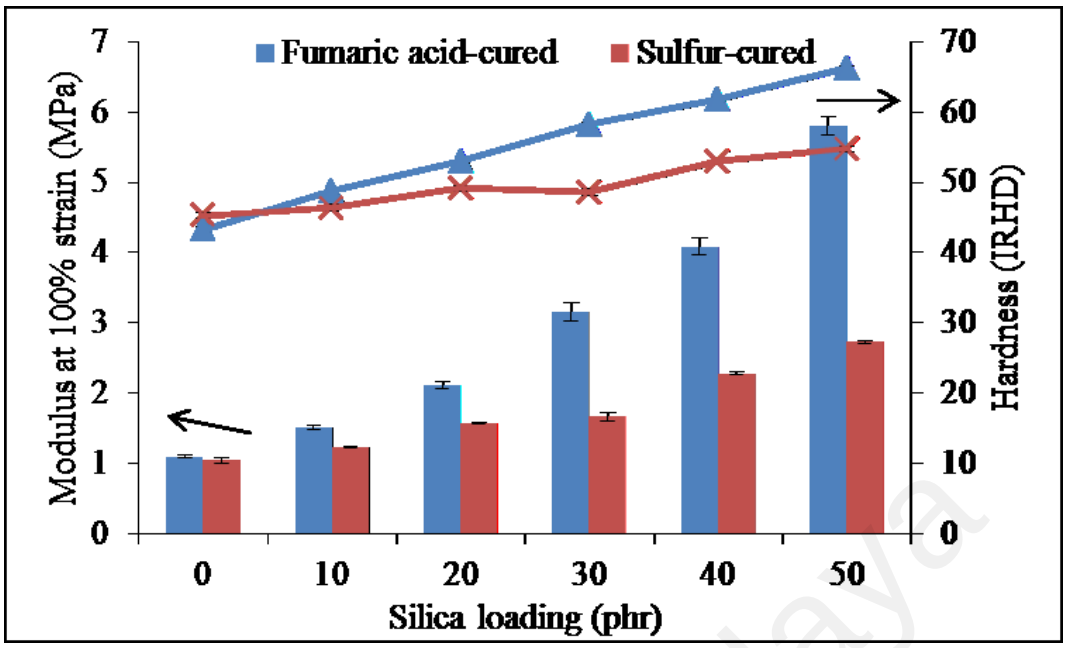

Figure 4.19: Modulus at 100 % strain and hardness of of fumaric acid-cured and sulfur-cured ENR50s filled with silica - Unaged

After exposed to heat aging at 100 ^{o}C for 7 days, tensile strength and elongation at break of fumaric acid-cured ENR50 filled with silica were shown to have excellent retention of more than 95 % and 85 %, respectively as shown in Figure 4.20. On the other hand, the tensile strength of sulfur-cured ENR50 filled with silica significantly decreased in similar order, ranging from 7 to 9 MPa, whilst elongation at break and modulus at 100% strain drastically decreased. These detrimental effects on the properties could be due to the oxidative scission processes both in the main chains and in the sulfidic crosslinks of ENR as reported by Gelling and Morrison (1985). Figure 4.21 reveals modulus at 100 % strain has slightly increased with increasing silica loading.

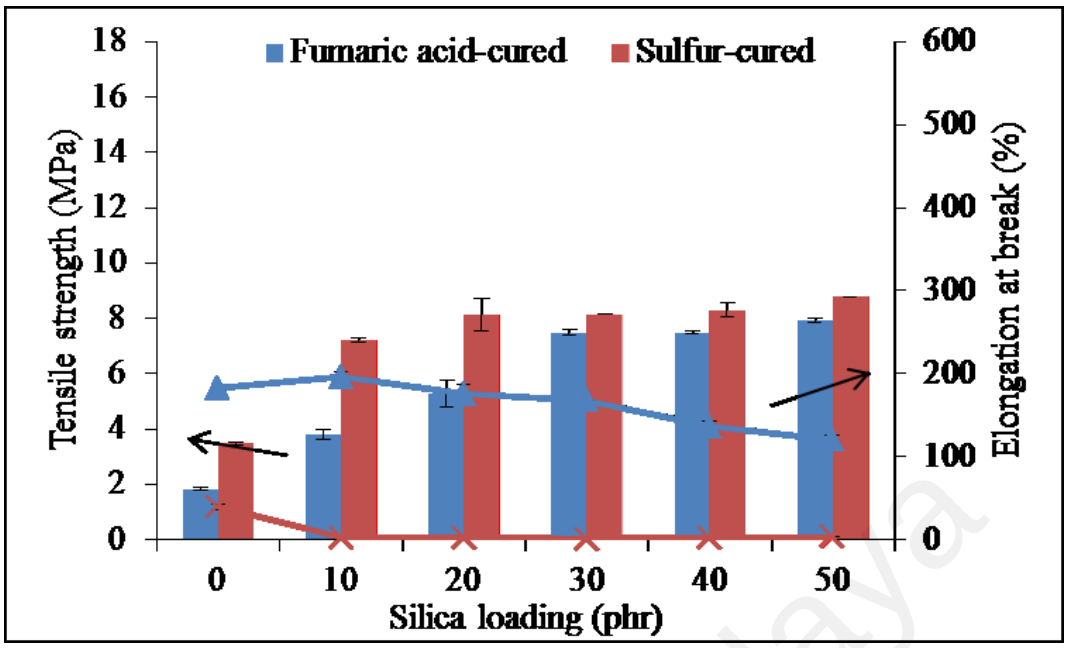

Figure 4.20: Tensile strength and elongation at break of fumaric acid-cured and sulfur-cured ENR50s filled with silica - Aged at 100 ^{o}C for 7 days

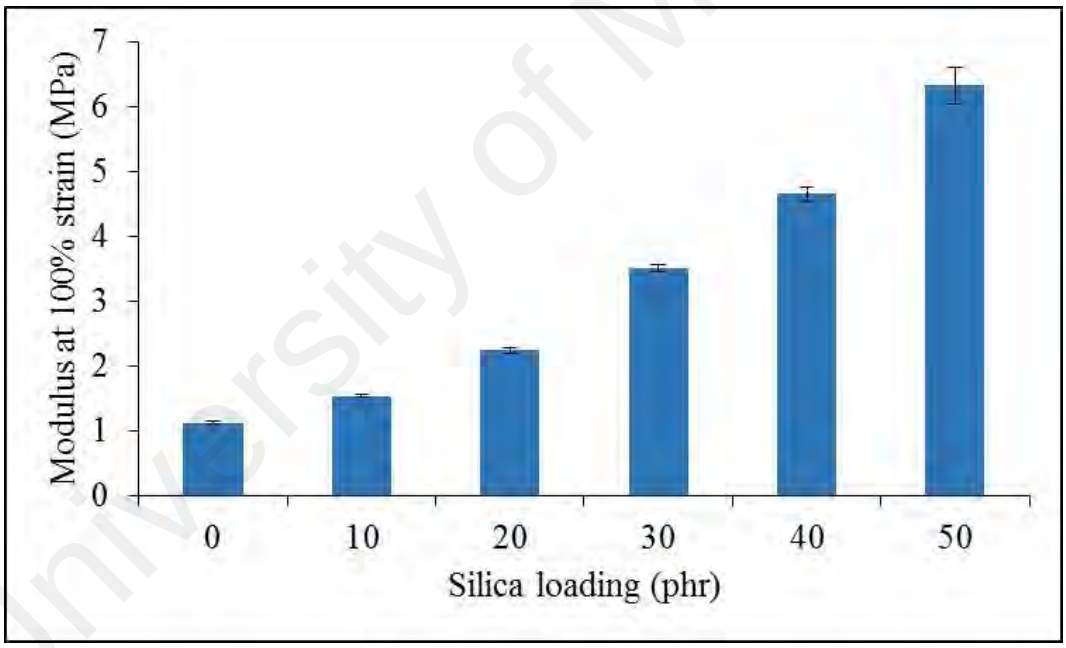

Figure 4.21: Modulus at 100 % strain of fumaric acid-cured ENR50 filled with silica - Aged at 100 ^{o}C for 7 days

4.5.6 Summary

The epoxide groups and double bonds in ENR could serve as the sites for crosslinking reactions. Fumaric acid-cured ENR50 filled with silica showed excellent retention in physical properties after being exposed to heat aging at 100 ^{o}C for 7 days.

In contrast, tensile strength, elongation at break and modulus at 100 % strain of sulfur-cured ENR50 revealed poor retention after aging.

CHAPTER 5: CONCLUSION AND SUGGESTION FOR FURTHER RESEARCH

5.1 Conclusion

The objectives of this study were to establish the predominant reactions between ENR and fumaric acid, and subsequently the interactions of ENR50 and fumaric acid filled with silica. Silica filler isolated from rice husk in the pure form was used in this study.

5.1.1 Properties of high purity amorphous silica

Silica that has been used in this study was isolated from rice husk, in which the conditions to produce high purity of silica was first established. In a systematic study, the combustion of un-leached, hydrochloric acid-leached and sulfuric acid-leached rice husks were performed in a muffle furnace at 600, 700, 800 and 900 ^{o}C for 2 h. Results demonstrated that all the samples produced amorphous silica (SiO_2) and the average particle size were in the range of 0.50 to 0.70 μm. The effect of combustion at different temperatures between 600 and 900 ^{o}C on the silica production is very small, particularly at temperature above 600 ^{o}C. Thus, amorphous silica with purity above 99 % as confirmed by XRF analysis was produced by hydrochloric and sulfuric acids leaching of the rice husk, followed by combustion at 600 ^{o}C for 2 h with BET surface area of 218 m^2/g and 209 m^2/g, respectively. Silica produced from sulfuric acid-leached rice husk was used in this study.

5.1.2 Interactions of silica-filled ENR50 with fumaric acid

This study was consisted of two parts. The aim of the first part was to study the crosslinking reactions between ENR50 and fumaric acid. ENR50 was mixed with various amount of fumaric acid at ambient temperature, followed by compression molding at 160 ^{o}C for 1 h. The amount of fumaric acid was in the range of 2 to 19.5 phr

to avoid excessive crosslinking in the sample. The initial ENR50 and fumaric acid compound showed no significant change in percentage of solvent swelling and in T_g with increasing amount of fumaric acid, indicating there was no reaction between ENR and fumaric acid at ambient temperature. Upon heating at 160 ^oC, the marked increment in rheometer torque and increase in T_g, with subsequent drastic decrease in percentage of solvent swelling with increasing amount of fumaric acid was consistent with the crosslinking reactions that occurred between ENR and fumaric acid. FTIR spectroscopy further confirmed that the predominant crosslinking reactions was due to the reaction between the epoxide groups of ENR and –COOH groups of fumaric acid, leading to the disappearing of epoxide peak and the formation of ester linkages. Greater amount of fumaric acid has also led to the higher extent of crosslinking.

The second part of this study focused on the interactions of silica-filled ENR50 with fumaric acid. Silica produced from sulfuric acid-leached rice husk was incorporated at loading of 0 to 50 phr into the ENR50 and fumaric acid (4 phr) compound, followed by curing at 160 ^oC to the respective t_{90}. The cure characteristic showed that M_H gradually increased from 24 to 60 dN m with increasing silica loading. Crosslinking reactions between ENR50 and fumaric acid has resulted in the reduction of percentage of solvent swelling by 90 % and decreased further by 67 to 75 % with silica loading, which presumably was due to the stiffening effect of the filler as there was no significant change in T_g. For physical properties, the tensile strength of fumaric acid-cured ENR50 has attained a tensile strength of 14 MPa at 50 phr silica loading, in spite of the decrease in elongation at break with increasing silica loading. As expected, the modulus at 100% strain and hardness increased with addition of more filler, but the modulus at 100 % strain decreased drastically from 13 MPa to 4 MPa, at 50 phr silica loading. Presumably, due to the silica exceeded the optimum level as filler and subsequently

reduced the modulus. These characteristics and properties were further compared with sulfur-cured ENR50 filled with silica. In comparison with sulfur vulcanization, the amount of fumaric acid was 1.5 phr similar to that of sulfur although sulfur vulcanization contains additives such as accelerators and activators. The extent of crosslinking was more prominent in the silica-filled ENR50 cured with fumaric acid that has been revealed by the significant increment in torque, crosslink density and T_g compared to those sulfur-cured ENR50 filled with silica. The tensile strength of fumaric acid-cured ENR50 marginally increased with increasing silica loading and has registered 8 MPa at 50 % silica loading, whilst sulfur-cured ENR50 attained 11 MPa at similar silica loading. On the other hand, since sulfur-cured ENR50 suffered from reversion, it was predictable that sulfur-cured ENR50 posed deleterious effect to the physical properties upon heat ageing at 100 ^{o}C for 7 days. But curing of ENR50 with fumaric acid has significantly suppressed the reversion behaviour and subsequently demonstrated significant ability in retention of the physical properties after aging. Besides fumaric acid could effectively cure ENR without additives such as accelerators, the physical properties and aging performance could be superior to those sulfur-cured ENR50.

Findings from this study revealed the potential usage of fumaric acid as crosslinking agent in ENR and the properties of rubber were influenced by the crosslink network structure. Furthermore, silica produced from rice husk can be used as filler in the rubber compound.

5.2 Suggestion for further research

The current scope of this study is restricted to the reactions between ENR50 and fumaric acid, and the longer cure time (t_{90}) was found necessary to complete the reaction. It would be of interest to investigate the reactions at 180 ^{o}C curing temperature

and the use of accelerator to speed up the reactions. Furthermore, it is expected that different amounts of fumaric acid could give comparable physical properties to those of sulfur vulcanization of silica-filled ENR50.

The work presented here studied the interactions of fumaric acid-cured ENR50 filled with silica at low loading. Since the significant reinforcement in rubber usually achieved with addition of more than 50 phr filler, it is interesting to investigate the effects of higher filler loading such as 70 and 80 phr of silica in the ENR50 and fumaric acid compounds. It would be rather interesting to determine the lime reactivity of amorphous silica produced from rice husk. In addition, silica filler usually employed in the form of precipitated silica, but in this study amorphous silica with high purity was used, in spite of precipitated amorphous silica could also be synthesized from rice husk ash (Ghosh & Bhattacherjee, 2013). The interactions of fumaric acid-cured ENR50 filled with silica could also be further compared with commercially available precipitated silica.

REFERENCES

Adam, F., Kandasamy, K., & Balakrishnan, S. (2006). Iron incorporated heterogeneous catalyst from rice husk ash. *Journal of Colloid and Interface Science, 304*(1), 137-143.

Aggarwal, D. (2003, March 12). Use of rice husks as fuel in process steam boilers. India: Tata Energy Research Institute, New Delhi.

Ahiduzzaman, M. (2007). Rice husk energy technologies in Bangladesh. *Agricultural Engineering International: the CIGR Ejournal, IX*(1), 1-9.

Ahmaruzzaman, M., & Gupta, V.K. (2011). Rice husk and its ash as low-cost adsorbents in water and wastewater treatment. *Industrial & Engineering Chemistry Research, 50*(24), 13589-13613.

Ajiwe, V.I.E., Okeke, C.A., & Akigwe, F.C. (2000). A preliminary study of manufacture of cement from rice husk ash. *Bioresource Technology, 73*(1), 37-39.

Akiba, M., & Hashim, A.S. (1997). Vulcanization and crosslinking in elastomers. *Progress Polymer Science, 22*, 475-521.

Alex, R., & De, P.P. (1991). Self-vulcanizable rubber-rubber blends based on epoxidised natural rubber and polychloroprene. *Kautschuk und Gummi, Kunststoffe, 44*(4), 333-335.

Alex, R., De, P.P., & De, S.K. (1989). Self-vulcanizable rubber blend system based on epoxidized natural rubber and carboxylated nitrile rubber. *Journal of Polymer Science: Part C: Polymer Letters, 27*, 361-367

Alex, R., De, P.P., & De, S.K. (1991). Self-vulcanizable ternary rubber blend based on epoxidized natural rubber, carboxylated nitrile rubber and polychloroprene rubber: 1. Effect of blend ratio, moulding time and fillers on miscibility. *Polymer, 32*(13), 2345-2350.

Ansell. (2010). What is a chemical allergy? In Ansell (Ed.), (pp. 1-16). Canada: Ansell Canada Inc.

Antal, M.J. (1983). Biomass pyrolysis: A review of the literature. Part 1 - Carbohydrate pyrolysis. *Advances in Solar Energy, 11*(1), 61-111.

Assureira, E. (2002, June 11). Rice husk – an alternative fuel in Perú. *Boiling Point, 48,* 35-36.

Baker, C.S.L., Gelling, I.R., & Newell, R. (1985). Epoxidized natural rubber. *Rubber Chemistry and Technology, 58*, 67-85.

Bandyopadhyay, S., De, P.P., Tripathy, D.K., & De, S.K. (1996a). 3-aminopropyltriethoxysilane as a promoter in the crosslinking of carboxylated

nitrile rubber by surface-oxidized carbon black. *Journal of Applied Polymer Science, 61*, 1813-1820.

Bandyopadhyay, S., De, P.P., Tripathy, D.K., & De, S.K. (1996b). Influence of surface oxidation of carbon black on its interaction with nitrile rubbers. *Polymer, 37*, 353-357.

Bandyopadhyay, S., De, P.P., Tripathy, D.K., & De, S.K. (1996c). Interaction between carboxylated nitrile rubber and precipitated silica: Role of (3-aminopropyl) triethoxysilane. *Rubber Chemistry and Technology, 69*(4), 637-647.

Bhattacharya, K.R., & Ali, S.Z. (2015). Rice husk and its utilisation. In K.R. Bhattacharya & S.Z. Ali (Eds.), *An introduction to rice-grain technology* (pp. 246-264). New Delhi: Woodhead Publishing India Pvt Ltd.

Billmeyer, F.W. (1984). Analysis and testing of polymers. In F.W. Billmeyer (Ed.), *Textbook of polymer science* (pp. 229-245). United States of America: A Wiley-Interscience Publication.

Borm, P.J., Tran, L., & Donaldson, K. (2011). The carcinogenic action of crystalline silica: A review of the evidence supporting secondary inflammation-driven genotoxicity as a principal mechanism. *Critical Reviews in Toxicology, 41*(9), 756-770.

Brunauer, S., Emmett, P.H., & Teller, E. (1938). Adsorption of gases in multimolecular layers. *Journal of the American Chemical Society, 60*(2), 309-319.

Burfield, D.R., Lim, K.L., & Law, K.S. (1984). Epoxidation of natural rubber latices: Methods of preparation and properties of modified rubbers. *Journal of Applied Polymer Science, 29*, 1661-1673.

Byers, J.T. (1987). Fillers Part 1: Carbon black. In M. Morton (Ed.), *Rubber technology* (pp. 59-70). New York: Van Nostrand Reinhold.

Chakraverty, A., Mishra, P., & Banderjee, H.D. (1985). Investigation of thermal decomposition of rice husk. *Thermochimica Acta, 94*, 261-275.

Chakraverty, A., Mishra, P., & Banerjee, H.D. (1988). Investigation of combustion of raw and acid-leached rice husk for production of pure amorphous white silica. *Journal of Materials Science, 23*(1), 21-24.

Chandrasekhar, S., Pramada, P.N., & Majeed, J. (2006). Effect of calcination temperature and heating rate on the optical properties and reactivity of rice husk ash. *Journal of Materials Science, 41*, 7926–7933.

Chandrasekhar, S., Pramada, P.N., & Praveen, L. (2005). Effect of organic acid treatment on the properties of rice husk silica. *Journal of Materials Science, 40*, 6535–6544.

Chandrasekhar, S., Pramada, P.N., Raghavan, P., & Satyanarayana, K.G. (2002). Microsilica from rice husk as a possible substitute for condensed silica fume for high performance concrete. *Journal of Materials Science Letters, 21*, 1245-1247.

Chandrasekhar, S., Satyanarayana, K.G., Pramada, P.N., & Raghavan, P. (2003). Review processing, properties and applications of reactive silica from rice husk – an overview. *Journal of Materials Science, 38*, 3159-3168.

Chang, F.W., Yang, H.C., Roselin, L.S., & Kuo, W.Y. (2006). Ethanol dehydrogenation over copper catalysts on rice husk ash prepared by ion exchange. *Applied Catalysis A: General, 304*, 30-39.

Chen, J.M., & Chang, F.W. (1991). The chlorination kinetics of rice husk. *Industrial & Engineering Chemistry Research, 30*, 2241-2247.

Conradt, R., Pimkhaokham, P., & Leela-Adisorn, U. (1992). Nano-structured silica from rice husk. *Journal of Non-crystalline Solids, 145*, 75-79.

Coran, A.Y. (2005). Vulcanization. In J.E. Mark, B. Erman & F.R. Eirich (Eds.), *The science and technology of rubber* (pp. 321-366). United States of America: Elsevier Acedemic Press.

Dannenberg, E.M. (1986). Bound rubber and carbon black reinforcement. *Rubber Chemistry and Technology, 59*, 512-524.

Davey, J.E., & Loadman, M.J.R. (1984). A chemical demonstration of the randomness of epoxidation of natural rubber. *British Polymer Journal, 16*, 134-138.

Davies, C.K.L., Wolfe, S.V., Gelling, I.R., & Thomas, A.G. (1983). Strain crystallization in random copolymers produced by epoxidation of *cis* 1,4-polyisoprene. *Polymer, 24*, 107-113.

Du, G., Liu, L., & Chen, J. (2015). White biotechnology for organic acids. In A. Pandey, R. Hofer, M. Taherzadeh, M. Nampoothiri & C. Larroche (Eds.), *Industrial Biorefineries and White Biotechnology* (pp. 409-435). United States of America: Elsevier Science.

Edwards, D.C. (1990). Review polymer-filler interactions in rubber reinforcement. *Journal of Materials Science, 25*, 4175-4185.

FAO. (2014). Rice Market Monitor (Vol. XVII, pp. 1-34). Italy Food and Agriculture Organization of the United Nations.

FAO. (2015). GIEWS Country Brief - Malaysia (pp. 1). Italy Food and Agriculture Organization of the United Nations.

Ferry, M.H., & Becker, A.V. (2004). Identification of polymers. In S.C. Bhatia (Ed.), *Handbook of polymer science and technology*. New Delhi, Bangalore: CBS Publishers & Distributors.

Fetterman, M.Q. (1973). Filler effect on the heat stability of vulcanized elastomeric compositions. *Rubber Chemistry and Technology, 46*(4), 927-937.

Flory, P.J., & Rehner, J. (1943). Statistical Mechanics of Cross-Linked Polymer Networks II. Swelling. *The Journal of Chemical Physics, 11*(11), 521-526.

Frohlich, J., Niedermeier, W., & Luginsland, H.D. (2005). The effect of filler–filler and filler–elastomer interaction on rubber reinforcement. *Composites Part A: Applied Science and Manufacturing, 36*, 449-460.

Fuad, M.Y.A., Ismail, Z., Ishak, Z.A.M., & Omar, A.K.M. (1995). Application of rice husk ash as fillers in polypropylene: Effect of titanate, zirconate and silane coupling agents. *European Polymer Journal, 31*(9), 885-893.

Fuad, M.Y.A., Ismail, Z., Mansor, M.S., Ishak, Z.A.M., & Omar, A.K.M. (1995). Mechanical properties of rice husk ash/polypropylene composites. *Polymer Journal, 27*(10), 1002-1015.

Fuad, M.Y.A., Jamaludin, M., Ishak, Z.A.M., & Omar, A.K.M. (1993). Rice husk ash as fillers in polypropylene: A preliminary study. *International Journal of Polymeric Materials and Polymeric Biomaterials, 19*, 75-92.

Gan, S.N., & Burfield, D.R. (1989). D.s.c. studies of the reaction between epoxidized natural rubber and benzoic acid. *POLYMER, 60*, 1903-1908.

Gelling, I.R. (1985). Modification of natural rubber latex with peracetic acid. *Rubber Chemistry and Technology, 58*, 86-96.

Gelling, I.R. (1987). Epoxidized natural rubber. *NR Technology, 18*, 21-29.

Gelling, I.R. (1991). Epoxidised natural rubber. *Journal of Natural Rubber Research, 6*(3), 184-205.

Gelling, I.R., & Morrison, N.J. (1985). Sulphur vulcanization and oxidative aging of epoxidized natural rubber. *Rubber Chemistry and Technology, 58*, 243-257.

Gelling, I.R., & Porter, M. (1988). Chemical modification of natural rubber. In A.D. Roberts (Ed.), *Natural rubber science and technology* (pp. 419-425). New York: Oxford University Press.

Ghosh, R., & Bhattacherjee, S. (2013). A review study on precipitated silica and activated carbon from rice husk. *Journal of Chemical Engineering & Process Technology, 4*(4), 1-7.

Hamad, M.A., & Khattab, I.A. (1981). Effect of the combustion process on the structure of rice hull silica. *Thermochimica Acta, 48*(3), 343-349.

Hamdan, H., Muhid, M.N.M., Endud, S., Listiorini, E., & Ramli, Z. (1997). 29Si MAS NMR, XRD and FESEM studies of rice husk silica for the synthesis of zeolites. *Journal of Non-crystalline Solids, 211*(1–2), 126-131.

Hashim, A.S., & Kohjiya, S. (1994). Curing of epoxidized natural rubber with *p*-phenylenediamine. *Journal of Polymer Science: Part A: Polymer Chemistry, 32*, 1149-1157.

Haxo, H.E., & Mehta, P.K. (1975). Ground rice-hull ash as a filler for rubber. *Rubber Chemistry and Technology, 48*, 271-288.

Ishak, Z.A.M., & Bakar, A.A. (1995). An investigation on the potential of rice husk ash as fillers for epoxidized natural rubber (ENR). *European Polymer Journal, 31*, 259-269.

Ismail, H., Ishiaku, U.S., Arinab, A.R., & Ishak, Z.A.M. (1997). The effect of rice husk ash as a filler for epoxidized natural rubber compounds. *International Journal of Polymeric Materials and Polymeric Biomaterials, 36*, 39-51.

Jacob, S.E., & Tace, S. (2006). Allergic contact dermatitis: Early recognition and diagnosis of important allergens. *Dermatology Nursing, 18*(5), 439-443.

James, J., & Rao, M.S. (1986). Silica from rice husk through thermal decomposition. *Thermochimica Acta, 97*, 329-336.

Kapur, P.C. (1985). Production of reactive bio-silica from the combustion of rice husk in a tube-in-basket (TiB) burner. *Powder Technology, 44*(1), 63-67.

Khong, Y.K., & Gan, S.N. (2013). Blends of phthalic anhydride-modified palm stearin alkyds with high carboxylic acid contents with epoxidized natural rubber. *Journal of Applied Polymer Science, 130*, 153-160.

Kilinçkale, F.M. (1997). The effect of $MgSO_4$ and HCl solutions on the strength and durability of pozzolan cement mortars. *Cement and Concrete Research, 27*(12), 1911-1918.

Krishnarao, R.V., Subrahmanyam, J., & Jagadish Kumar, T. (2001). Studies on the formation of black particles in rice husk silica ash. *Journal of the European Ceramic Society, 21*, 99-104.

Kumar, A., Mohanta, K., Kumar, D., & Prakash, O. (2012). Properties and industrial applications of rice husk: A review. *International Journal of Emerging Technology and Advanced Engineering, 2*(10), 86-90.

Leblanc, J.L. (2002). Rubber-filler interactions and rheological properties in filled compounds. *Progress in Polymer Science, 27*, 627-687.

Lee, S.Y. (2009). *Reactions of epoxidized natural rubber with palm oil-based alkyds and medium-chain-length polyhydroxyalkanoates.* (Unpublished doctoral dissertation), University of Malaya, Kuala Lumpur, Malaysia.

Liou, T.H. (2004a). Evolution of chemistry and morphology during the carbonization and combustion of rice husk. *Carbon, 42*, 785-794.

Liou, T.H. (2004b). Preparation and characterization of nano-structured silica from rice husk. *Materials Science and Engineering, A364*, 313-323.

Liou, T.H., Chang, F.W., & Lo, J.J. (1997). Pyrolysis kinetics of acid-leached rice husk. *Industrial & Engineering Chemistry Research, 36*, 568-573.

Loo, C.T. (1985, 21-25 October). *Vulcanisation of epoxidised natural rubber with dibasic acids.* Paper presented at the International Rubber Conference, Kuala Lumpur.

Loo, C.T. (1989). Malaysia Patent No. MY 106610.

Manna, A.K., De, P.P., & Tripathy, D.K. (2002). Dynamic mechanical properties and hysteresis loss of epoxidized natural rubber chemically bonded to the silica surface. *Journal of Applied Polymer Science, 84*, 2171-2177.

Manna, A.K., De, P.P., Tripathy, D.K., & De, S.K. (1997). Chemical interaction between surface oxidized carbon black and epoxidized natural rubber. *Rubber Chemistry and Technology*, 624-633.

Manna, A.K., De, P.P., Tripathy, D.K., De, S.K., & Peiffer, D.G. (1999). Bonding between precipitated silica and epoxidized natural rubber in the presence of silane coupling agent. *Journal of Applied Polymer Science, 74*, 389–398.

Melotto, M.A. (1990). Factory processing and laboratory testing. In R.F. Ohm (Ed.), *The Vanderbilt rubber handbook* (pp. 496-541). Norwalk, CT: R.T.Vanderbilt Company, Inc.

Mukhopadhyay, S., & De, S.K. (1991). Self-vulcanizable rubber blend systems based on epoxidized natural rubber and chlorosulfonated polyethylene: Effect of blend composition, epoxy content of epoxidized natural rubber, and reinforcing black filler on physical properties. *Journal of Applied Polymer Science, 42*, 2773-2786.

Nasir, M., Poh, B.T., & Ng, P.S. (1988). Effect of γ-mercaptopropyltrimethoxysilane coupling agent on t_{90}, tensile strength and tear strength of silica-filled NR, NBR and SBR vulcanizates. *European Polymer Journal, 24*(10), 961-965.

Nasir, M., Poh, B.T., & Ng, P.S. (1989). The effect of γ-mercaptopropyltrimethoxysilane coupling agent on t_{90}, tensile strength and tear strength of silica-filled ENR vulcanisates. *European Polymer Journal, 25*(3), 267-273.

NCBI. (2016, Apr 12, 2016). Fumaric acid. 2004-09-16. from https://pubchem.ncbi.nlm.nih.gov/compound/444972

Norman, D.T. (1990). Rubber grade carbon blacks. In R.F. Ohm (Ed.), *The Vanderbilt rubber handbook* (pp. 397-422). Norwalk, CT: R.T.Vanderbilt Company, Inc.

Olawale, O., Oyawale, F.A., Makinde, O.W., & Ogundele, K.T. (2012). Effect of oxalic acid on rice husk. *International Journal of Applied Sciences and Engineering Research, 1*(5), 663-668.

Panpa, W., & Jinawath, S. (2009). Synthesis of ZSM-5 zeolite and silicalite from rice husk ash. *Applied Catalysis B: Environmental, 90*, 389-394.

Patel, M., Karera, A., & Prasanna, P. (1987). Effect of thermal and chemical treatments on carbon and silica contents in rice husk. *Journal of Materials Science, 22*, 2457-2464.

Pire, M., Lorthioir, C., Oikonomou, E.K., Norvez, S., Iliopoulos, I., Rossignol, B.L., & Leibler, L. (2012). Imidazole-accelerated crosslinking of epoxidized natural rubber by dicarboxylic acids: A mechanistic investigation using NMR spectroscopy. *Polymer Chemistry, 3*, 946-953.

Pire, M., Norvez, S., Iliopoulos, I., Rossignol, B.L., & Leibler, L. (2010). Epoxidized natural rubber/dicarboxylic acid self-vulcanized blends. *Polymer, 51*, 5903-5909.

Pire, M., Norvez, S., Iliopoulos, I., Rossignol, B.L., & Leibler, L. (2011). Imidazole-promoted acceleration of crosslinking in epoxidized natural rubber/dicarboxylic acid blends. *Polymer, 52*, 5243-5249.

Poh, B.T., Kwok, C.P., & Lim, G.H. (1995). Reversion behaviour of epoxidized natural rubber. *European Polymer Journal, 31*(3), 223-226.

Rahman, I.A., Ismail, J., & Osman, H. (1997). Effect of nitric acid digestion on organic materials and silica in rice husk. *Journal of Materials Chemistry, 7*(8), 1505–1509.

Rajeev, R.S., & De, S.K. (2002). Crosslinking of rubbers by fillers. *Rubber Chemistry and Technology, 75*, 475-509.

Rao, G.R., Sastry, A.R.K., & Rohatgi, P.K. (1989). Nature and reactivity of silica available in rice husk and its ashes. *Bulletin of Materials Science, 12*(5), 469-479. doi: 10.1007/bf02744917

Real, C., Alcala, M.D., & Criado, J.M. (1996). Preparation of silica from rice husks. *Journal of the American Ceramic Society, 79*(8), 2012–2016.

Roa Engel, C.A., Straathof, A.J.J., Zijlmans, T.W., van Gulik, W.M., & van der Wielen, L.A.M. (2008). Fumaric acid production by fermentation. *Applied Microbiology and Biotechnology, 78*(3), 379-389.

Roychoudhury, A., & De, P.P. (1992). FTIR and NMR studies on crosslinking reaction between chlorosulfonated polyethylene and epoxidized natural rubber. *Rubber Chemistry and Technology, 66*, 230-241.

Roychoudhury, A., & De, P.P. (1993). Reinforcement of epoxidized natural rubber by carbon black: Effect of surface oxidation of carbon black particles. *Journal of Applied Polymer Science, 50*, 181-186.

Roychoudhury, A., De, P.P., Bhowmick, A.K., & De, S.K. (1992). Self-crosslinkable ternary blend of chlorosulphonated polyethylene, epoxidized natural rubber and carboxylated nitrile rubber. *Polymer, 33*(22), 4737-4740.

Rozman, H.D., Lee, M.H., Kumar, R.N., Abusamah, A., & Mohd. Ishak, Z.A. (2000). The effect of chemical modification of rice husk with glycidyl methacrylate on the mechanical and physical properties of rice husk-polystyrene composites. *Journal of Wood Chemistry and Technology, 20*(1), 93-109.

Sadrul Islam, A.K.M., & Ahiduzzaman, M. (2013). Green electricity from rice husk: A model for Bangladesh. In M. Rasul (Ed.), Thermal power plants - advanced applications (pp. 127-141). Croatia: InTech.

Shafizadeh, F. (1968). Pyrolysis and combustion of cellulosic materials. In L.W. Melville & R.S. Tipson (Eds.), *Advances in Carbohydrate Chemistry* (Vol. Volume 23, pp. 419-474). New York: Academic Press.

Shafizadeh, F., & DeGroot, W.F. (1976). Combustion characteristics of cellulosic fuels. In F. Shafizadeh, K.V. Sarkanen & D.A. Tillman (Eds.), *Thermal uses and properties of carbohydrates and lignins* (pp. 1-18). New York: Academic Press.

Sim, P.H. (2005, May 18). Product focus: Maleic anhydride. *Chemical Week, 167,* 26-27.

Solomons, T.W.G., & Fryhle, C.B. (2000). *Organic chemistry* (7th ed.). New York: John Wiley & Sons, Inc.

Sood, Y., Dhawan, J., & Kaur, A. (2014). Fumaric acid production by *Rhizopus oryzae* and its facilitated extraction via organic liquid membrane. *African Journal of Biotechnology, 13*, 1182-1187.

Sullivan, J.B., Van Ert, M.D., & Lewis, R. (2001). Tire and rubber manufacturing industry. In J.B. Sullivan & G.R. Krieger (Eds.), *Clinical environmental health and toxic exposures* (pp. 475-489). Philadelphia, USA: Lippincott Williams & Wilkins.

Sun, L., & Gong, K. (2001). Silicon-based materials from rice husks and their applications. *Industrial & Engineering Chemistry Research, 40*, 5861-5877.

Theeba, M., Bachmann, R.T., Illani, Z.I., Zulkefli, M., Husni, M.H.A., & Samsuri, A.W. (2012). Characterization of local mill rice husk charcoal and its effect on compost properties. *Malaysian Journal of Soil Science, 16*, 89-102.

Tsay, M.T., & Chang, F.W. (2000). Characterization of rice husk ash-supported nickel catalysts prepared by ion exchange. *Applied Catalysis A: General, 203*(1), 15-22.

Ugheoke, I.B., & Mamat, O. (2012). A critical assessment and new research directions of rice husk silica processing methods and properties. *Maejo International Journal of Science Technology, 6*(3), 430-448.

Umeda, J., Katsuyoshi, K., & Yoshisada, M. (2007). Environmentally benign reuse of agricultural wastes to prepare high-purity silica from rice husks. *Transactions of JWRI, 36*(2), 17-21.

Varughese, S., & Tripathy, D.K. (1992). Chemical interaction between epoxidized natural rubber and silica: Studies on cure characteristics and low-temperature dynamic mechanical properties. *Journal of Applied Polymer Science, 44*, 1847-1852.

Venezia, A.M., Parola, V.L., Longo, A., & Martorana, A. (2001). Effect of alkali ions on the amorphous to crystalline phase transition of silica. *Journal of Solid State Chemistry, 161*, 373-378.

Wagner, M.P. (1987). Fillers Part 2: Nonblack fillers. In M. Morton (Ed.), *Rubber technology* (pp. 89-95). New York: Van Nostrand Reinhold.

Witnauer, L.P., & Swern, D. (1950). X-ray diffraction and melting point-Composition studies on the 9,10-epoxy- and dihydroxystearic acids and 9,10-epoxyoctadecanols. *Journal of the American Chemical Society, 72*(8), 3364-3368.

Wolff, S. (1996). Chemical aspects of rubber reinforcement by fillers. *Rubber Chemistry and Technology, 69*, 325-346.

Wolff, S., & Wang, M.J. (1992). Filler-elastomer interactions. Part IV. The effect of the surface energies of fillers on elastomer reinforcement. *Rubber Chemistry and Technology, 65*(2), 329-342.

Yadav, L.D.S. (2005). *Organic Spectroscopy*. India: Springer-Science+Business Media.

Yalcin, N., & Sevinc, V. (2001). Studies on silica obtained from rice husk. *Ceramics International, 27*, 219-224.

Zhang, M.H., Lastra, R., & Malhotra, V.M. (1996). Rice-husk ash paste and concrete: Some aspects of hydration and the microstructure of the interfacial zone between the aggregate and paste. *Cement and Concrete Research, 26*(6), 963-977.

Zhang, M.H., & Malhotra, V.M. (1996). High-performance concrete incorporating rice husk ash as a supplementary cementing material. *Materials Journal, 93*(6), 629-636.

LIST OF PUBLICATIONS AND PAPERS PRESENTED

1. Rohani Abu Bakar, Rosiyah Yahya & Seng Neon Gan (2016) Crosslinking reactions of silica-filled epoxidized natural rubber (ENR) with fumaric acid. *Rubber Chemistry and Technology*, *89 (3),* 465-476.
2. Rohani Abu Bakar, Rosiyah Yahya & Seng Neon Gan (2016) Comparison between silica-filled epoxidized natural rubber crosslinked with fumaric acid and vulcanized with sulphur. *Submitted to Journal of Rubber Research – under review.*
3. Rohani Abu Bakar, Rosiyah Yahya & Seng Neon Gan (2016) Production of high purity amorphous silica from rice husk. *Procedia Chemistry*, *19,* 189 – 195.
4. Rohani Abu Bakar, Rosiyah Yahya & Seng Neon Gan (2016). Curing of silica-filled epoxidised natural rubber with fumaric acid *versus* sulfur vulcanisation, International Symposium on Advanced Polymeric Materials, Institute of Materials Malaysia. 16th – 18th May 2016. Putra World Trade Centre, Kuala Lumpur.
5. Rohani Abu Bakar, Rosiyah Yahya & Seng Neon Gan (2015). Production of high purity amorphous silica from rice husk, 5th International Conference on Recent Advances in Materials, Minerals and Environment (RAMM) & 2nd International Postgraduate Conference on Materials, Mineral and Polymer (MAMIP), Universiti Sains Malaysia. 4th – 6th August 2015. Vistana Hotel, Penang.
6. Rohani Abu Bakar, Rosiyah Yahya & Seng Neon Gan (2014). High purity silica from rice husk produced at various combustion temperatures, 18th Malaysian International Chemical Congress, Institut Kimia Malaysia. 3rd – 5th November 2014. Putra World Trade Centre, Kuala Lumpur.

APPENDIX A: FTIR SPECTRA OF SILICA PRODUCED FROM RICE HUSK

A.1 FTIR spectra of silica after combustion of the rice husk at 700 ^{o}C

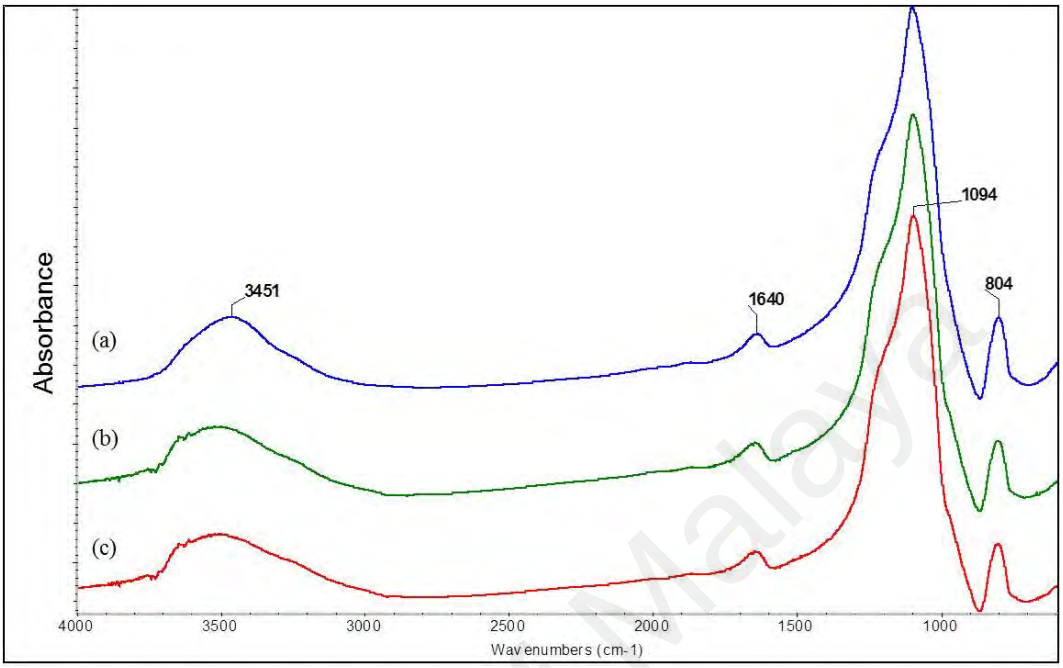

FTIR spectra of silica from (a) un-leached (b) hydrochloric acid-leached and (c) sulfuric acid-leached rice husks

A.2 FTIR spectra of silica after combustion of the rice husk at 800 ^{o}C

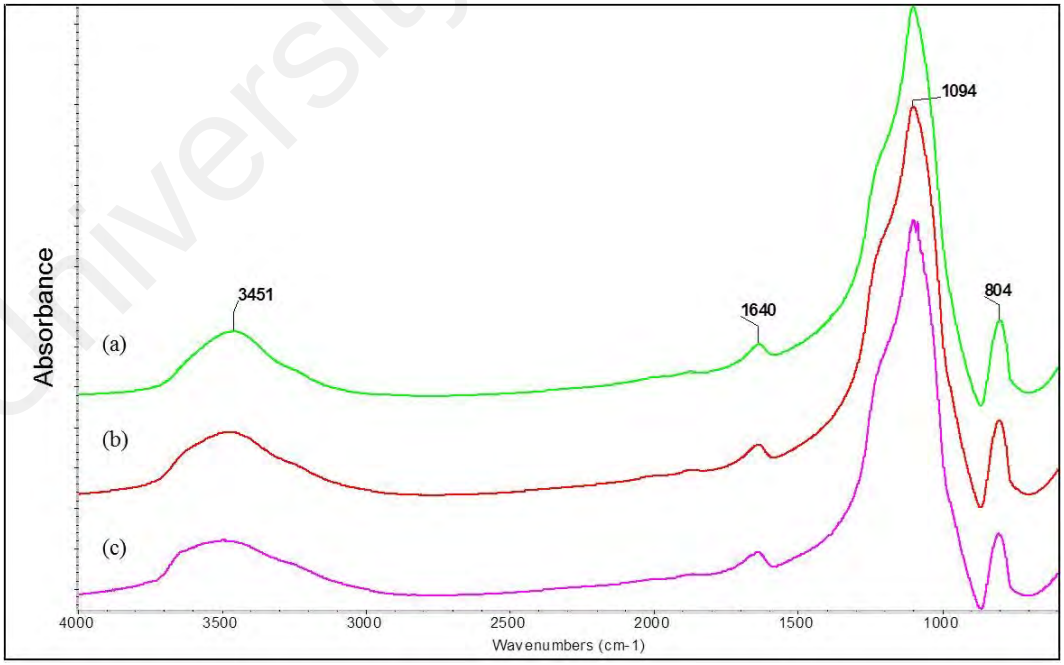

FTIR spectra of silica from (a) un-leached (b) hydrochloric acid-leached and (c) sulfuric acid-leached rice husks

A.3 FTIR spectra of silica after combustion of the rice husk at 900 ^{o}C

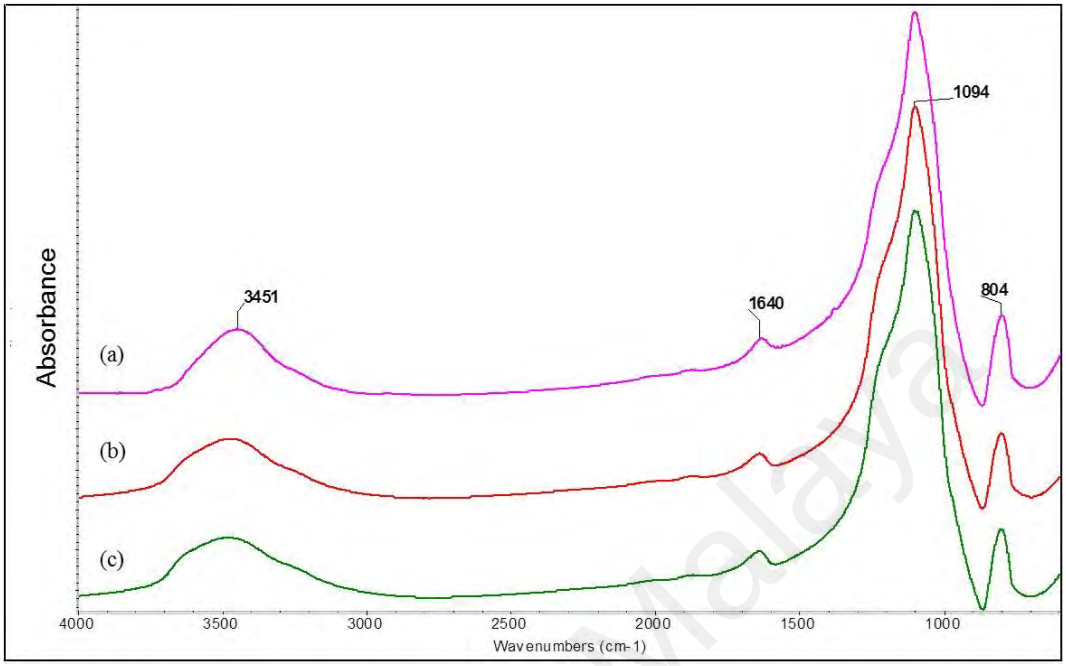

FTIR spectra of silica from (a) un-leached (b) hydrochloric acid-leached and (c) sulfuric acid-leached rice husks

APPENDIX B: DSC THERMOGRAM OF THE REACTION BETWEEN ENR50 AND FUMARIC ACID

B.1 DSC thermogram of E-FA2, E-FA11.5 and E-FA19.5 samples mixed at ambient temperature

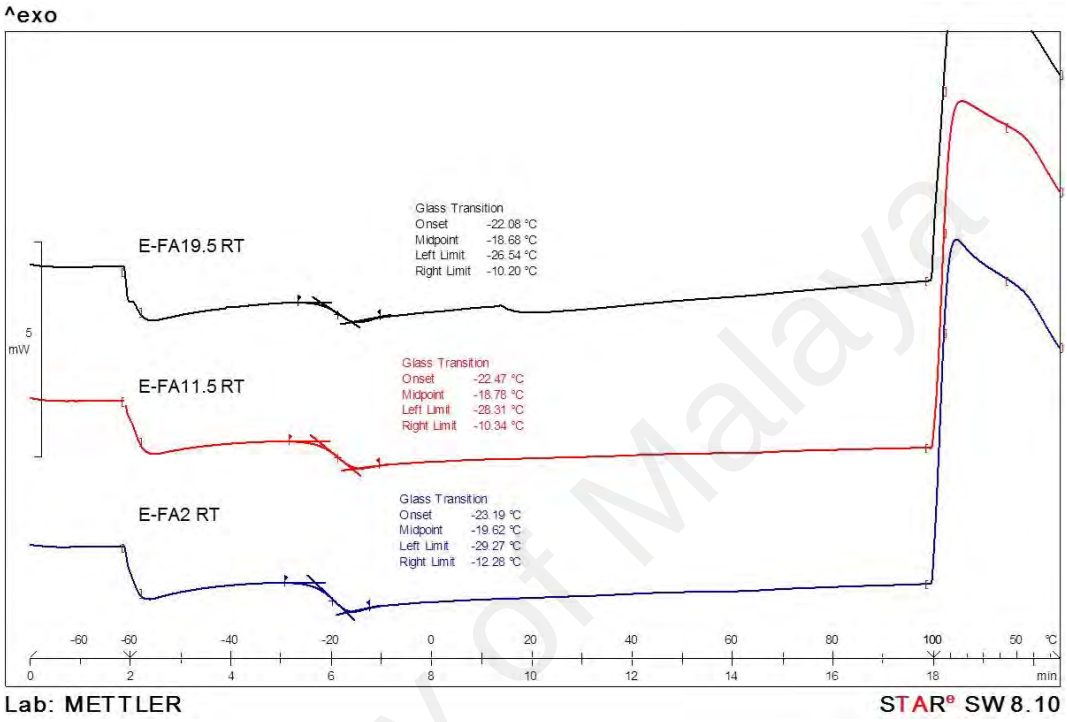

B.2 DSC thermogram E-FA2, E-FA11.5 and E-FA19.5 samples after heating at 160°C

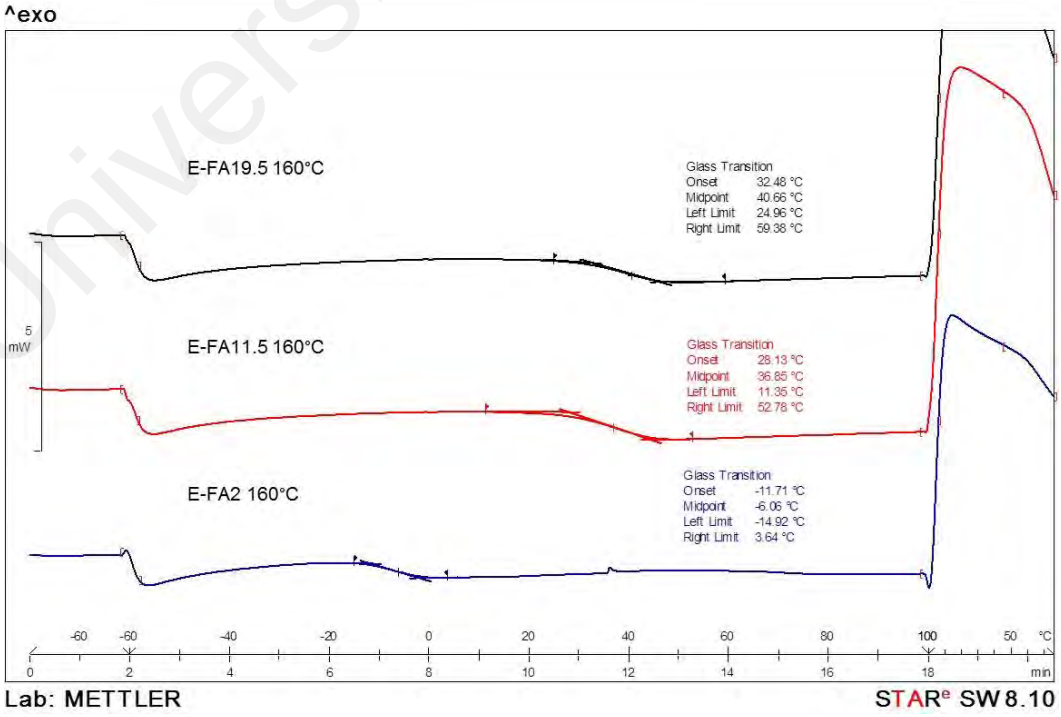

APPENDIX C: DSC THERMOGRAM OF THE SILICA-FILLED ENR50 WITH FUMARIC ACID AND SULFUR-CURED ENR50

C.1 DSC thermogram of silica-filled ENR50 mixed with fumaric acid at ambient temperature

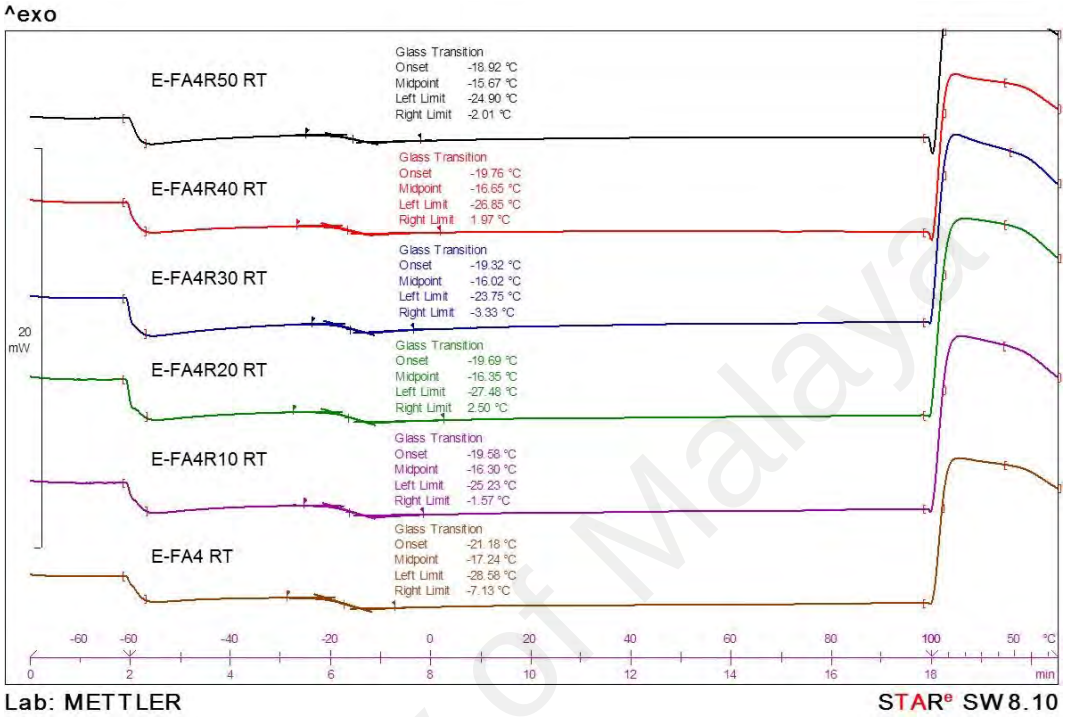

C.2 DSC thermogram of silica-filled ENR50 with fumaric acid after heating at 160 ^{o}C

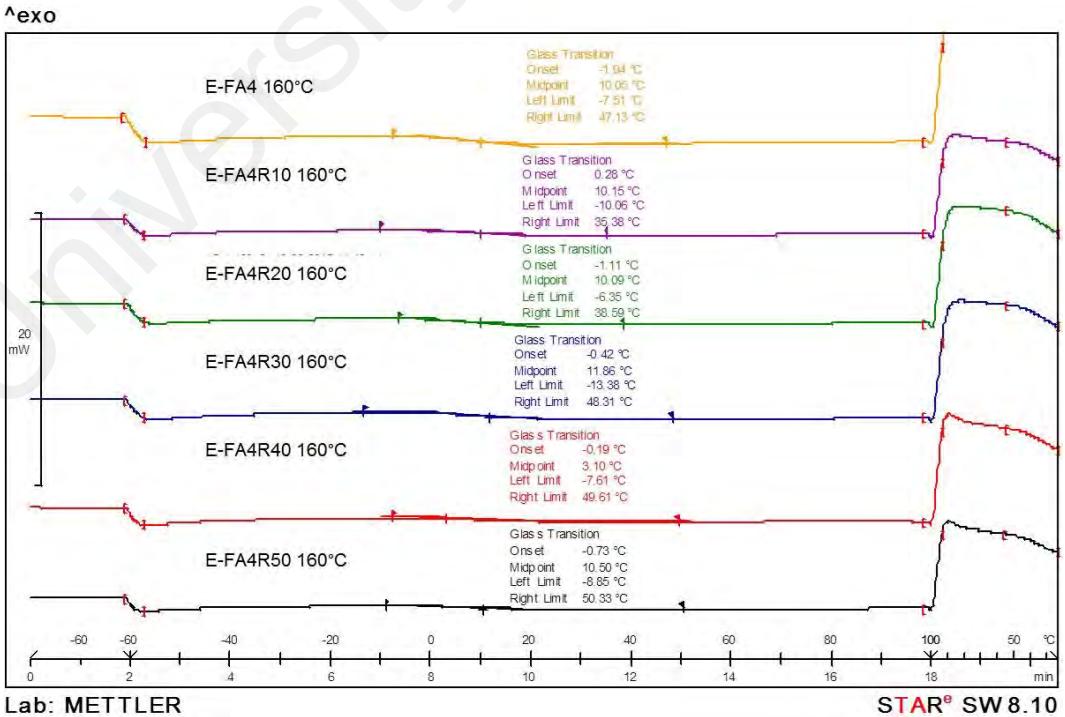

C.3 DSC thermogram of ENR50 mixed with fumaric acid (1.5phr) and silica at various loading (0 – 50 phr), at ambient temperature

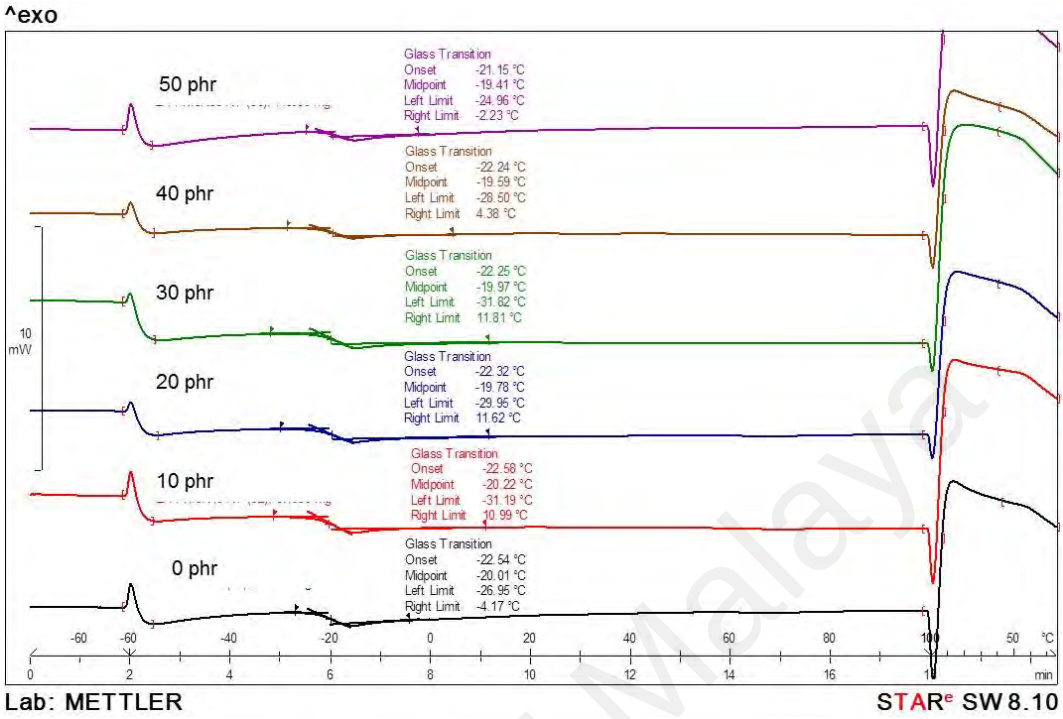

C.4 DSC thermogram of ENR50 mixed with sulfur (1.5phr) formulation and silica at various loading (0 – 50 phr), at ambient temperature

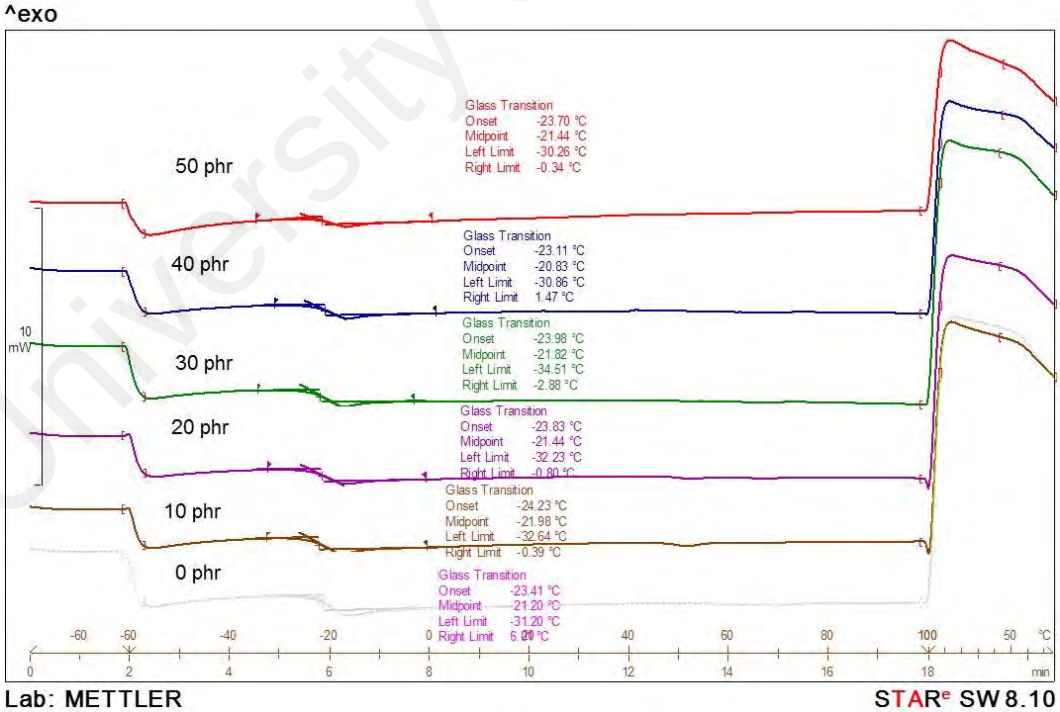

C.5 DSC thermogram of fumaric acid- cured ENR50 filled with silica at various loading (0 – 50 phr), after curing at 160 ^{o}C

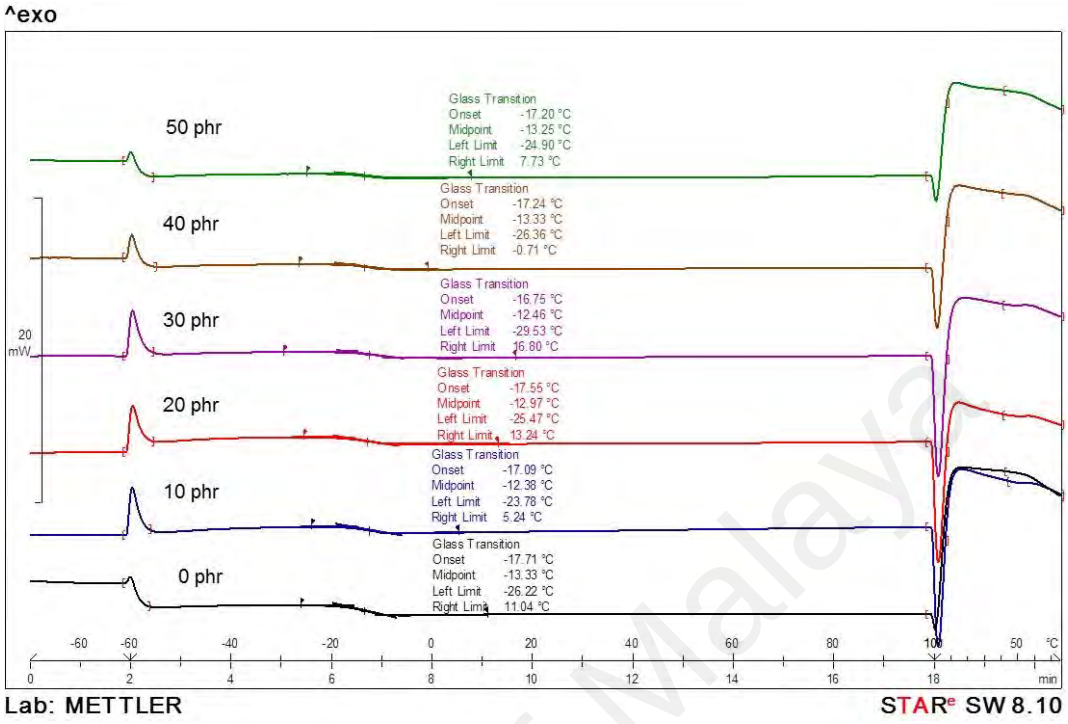

C.6 DSC thermogram of sulfur-cured ENR50 filled with silica at various loading (0 – 50 phr), after curing at 160 ^{o}C

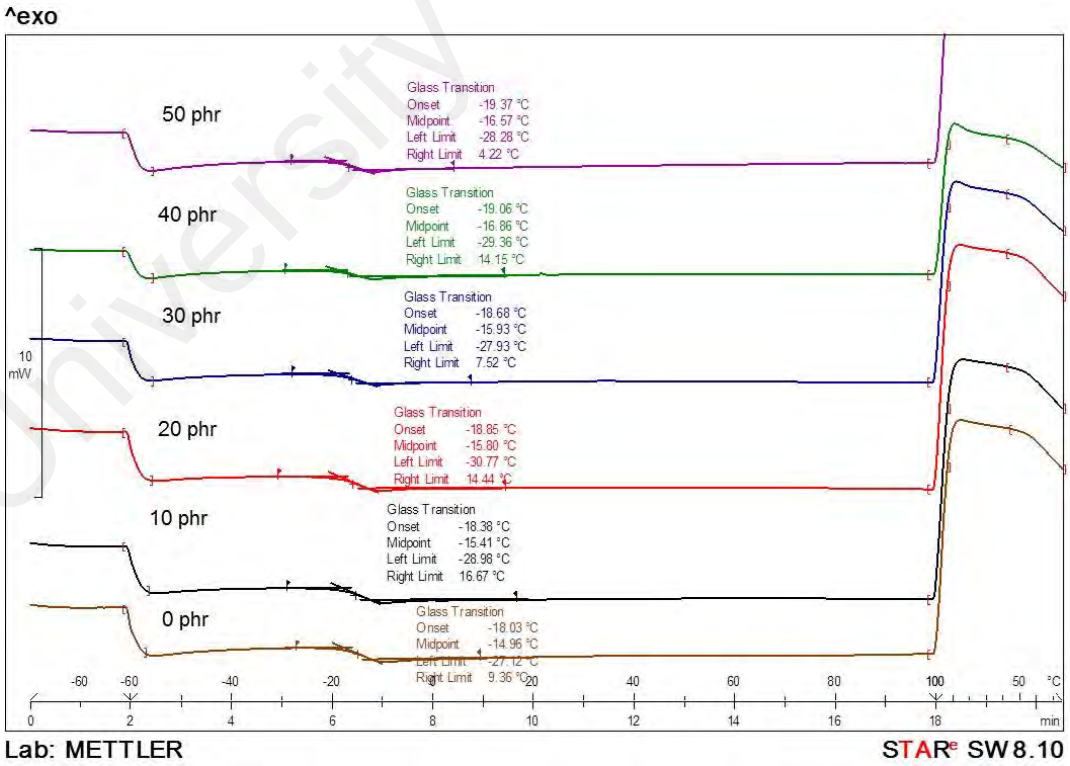

APPENDIX D: FTIR SPECTRA OF SULFUR-CURED ENR50 FILLED WITH SILICA

D.1 FTIR spectra of sulfur-cured ENR50 filled with silica at loading of (a) 0 (b) 10 (c) 20 (d) 30 (e) 40 and (f) 50 phr

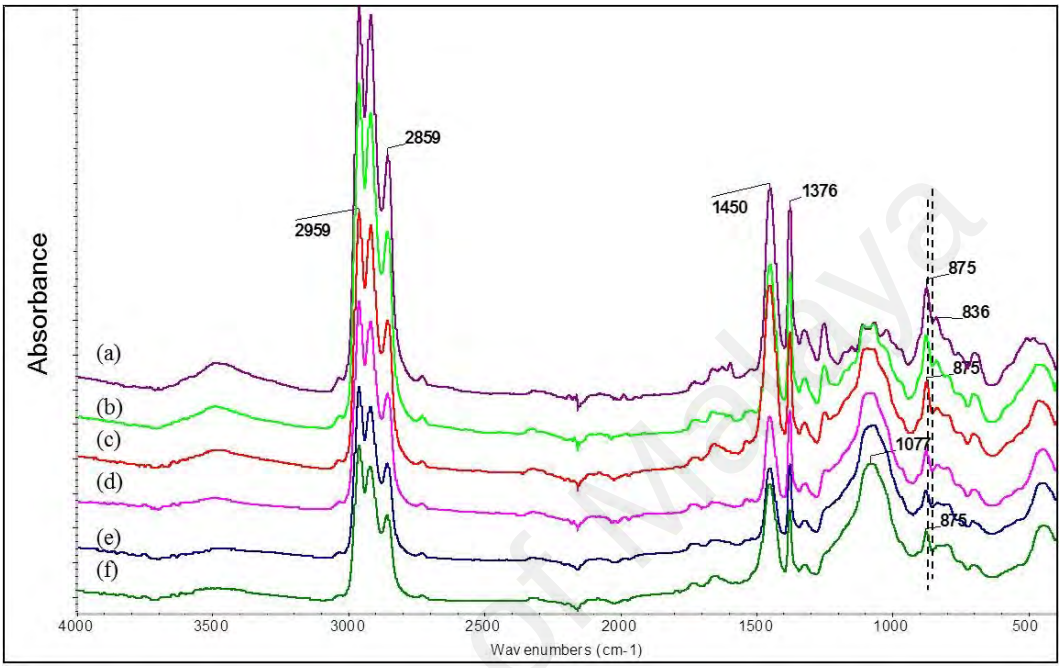

APPENDIX E: PHYSICAL PROPERTIES DETERMINATION

E.1 Physical properties of silica-filled ENR50 cured with 4 phr fumaric acid - Unaged

Silica loading (phr)	Tensile strength (MPa)	Elongation at break (%)	Modulus at 100 % strain (MPa)	Hardness (IRHD)
0	4.61±0.1	113±9	4.08±0.2	64
10	10.06±0.5	143±7	6.34±0.1	71
20	11.26±0.8	129±11	8.73±0.4	75
30	12.95±0.7	117±9	11.70±0.3	79
40	14.09±0.2	113±11	13.28±0.8	83
50	14.13±0.7	82±7	4.37±0	86

E.2 Tensile strength and elongation at break of silica-filled ENR50 cured with fumaric acid

Silica loading (phr)	Tensile strength (MPa)			Elongation at break (%)		
	Unaged	Aged	% Retention	Unaged	Aged	% Retention
0	1.96±0.2	1.84±0.1	94	196±10	183±3	93
10	3.71±0.1	3.81±0.2	103	202±0	196±6	97
20	5.44±0.6	5.27±0.5	97	193±14	176±11	90
30	7.36±0.3	7.48±0.1	102	183±4	168±1	92
40	7.49±0.2	7.48±0.1	100	160±2	136±7	85
50	8.39±0.8	7.93±0.1	95	136±12	120±5	88

E.3 Tensile strength and elongation at break of sulfur-cured ENR50 filled with silica

Silica loading (phr)	Tensile strength (MPa)			Elongation at break (%)		
	Unaged	Aged	% Retention	Unaged	Aged	% Retention
0	2.12±0.2	3.48±0.1	164	230±19	39±4	17
10	4.02±0.6	7.21±0.1	179	305±31	2±0	0.7
20	13.59±0.0	8.12±0.6	60	437±47	2±0	0.5
30	15.51±0.0	8.14±0.0	52	484±4	1±0	0.2
40	13.37±0.7	8.30±0.3	62	423±12	2±0	0.1
50	11.16±0.5	8.79±0.0	79	335±18	3±0	0.9

E.4 Modulus at 100 % strain and hardness of fumaric acid-cured and sulfur-cured ENR50s filled with silica

Silica loading (phr)	Modulus at 100% strain (MPa)		Hardness (IRHD)
Fumaric acid-cured ENR50	Unaged	Aged	Unaged
0	1.10±0	1.12±1.5	43
10	1.51±0	1.54±1.1	49
20	2.11±0	2.24±2	53
30	3.15±0.1	3.50±1.5	58
40	4.08±0.1	4.65±2.3	62
50	5.80±0.1	6.33±4.5	66
Sulfur-cured ENR50	Unaged	Aged	Unaged
0	1.04±0	ND	45
10	1.23±0	ND	46
20	1.58±0	ND	49
30	1.67±0	ND	49
40	2.28±0	ND	53
50	2.73±0	ND	55

ND – not detected

APPENDIX F: CROSSLINK DENSITY *VIA* FLORY REHNER EQUATION

Sample	Silica loading (phr)	W_1	W_2	W_1-W_2	ρ	ρ/ρ_s	$W_2+\rho/\rho_s(W_1-W_2)$	$V_r=(W_2/(W_2+\rho/\rho s(W1-W2))$	$(1-V_r)$	ln $(1-V_r)$	χV_r^2	$V_r^{1/3}$	$\ln(1-V_r)-V_r-\chi V_r^2$	$2\rho V_o V_r^{1/3}$	$\eta_{phy}=2M_c^{-1}$
Sulfur-cured ENR50	0	0.8963	0.2400	0.6563	1.0589	1.2171	1.0388	0.2310	0.7690	-0.2627	0.0224	0.6136	0.0093	137.8887	0.0000671
	10	0.8416	0.2481	0.5935	1.1053	1.2705	1.0022	0.2476	0.7524	-0.2845	0.0257	0.6279	0.0111	147.2936	0.0000756
	20	0.7676	0.2513	0.5163	1.1568	1.3297	0.9378	0.2680	0.7320	-0.3119	0.0302	0.6447	0.0138	158.2724	0.0000872
	30	0.7325	0.2520	0.4805	1.1819	1.3585	0.9047	0.2785	0.7215	-0.3265	0.0326	0.6531	0.0154	163.8060	0.0000937
	40	0.7073	0.2564	0.4509	1.2156	1.3972	0.8864	0.2892	0.7108	-0.3414	0.0351	0.6613	0.0170	170.6015	0.0000999
	50	0.6192	0.2455	0.3737	1.2474	1.4338	0.7813	0.3142	0.6858	-0.3772	0.0415	0.6798	0.0215	179.9651	0.0001195
Fumaric acid-cured ENR50	0	0.7067	0.2262	0.4805	1.0199	1.1723	0.7895	0.2866	0.7134	-0.3377	0.0345	0.6593	0.0166	142.6971	0.0001164
	10	0.6607	0.2289	0.4318	1.0691	1.2289	0.7596	0.3014	0.6986	-0.3586	0.0381	0.6704	0.0191	152.1129	0.0001257
	20	0.6217	0.2470	0.3746	1.1146	1.2811	0.7270	0.3398	0.6602	-0.4152	0.0485	0.6978	0.0269	165.0619	0.0001631
	30	0.5461	0.2323	0.3138	1.1552	1.3278	0.6490	0.3579	0.6421	-0.4430	0.0538	0.7100	0.0313	174.0586	0.0001799
	40	0.4977	0.2197	0.2780	1.1831	1.3599	0.5977	0.3676	0.6324	-0.4582	0.0568	0.7164	0.0339	179.8608	0.0001884
	50	0.4641	0.2183	0.2458	1.2129	1.3941	0.5610	0.3891	0.6109	-0.4928	0.0636	0.7301	0.0401	187.9180	0.0002136